XANTHATE-DERIVED PHOTOSENSITIVE MONOMERIC INITIATORS: SYNTHESIS, CHARACTERIZATION AND POLYMERIZATION STUDIES

THESIS SUBMITTED
TO THE UNIVERSITY OF KERALA
IN PARTIAL FULFILMENT OF THE REQUIREMENTS
FOR THE DEGREE OF
DOCTOR OF PHILOSOPHY
IN CHEMISTRY
UNDER THE FACULTY OF SCIENCE

BY

RAJU FRANCIS

PHOTOCHEMISTRY RESEARCH UNIT
REGIONAL RESEARCH LABORATORY (CSIR)
THIRUVANANTHAPURAM - 695 019, KERALA, INDIA

MAY, 1998

PHOTOCHEMISTRY RESEARCH UNIT
REGIONAL RESEARCH LABORATORY (CSIR)
TRIVANDRUM-695 019, INDIA

Telephone : 91-471-490392 Fax : 91-471-490186
E. mail: ajay@csrrltrd.ren.nic.in

Dr. A. AJAYAGHOSH
SCIENTIST

CERTIFICATE

Certified that the work embodied in this thesis entitled: **"Xanthate-Derived Photosensitive Monomeric Initiators: Synthesis, Characterization and Polymerization Studies"** has been carried out by Mr. Raju Francis under my supervision and the same has not been submitted elsewhere for a degree.

A. Ajayaghosh
(Thesis Supervisor)

STATEMENT

I hereby declare that the matter embodied in this thesis entitled: **"Xanthate-Derived Photosensitive Monomeric Initiators: Synthesis, Characterization and Polymerization Studies"** is the result of the investigations carried out by me at the Photochemistry Research Unit of the Regional Research Laboratory, Thiruvananthapuram under the guidance of Dr. A. Ajayaghosh, Scientist and the same has not been submitted elsewhere for a degree.

In keeping with the general practice of reporting scientific observations, due acknowledgement has been made wherever the work described is based on the findings of other investigators.

Raju Francis

CONTENTS

ACKNOWLEDGEMENTS

It is with great pleasure that I place on record my deep sense of gratitude to Dr. A. Ajayaghosh, my Ph.D. thesis supervisor, for suggesting the research problem, discussions at various stages of my work and helping me for a successful completion of this work.

I am indebted to Professor M. V. George, for his help and encouragement throughout the tenure of my work.

I would like to express my sincere gratitude to Dr. G. Vijay Nair, Director and Dr. A. D. Damodaran, former Director, RRL, Trivandrum for permitting me to utilize all the laboratory and library facilities during the tenure of my Ph. D. work at RRL, Trivandrum.

I am grateful to Dr. Suresh Das, Head, Photochemistry Research Unit, RRL, Trivandrum for his help. Thanks are due to all members of the Photochemistry Research Unit and particularly to Dr. K. R. Gopidas and Dr. C. R. Chenthamarakshan, for their help and support. Help received from the members of the Organic Chemistry Division, Fine Ceramics Division and Polymer Division, Mr. Mukundan (TGA analysis) and Miss. Soumini Mathew (NMR spectra) is gratefully acknowledged. Thanks are also due to Prof. P. Indrasenan, Head, Department of chemistry and Professor C. P. Joshua, former Head of the department of chemistry, University of Kerala for their interest in my work. I would like to thank all my teachers who have motivated me at different stages of my education. I express my sincere thanks to Mrs. Sarada Nair for her help in typing the thesis. Partial financial assistance from CSIR and one year leave granted by the Ministry of Education, Government of Kerala are gratefully acknowledged.

Also, I place on record my sincere gratitude to Rev. Fr. Dr. James Maruthukunnel, Principal and Rev. Fr. Jose Kappukattu, Manager, St.Joseph's College, Devagiri, Calicut for their interest and help in completing my thesis work.

Finally, I wish to express my deepest gratitude to my parents, brothers and sister for their constant encouragement, patience and support throughout my life. It would not have been possible for me to complete my Ph. D. thesis without the cooperation and encouragement of my wife Maya, for which I am deeply indebted.

Trivandrum

May, 1998 Raju Francis

PREFACE

Light induced polymerization of acrylic and vinylic monomers is a key process in the development of photosensitive polymeric coatings, printing inks and photoresist materials, which have wide ranging industrial applications. Therefore, synthesis of new photosensitive monomers and photoinitiators, studies on the photochemical processes involved during polymerization using such monomers and initiators and methods to achieve controlled synthesis of polymers have great significance both from the fundamental and technological points of view. The synthesis and use of several monomeric and polymeric photoinitiators have been reported in the literature. However, majority of these photoinitiators lead to uncontrolled polymerization which is the common drawback of normal free radical induced polymerizations.

The known photochemistry of xanthates and their application in organic synthesis have generated considerable interest in this class of compounds. The main objectives of the present investigation are the synthesis of new xanthate based photosensitive monomeric initiators and study of their role in the controlled thermal and photoinduced free radical polymerization processes. Three new photoinitiators containing polymerizable double bonds namely S-methacryloyl O-ethyl xanthate (MAX), S-maleimidobenzoyl O-ethyl xanthate (MBX) and S-(*p*-vinyl)benzoyl O-ethyl xanthate (VBX) have been chosen for the studies because of their easy synthetic accessibility and favorable light absorption properties. In addition, the photochemistry of xanthates is fairly well documented in the current literature.

The first Chapter of the thesis consists of a brief review on the role of monomeric and polymeric initiators in light induced polymerization reactions. A

brief account of various photoinitiators used for free radical initiated polymerization processes has been given with particular emphasis concerning the use of sulfur-containing photoinitiators. In addition, the recent information available on the use of polymeric photoinitiators in free radical induced graft and block copolymer syntheses have been presented.

Chapter 2 of the thesis describes the synthesis, characterization and thermal copolymerization behaviour of MAX, MBX and VBX. Several copolymers of these monomers with methyl methacrylate (MMA) and styrene (St) have been prepared. Detailed analysis of the copolymer composition and molecular weight has revealed that the new monomers show considerable differences in their copolymerization behaviour. MAX and MBX are electron deficient monomers and show tendency to form alternate copolymers during their copolymerization with styrene. In addition, MAX and MBX gave copolymers with narrow polydispersities and showed considerable reduction in their molecular weights with increase in MAX concentration. On the other hand, copolymers of VBX with MMA and St showed increase in molecular weights as well as polydispersities with increase in VBX concentration.

In the third Chapter, the role of MAX, MBX and VBX as photoinitiators in controlling the polymerization processes of MMA and St is discussed. MMA and St showed distinctly different polymerization behaviour towards the new initiators. It has been found that the thermal copolymerization behaviour of MAX, MBX and VBX with MMA and St, as discussed in Chapter 2, plays a key role in controlling their photopolymerization behaviour. Photopolymerization of MMA using MAX and MBX showed considerable control over molecular weight, polydispersity and end functionalization of the polymer chain. In the case of the photopolymerization of St, both MAX and VBX behaved as a comonomer, in addition to its role as the photoinitiator. This was particularly important in the case of the

photopolymerization of St using MBX which leads to the formation of exceptionally high molecular weight hyper branched graft copolymers along with the formation of crosslinked polymers. Photopolymerization of MMA and St did not show any appreciable difference in their polymerization behaviour when VBX was used as the photoinitiator.

The last Chapter of the thesis describes the use of soluble and crosslinked macroinitiators containing xanthate chromophores for photoinduced graft and block copolymer synthesis. The copolymers of MAX with MMA and St containing pendant xanthate groups have been found useful for the efficient photografting of St and MMA. The homopolymer formation could be effectively suppressed in these cases. Highly efficient photografting of MMA could be achieved using a heterogeneous photoinitiator containing xanthate chromophore. Polymers obtained by the photopolymerization of MMA using MAX as the photoinitiator have been found useful for the photoinduced block copolymerization. This has been illustrated by the block copolymerization of methyl acrylate (MA) using 300 nm light on to poly(methyl methacrylate) (PMMA) containing a thiocarbonylthiyl group at the chain end. The mechanism of block copolymerization is found to be analogous to the iniferter method described earlier by Otsu et al., which has the characteristics of a pseudo living radical process.

CHAPTER 1

ROLE OF PHOTOACTIVE MONOMERS AND POLYMERIC INITIATORS IN LIGHT INDUCED POLYMERIZATION REACTIONS : A BRIEF REVIEW

1.1. Introduction

Recent developments in the areas of organic chemistry, macromolecular sciences and photochemistry have significantly contributed to the designing of novel polymeric materials for advanced technological applications. Light induced polymerization of acrylic and vinylic monomers is the key process in the development of photosensitive coatings, printing inks and photoresist materials.[1-10] These materials have wide-ranging industrial applications, mainly in printing and microelectronic industries. Synthesis of new photosensitive monomers and photoinitiators, studies on the photochemical processes involved during polymerization and methods to control the polymerization processes have great significance, both from fundamental and technological points of view. The importance of this area of research is evident from the large number of publications, reviews and patents appearing in the literature. The purpose of the present review is to give a summary of the recent developments in the area of light-induced polymerization processes, using monomeric and polymeric photoinitiators. Special emphasis is given to the use of polymeric photoinitiators, and in particular *photoiniferters* for light induced block and graft copolymer synthesis. Before attempting this, it would be appropriate to mention briefly about the various types of photoinitiators, which are used in the photopolymerization of unsaturated monomers.

1.2. Photoinitiators for Free Radical Initiated Polymerization

The use of photochemically generated free radicals in the polymerization of unsaturated monomers has made great strides in recent years, mainly because of the wide application of these processes in photoactive polymer-based coating and printing formulations. The photoinitiation step in such reactions usually requires the presence of a light absorbing molecule, which is referred to as the photoinitiator. Direct absorption of light by most of the commonly used monomers being rather inefficient, light sensitive molecules are required to generate reactive species to initiate the polymerization of unsaturated monomers. Compared with other modes of initiation of free radical polymerization, light induced initiation has the advantage of being applicable at low temperatures, especially at room temperature. Photoinitiated polymerization has more control when compared to thermally initiated free radical polymerization.

In general, free radical photoinitiators can be classified into those which undergo intramolecular bond cleavage (type I) and those which abstract hydrogen atoms from hydrogen atom donors (type II). Many members of the type I initiators belong to carbonyl compounds. Benzoin and its ether derivatives[11-14] are the well-studied type I initiators which undergo Norrish type I cleavage on photolysis as shown in Scheme I.

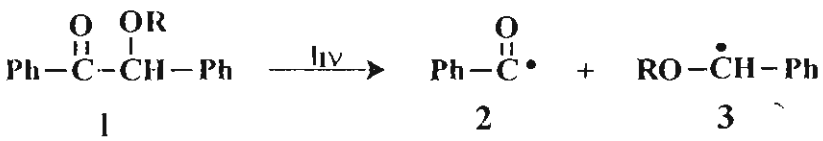

Scheme 1

The benzoyl radical initiates polymerization whereas the ether radical can function as both initiator as well as terminator, depending upon the polymerization

conditions. Structures of some of the industrially important photoinitiators of the benzoin family are shown in Chart 1.

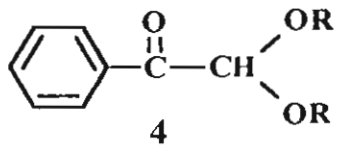

4

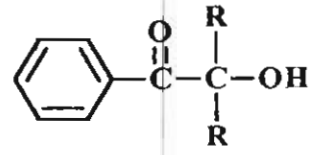

5

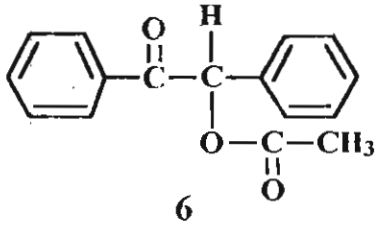

6

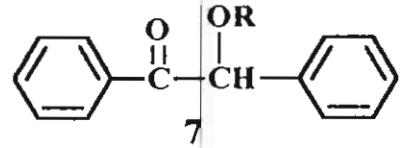

7

Chart 1

In addition to benzoin and its derivatives, acyloxime esters (**8**), acylphosphine oxides (**9**) and acylphosphonates (**10**) are also known to be efficient photoinitiators for free radical polymerization.[15-20]

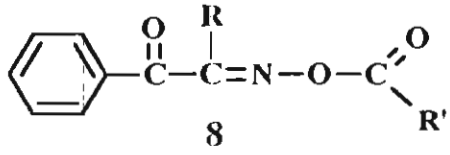

8

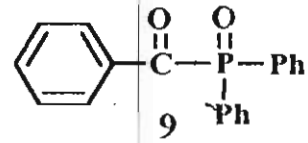

9

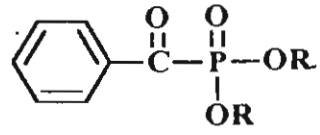

10

Chart 2

Photoinitiators which generate radicals by hydrogen abstraction are generally aromatic ketones which includes benzophenone (**11**), benzil (**12**), quinone (**13**), thioxanthone (**14**), Michler's ketone (**15**) and ketocoumarin (**16**) (Chart 3).[21-30] In the presence of appropriate electron donors such as amines, these ketones will form exciplexes. The exciplex thus formed will subsequently undergo hydrogen atom transfer from the amine moiety to the ketone, thereby forming ketyl radicals (**A**) and α-amino radicals (**B**) (Scheme 2). The α-amino radicals are reported to be more efficient in initating polymerization processes when compared to the ketyl radicals.[31,32] Thioxanthones and ketocoumarins absorb light relatively strongly in the near UV-visible region, which in association with tertiary amines find application as photoinitiators for thin-film and imaging technology.

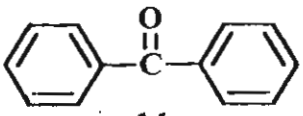

11

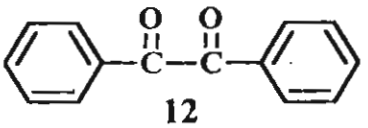

12

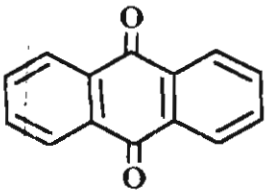

13

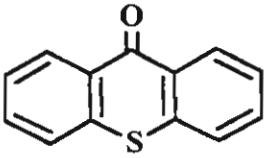

14

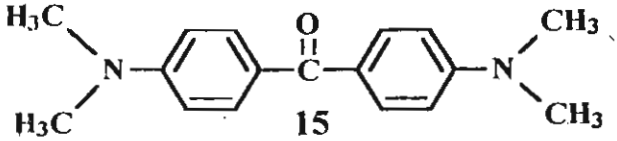

15

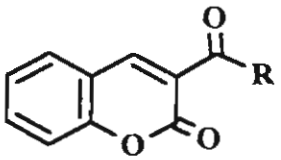

16

Chart 3

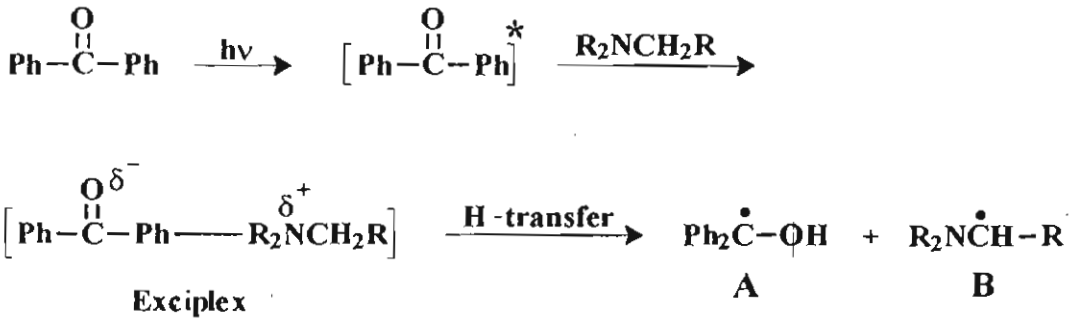

Scheme 2

1.3. Sulfur-Containing Photoinitiators

Several photoinitiators which contain photoactive C-S or S-S bonds have been synthesized and used for the photoinduced free radical polymerization of unsaturated monomers. They undergo homolytic photocleavage depending upon their molecular structures. For example, irradiation of thiobenzoic S-aryl and thiobenzoic S-alkyl esters have been reported to give the corresponding benzaldehyde, benzil and bisaryldisulfide (or *bisalkyldisulphide*), formed *via* the corresponding aroyl and thiyl radicals (Scheme 3).[33,34] Evidence for this fragmentation mode has been provided by ^{1}H NMR-CIDNP experiments.[35] *Several other sulfur containing photoinitiators such as phenyl phenacyl sulfide* ***23****,* desyl aryl *sulfide* ***24****, dibenzoyl disulfide* ***25*** *and diphenyldithiocarbonate* ***26*** (Chart 4) are known to initiate free radical polymerization of acrylic and vinylic monomers.[36-39] Other interesting classes of sulfur containing photoinitiators are tetraalkylthiuram disulfides (TD) **27** and N,N-dialkyldithiocarbamates **28** (Chart 5).

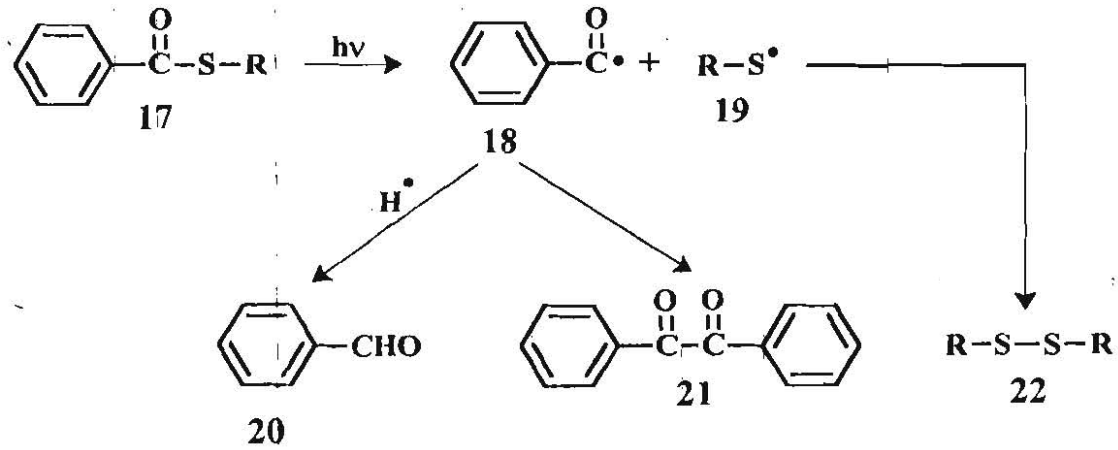

Scheme 3

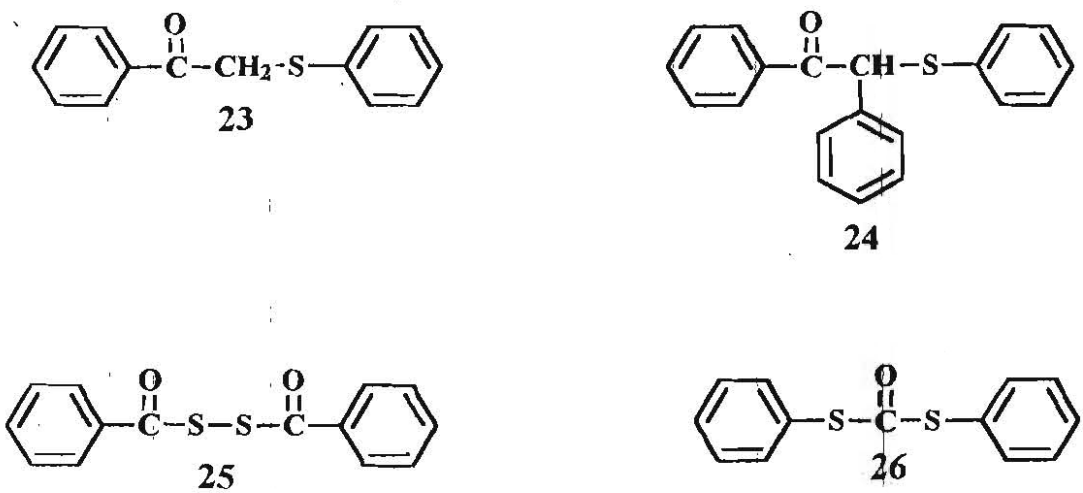

Chart 4

During 1955-1996, several studies were carried out by Forington et al.[40], Otsu et al.[41-44] and Bevington et al.[45,46] to reveal the mechanism of radical polymerization of unsaturated monomers with TD. These studies have revealed that TD is a poor initiator. However, it has been shown that polymers with reactive end functional groups, which can further act as photoinitiators and which, are

useful for block copolymer synthesis can be obtained by using TD as photoinitiator. Extensive studies have been reported by Otsu and coworkers on the photopolymerization of styrene and MMA using various dithiocarbamates as photoinitiators.[47-50] They have put forward the iniferter (initiator-transfer agent-terminator) concept in free radical polymerization which involves a living free radical polymerization mechanism. However, the use of low wavelength light (≤ 300 nm) complicates the polymerization processes and as a result, polymers obtained from such systems are found to have large polydispersities.

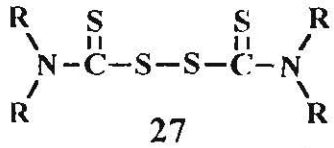

27

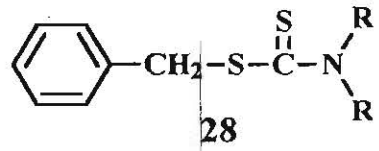

28

Chart5

Recent studies have revealed the use of benzoyl xanthate for the photopolymerization of MMA.[51] Benzoyl xanthate upon irradiation is known to undergo homolytic bond scission at the C(=O)-S bond position, generating benzoyl and thiocarbonyl thiyl radicals, as shown in Scheme 4.[52,53] Laser flash photolysis studies of a few representative aroyl xanthates have revealed the formation of two transient intermediates, assigned as benzoyl (**30**) and thiyl radicals (**31**). In this case, the benzoyl radical is the initiating species whereas the thiocarbonyl thiyl radical is a primary radical terminator.

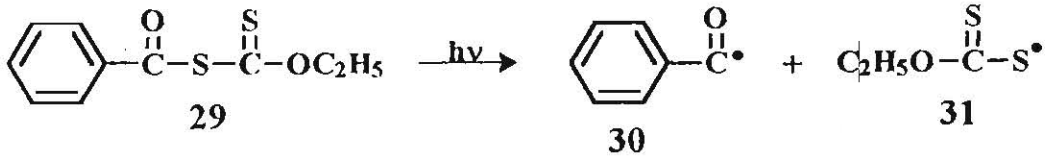

29 30 31

Scheme 4

1.4. Polymeric Free Radical Photoinitiators

Polymeric photoinitiators can be prepared either by the polymerization or copolymerization of a photoinitiator moiety attached to a polymerizable group or by the covalent linking of a photoinitiator group to a polymer backbone. Polymeric photoinitiators are found to be more reactive compared to the corresponding monomeric initiators in several cases. This could be due to the high local concentration of the radical centers on the polymeric initiator backbone and also due to the energy migration from one photoinitiator group to another along the polymer chain. They have other advantages such as low odor, low volatility and long shelf life. Therefore, polymeric photoinitiators are highly beneficial for the designing of UV curable coating formulations. However, the most important use of polymeric photoinitiators is in photoinduced graft and block copolymer synthesis. These aspects are discussed in the following section and due credit has been given to the earlier reviews on this subject.[54-58]

1.4.1. Polymers Containing Pendant Photoinitiator Groups. Photoinduced Graft Copolymer Synthesis

Polymers containing pendant photoinitiator moieties are obtained either by copolymerization of a polymerizable initiator or by covalent attachment of an initiator moiety on to a polymer backbone. Out of these two approaches, the former is preferable because copolymers with any composition and well-defined structures can be obtained. The importance of such polymeric photoinitiators is due to their use in the designing of photocurable coating formulations and in photoinduced graft copolymer synthesis. Graft copolymerization is known to be a powerful tool for the structural and physical modification of polymers. Several of the known photoinitiator groups have been incorporated on to polymer backbone as pendants and have been used for the photoinduced graft copolymerization of appropriate monomers.

1.4.1.1. Type I polymeric photoinitiators

Several of the type I photoinitiators containing a polymerizable double bonds have been reported. One of the earliest reports under this category deals with the synthesis of a polymeric photoinitiator **32** containing pendant benzophenone, substituted with a perester group.[59,60] Both, homopolymers and copolymers of **32** have been synthesized and characterized. These polymers undergo homolytic cleavage at the perester linkage upon irradiation at 366 nm, as shown in Scheme 5. The polymer **33** was found to be more efficient than its monomeric analog for the polymerization of styrene.

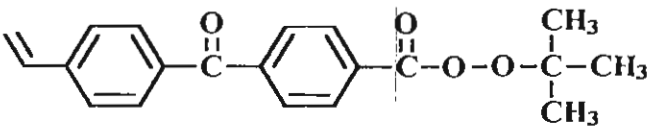

32

Several polymeric initiators containing pendant benzoin derivatives have been reported as efficient initiators for polymerization of acrylic and vinylic monomers.[61-65] A possible pathway of derivatizing benzoin is through the hydroxyl group. The acrylic derivative of benzoin undergoes efficient thermal polymerization with several common monomers, resulting in the formation of the corresponding polymeric photoinitiator **38** (Scheme 6).[66] The photoinitiation efficiency of **38** was found to be low in view of the relatively low initiation efficiency of benzoin esters in general.[67] Therefore, a range of polymeric photoinitiators based on α-hydroxymethylbenzoin have been synthesized and a representative example of this is shown in structure **39**.[61,62] The polymeric photoinitiator **39** undergoes efficient α-cleavage and shows better photoinitiation efficiency when compared to the corresponding monomeric initiator. Several other polymerizable monomers of benzoin and their derivatives such as **40** and **41** have

also been synthesized (Chart 6). Polymers of these monomers show reactivity similar to their low molecular weight counterparts, which are commercially used.[68] Recently, Fouassier et al. have carried out detailed studies on the reactivity and excited state properties of several polymeric photoinitiators containing pendant benzoin methyl ether and related groups.[69,70]

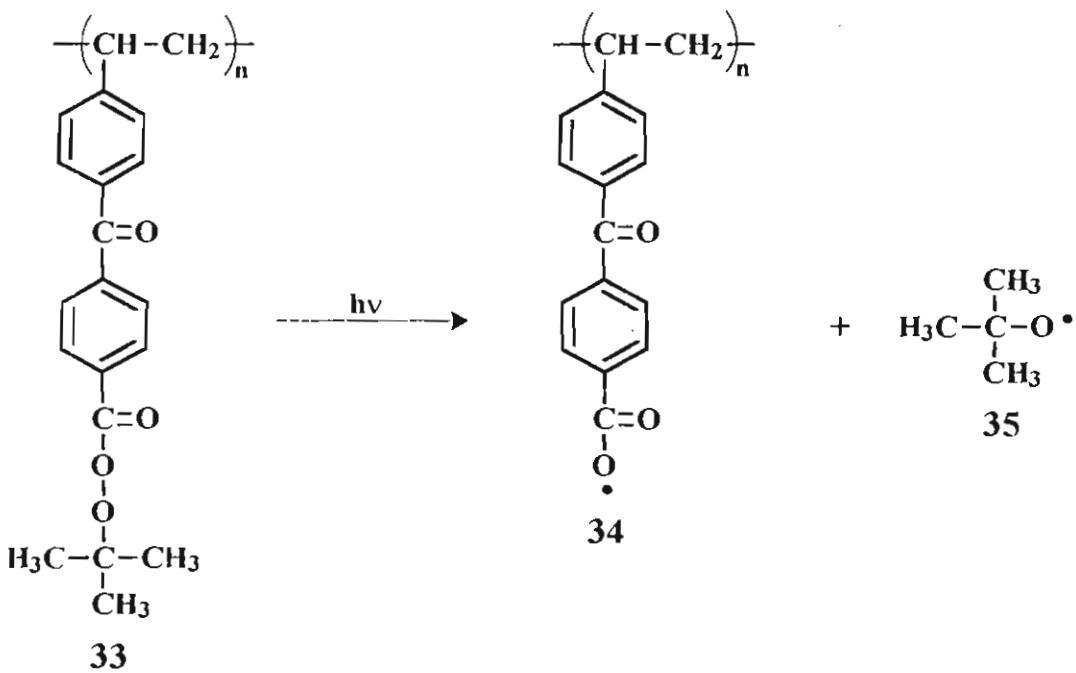

Scheme 5

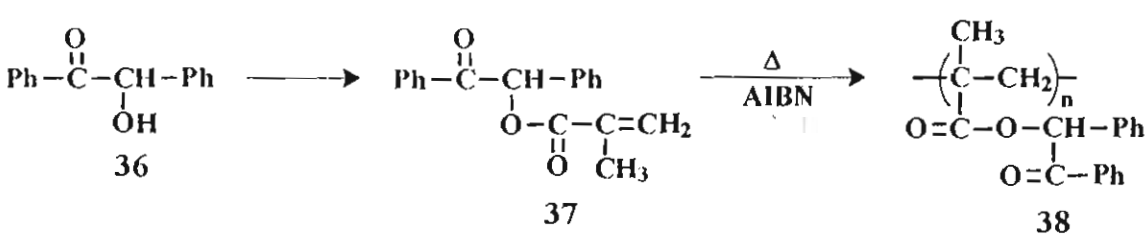

Scheme 6

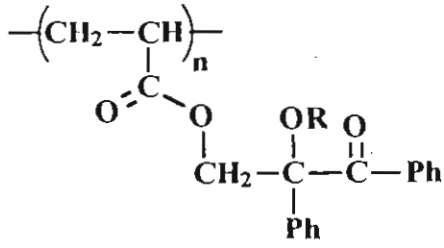

39

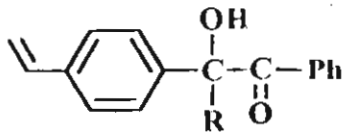

40

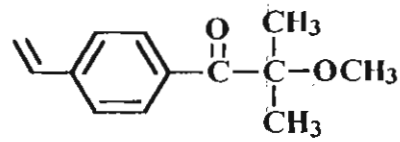

41

R = H, CH_3, Ph

Chart 6

Photophysical studies by laser flash photolysis of polymeric and low molecular weight benzoin methyl ether derivatives have revealed not only the lifetime of their triplets but also the relative quantum yields of initiation and polymerization rates for the photopolymerization of MMA. These studies indicate that the polymeric photoinitiators display higher reactivity than the low molecular weight analogues.

1.4.1.2. Polymeric photoinitiators containing pendant *iniferter* groups

As mentioned in Section 1.3, Otsu et al. have shown that certain sulfur-containing photoinitiators such as alkyl dithiocarbamates initiate polymerization of acrylic and vinylic monomers by a 'pseudo living' radical mechanism, which is also known as the '*iniferter*' mechanism. Several people have utilized the photoinitiation property of *iniferters* in graft copolymer synthesis.[71-73] For this purpose, polymers containing dithiocarbamate groups have been synthesized by reacting halogenated linear polymers with sodium dialkyl dithiocarbamates.

Similarly, polymers such as poly(vinyl chloride), partially chloromethylated polystyrene and chloromethylated polydimethylsiloxane have been converted into their corresponding dithiocarbamate derivatives for the subsequent grafting of appropriate monomers. This approach has special significance in the synthesis of several graft copolymers, which are useful for biomedical applications. For example, the properties of polydimethylsiloxane have been modified by photoinduced graft copolymerization using the '*iniferter*' method (Scheme 7).[74] By using this method, hydrophilic vinyl monomers such as 2-hydroxyethyl methacrylate, acrylamide, 2-methylaminoethyl methacrylate, sodium styrene sulfonate, N-vinyl-2-pyrrolidone and methacrylic acid were photografted on to the polymer **44**. These graft copolymers were found to have improved hydrophilicity, necessary for several biomedical applications.

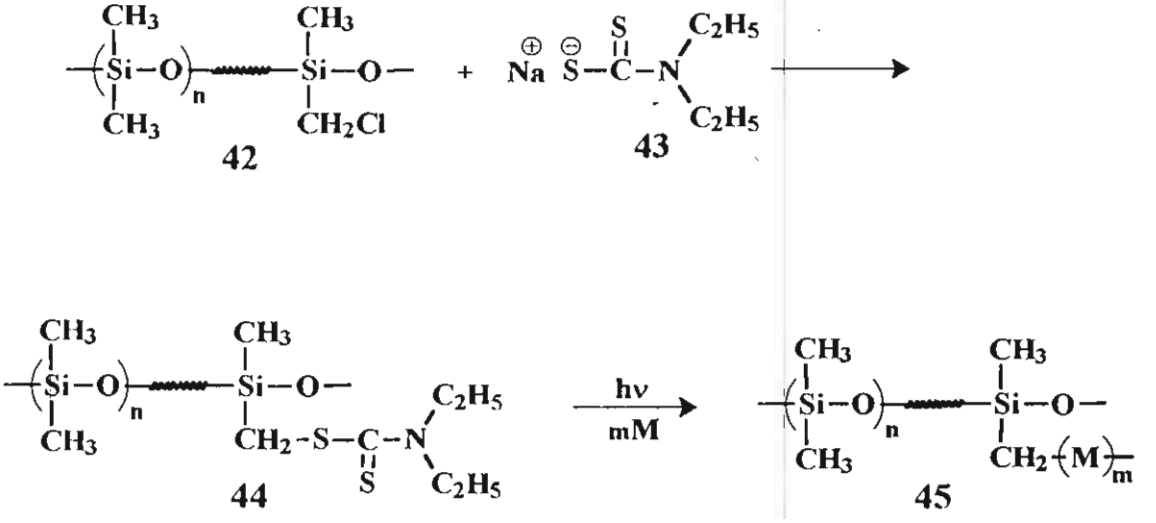

Scheme 7

Miyama and Sato have used the dithiocarbamate pendant groups for the photoinduced grafting of various monomers such as methoxyethyleneglycol methacrylate and N,N-dimethyl methacrylate on to poly(vinyl chloride).[75] Dimethylamino groups of the graft polymer are quaternized to give positive charges on to which antithrombogenic reagent heparin molecules are ionically bounded. Otsu and coworkers have synthesized a monomeric iniferter, 4-vinylbenzyl N,N-diethyldithiocarbamate (**46**). Several copolymers of the monomer **46** have been synthesized and they have been used for the preparation of graft copolymers (Scheme 8).[76] Recently, Nakayama et al. have reported surface photograft copolymerization *via* benzyl N,N-diethyldithiocarbamate free-radical chemistry.[77] This method appears to be a powerful tool for well-controlled surface

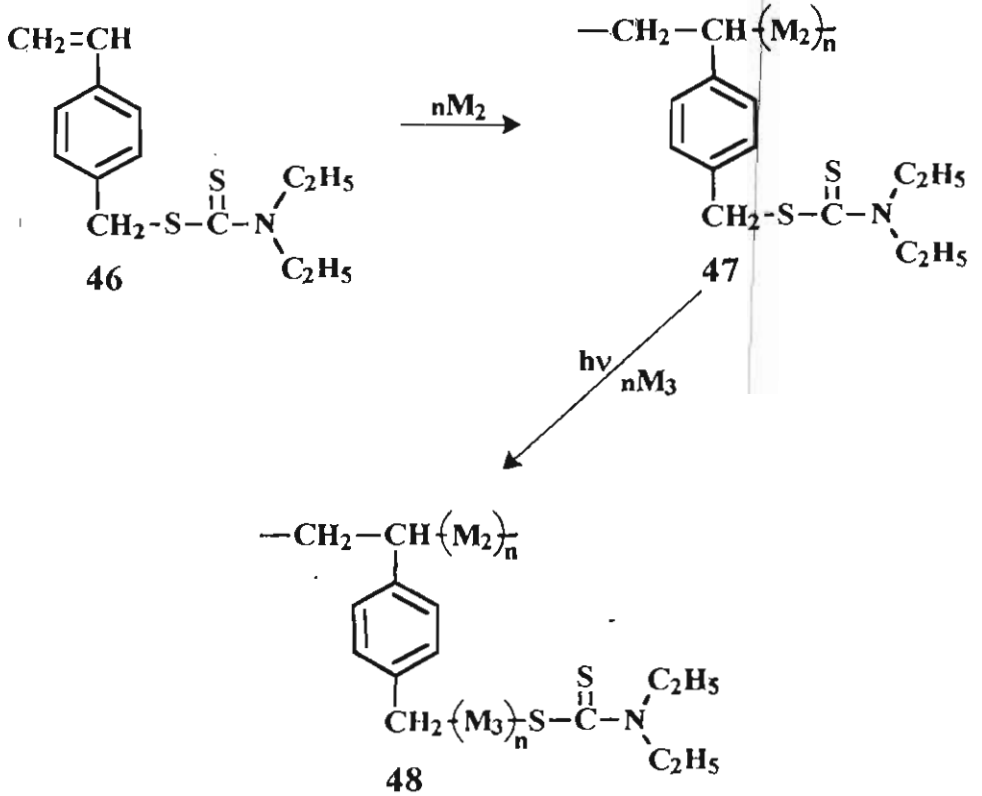

Scheme 8

macromolecular engineering for biomedical applications. Also it is claimed to be useful for functional surface design for artificial organs, micromachines and microbiosensors.

1.4.1.3. Polymers containing pendant type II initiators. Photografting by H-abstraction mechanism

Photoinduced radical polymerization property of ketone-amine systems has been exploited, in several cases, for graft copolymer synthesis. For example, the recent literature contain a good number of reports on the use of polymers carrying benzophenone as pendant group for graft copolymer synthesis.[78-80] Upon irradiation in the presence of an appropriate amine, the triplet of the polymeric benzophenone abstracts a hydrogen atom from the amine to form the polymeric radical **51** and the α-amino radical **52** (Scheme 9). A disadvantage of this method is that the initiation efficiency of the α-amino radical is much higher compared to the polymeric radical **51**, which leads to homopolymerization of monomers thereby reducing the graft efficiency. However, the polymeric initiator **49** is reported to have higher reactivity than its monomeric analogue.[81] Laser flash photolysis studies reveal that the triplet lifetime of the polymeric benzophenone is lower than that of its low molecular weight analogue.[82]

In an attempt to improve the graft yield, Kinstle and Watson have used a polymer carrying N,N-diethylamino groups in the presence of benzophenone as the triplet sensitizer (Scheme 10).[78] In this case an α-amino radical which is attached to a polymer backbone is formed. In the presence of an appropriate monomer high graft efficiency could be obtained in this way. The rather low homopolymer yield was attributed to the relatively inefficient initiating power of benzophenone ketyl radicals, and to some extent, to chain transfer reactions occurring between growing macroradicals and monomer or solvent molecules. A polymeric analogue of Michler's ketone has been prepared by modifying low

molecular weight polystyrene.[83] In this case, intramolecular hydrogen abstraction is found to be in competition with intermolecular hydrogen abstraction from the solvent. This polymer is reported to be inefficient as photoinitiator due to the overall intramolecular quenching of the triplet ketone by the amine moiety.

A new class of polymeric photoinitiators having thioxanthone as a pendant group has been described in the literature.[84-86] Detailed studies on the excited state properties of copolymers of 2-acryloxythioxanthone with MMA have revealed that the efficiency of the ketyl radical formation is lower for the copolymer **58** when compared to the low molecular weight thioxanthone photoinitiators.[86]

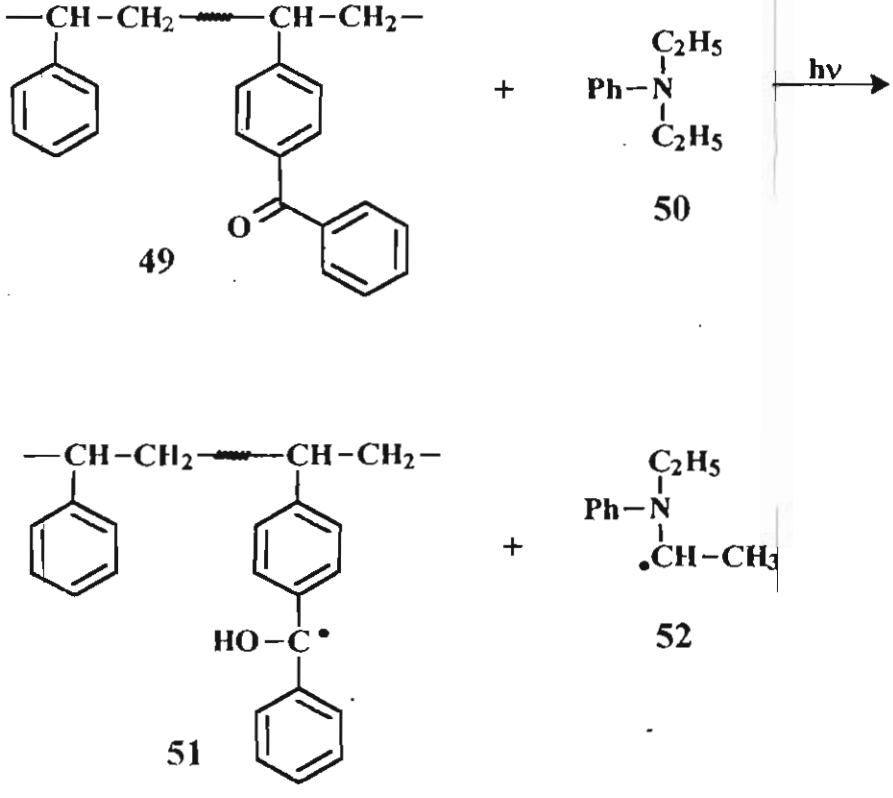

Scheme 9

1.4.1.4. Use of organometallic complexes in photoinduced graft copolymerization

It has been shown that polymers, carrying pendant halocarbon moieties such as CBr_3, upon irradiation in the presence of $Mn_2(CO)_{10}$ or $Re_2(CO)_{10}$ can generate polymeric radicals (Scheme 11). These radicals can initiate grafting of various monomers to a variety of polymeric surfaces.[87]

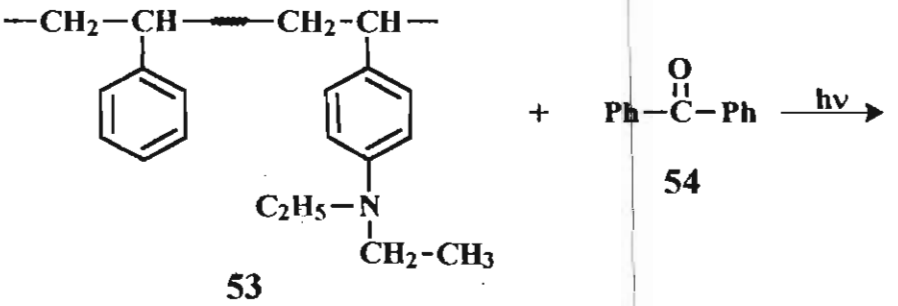

53 54

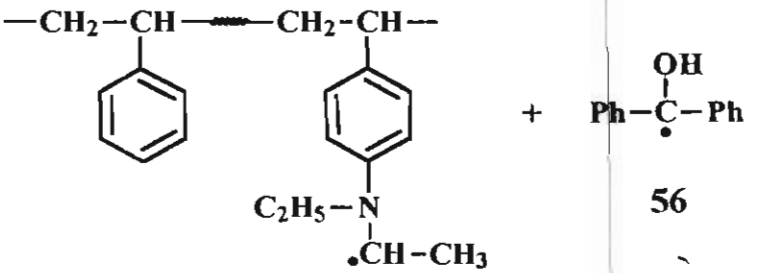

55 56

Scheme 10

The major advantage of this method is that the homopolymer formation is avoided because no radicals except the polymeric radicals are formed in the system. Several persulfate salts of ruthenium tris(bipyridyl) complexes have been used for the grafting of monomers such as acrylamide, acrylic acid and acrylonitrile on to cellulose triacetate.[88] Since a number of ruthenium complexes

have been described and their photophysical properties are known, it may be possible to design several polymeric photoinitiators based on ruthenium complexes.

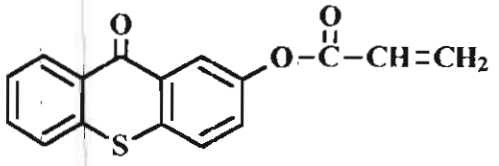

57

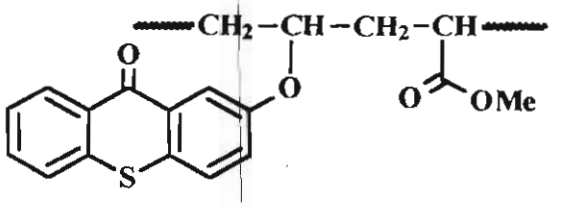

58

Chart 7

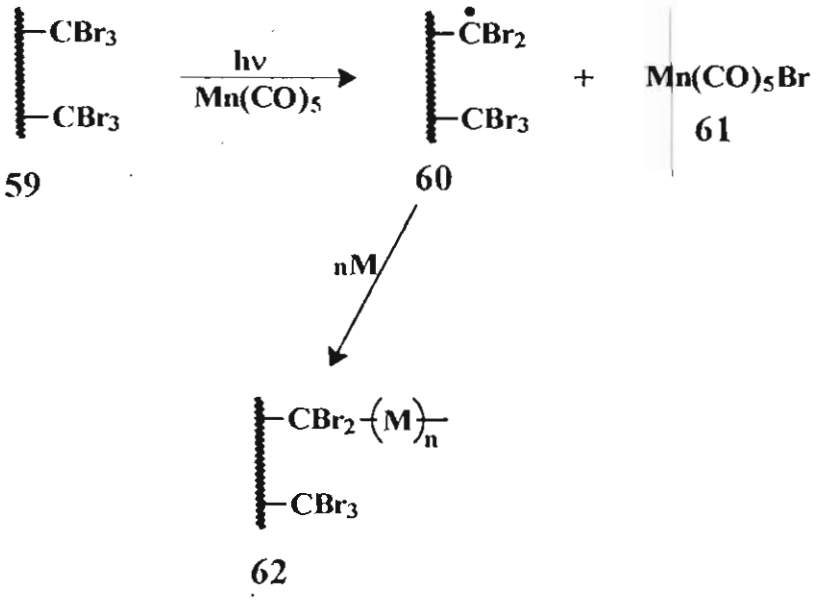

Scheme 11

1.4.2. Light Induced Synthesis of Block Copolymers

Photoinduced block copolymerization is a versatile approach towards the modification of structure and properties of polymers.[89,90] Photochemical block copolymerization consists of a photochemical reaction by which active radical

centers are produced at the end of a polymeric chain which initiate the incorporation of a second monomer to form blocks of new polymeric chains. The method, therefore, consists of two or more steps. The first stage is the synthesis of prepolymers containing one or several photosensitive groups. The subsequent steps involve the photolysis of the prepolymers in the presence of various monomers. The photosensitive groups can be located either in the main chain or at the chain ends of the prepolymer.

1.4.2.1. Block copolymerization using polymers carrying photolabile groups in the main chain

Prepolymers carrying small amount of photoactive groups, which are useful for photoinduced block copolymer synthesis can be obtained by the polycondensation approach. In this case, the structure of the resulting block copolymers depend upon the mode of termination processes involved as shown in Scheme 12.

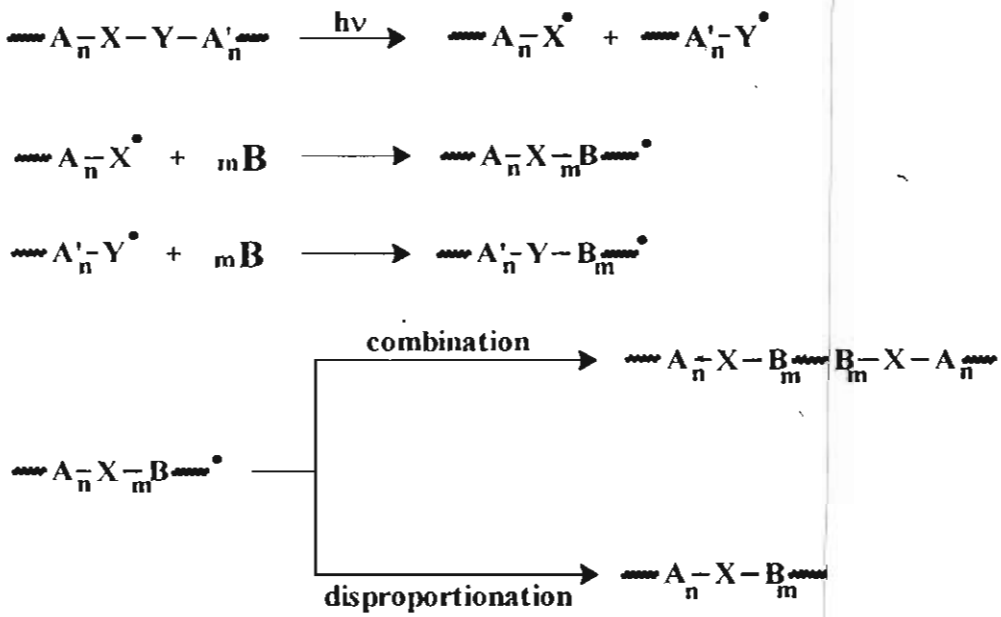

Scheme 12

Lanza et al. have utilized the photodissociation of keto oxime esters for the synthesis of block copolymers.[91] Polycondensation of adipoyl chloride **65** and tetrachlorobisphenol-A **63**, in the presence of small amounts of the keto oxime **64** have resulted in a polyester **66** containing small amounts of keto oxime ester linkage. This polymer, on photolysis in the presence of styrene gave block copolymers in 90-95% yield (Scheme 13). The length of styrene sequences in the block polymer could be adjusted by changing the initial monomer concentration.

Photoactive benzoin methyl ester groups have been introduced into polycarbonates by the condensation polymerization of bisphenol-A with phosgene in the presence of 4,4'-dihydroxybenzoin methyl ether as shown in Scheme 14.[92,93] On photolysis, the polycarbonate undergoes main-chain scission due to the photodissociation of the benzoin methyl ether group as evidenced by the decrease in viscosity. When irradiation was carried out in the presence of MMA a block copolymer was formed in high yield. Differential scanning calorimetric studies has revealed the existence of two distinct glass transitions at 90° and 176 °C, corresponding to PMMA and polycarbonate sequences. The number of the benzoin methyl ether groups in the polycarbonate prepolymer could adjust the length of the polycarbonate blocks whereas the length of the PMMA blocks was controlled by the polymerization conditions.

Craubner has reported the synthesis of several block copolymers by using polymers containing N-nitroso groups.[94] The principle of this method is based on the photoisomerization of nitrosoamide groups into diazoesters, which afford two macroradicals with evolution of nitrogen (Scheme 15). Block copolymers containing sequences of a polypeptide and of poly (methyl methacrylate) were prepared by Vlasov et al.[95] Disulfide groups were incorporated into the peptide chain by polymerization of a N-carboxyanhydride (NCA) of an amino acid in the presence of an appropriate disulfide. For example, a polypeptide carrying a

disulfide on UV irradiation in the presence of an appropriate monomer gave the corresponding block copolymers as per Scheme16.

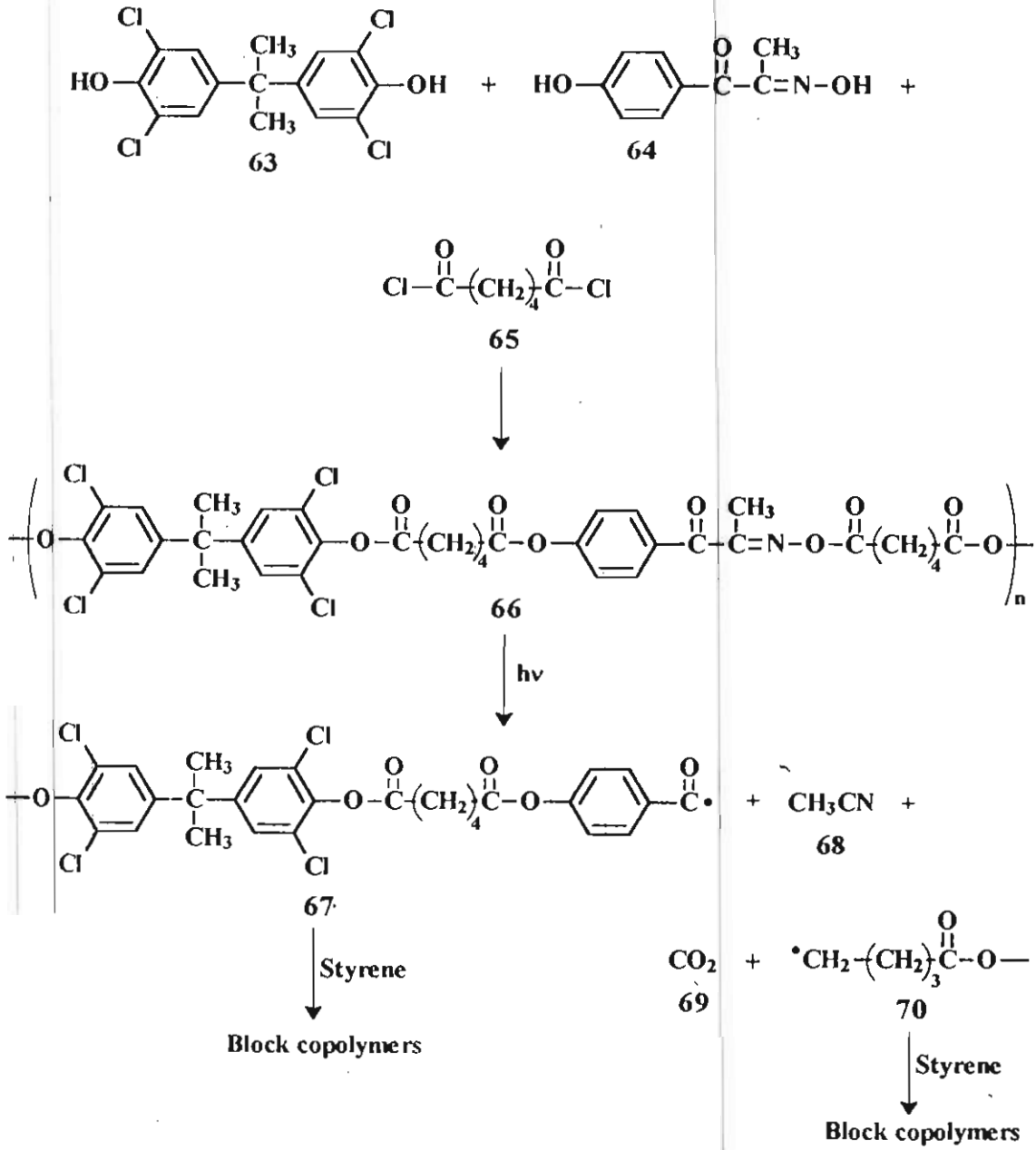

Scheme 13

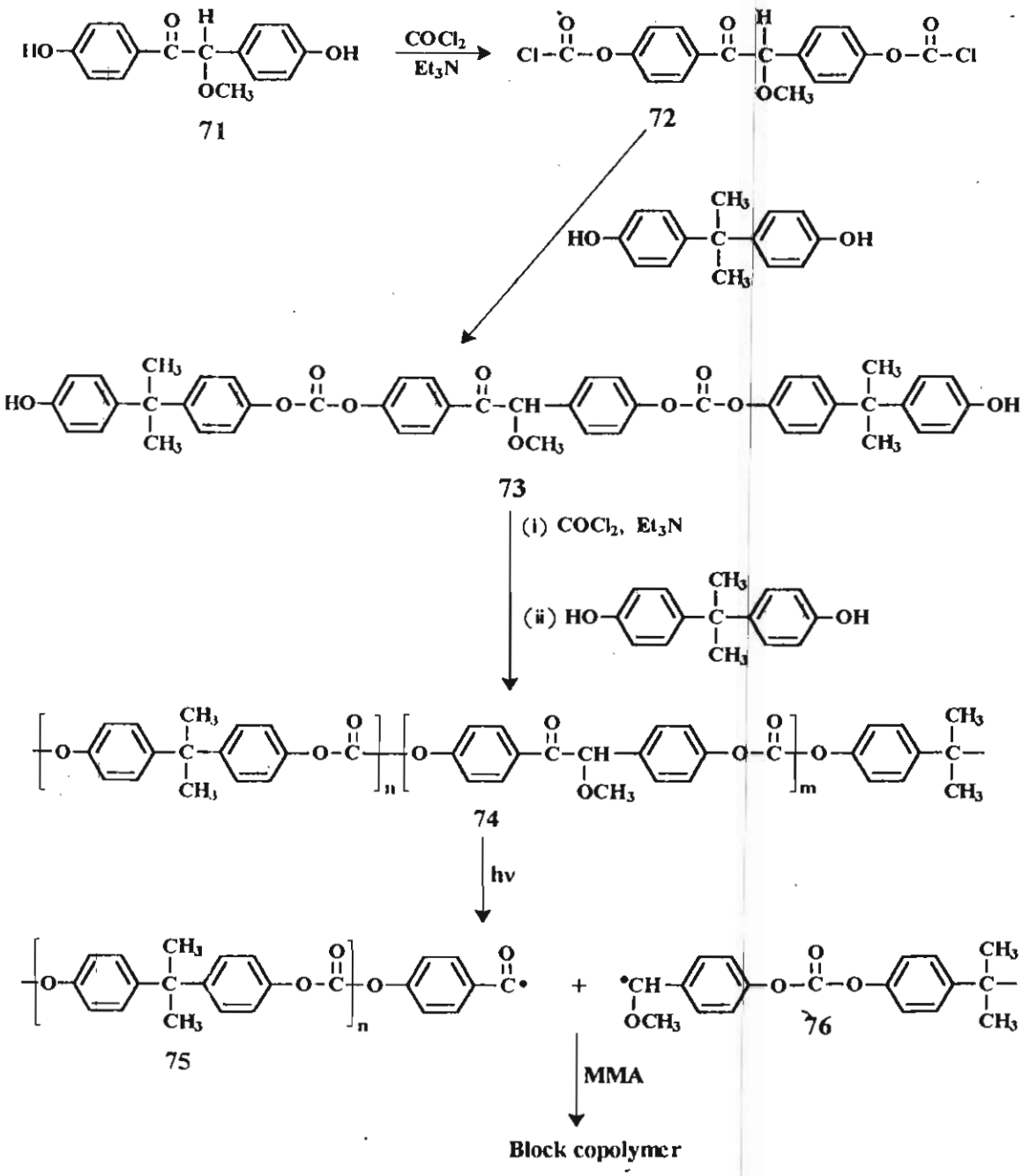

Scheme 14

A similar method was applied by Mezger and Cantow to synthesize block copolymers containing blocks of cellulose triester and polystyrene.[96,97] Cellulose

triesters containing terminal hydroxy groups were prepared by hydrolytic degradation. The product thus obtained was reacted with 4,4-dithiobis(phenylisocyanate) to form the polymeric disulfide (**85**), which on irradiation in the presence of styrene or MMA gave block copolymers (Scheme 17). The cellulose content of the block copolymer **87** was estimated to be nearly 10-40% by weight. Due to the low glass transition temperature of the MMA blocks, the copolymer **87** exhibited rubber like elasticity at room temperature and hence processable as thermoplastics. The major disadvantage of the use of polymeric initiators having photolabile groups which are incorporated within the

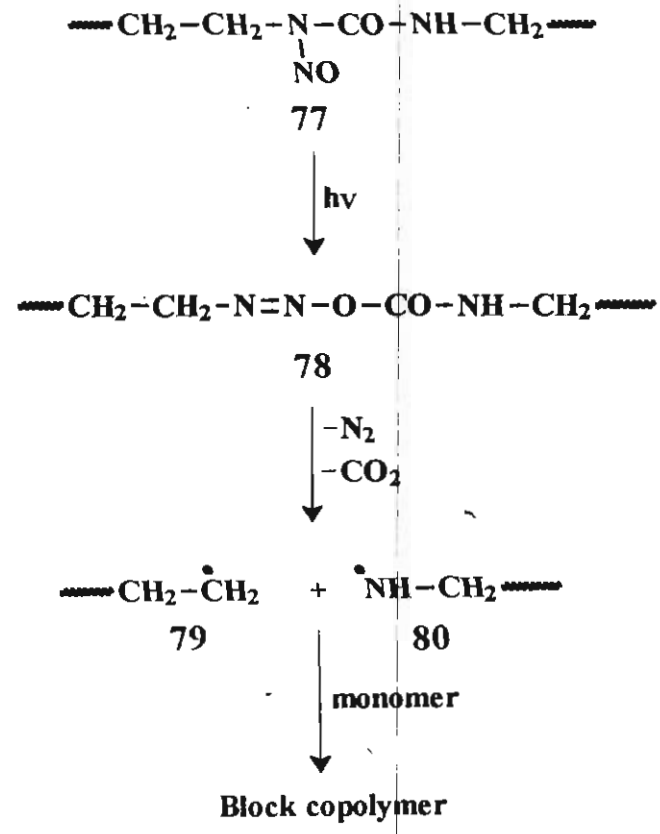

Scheme 15

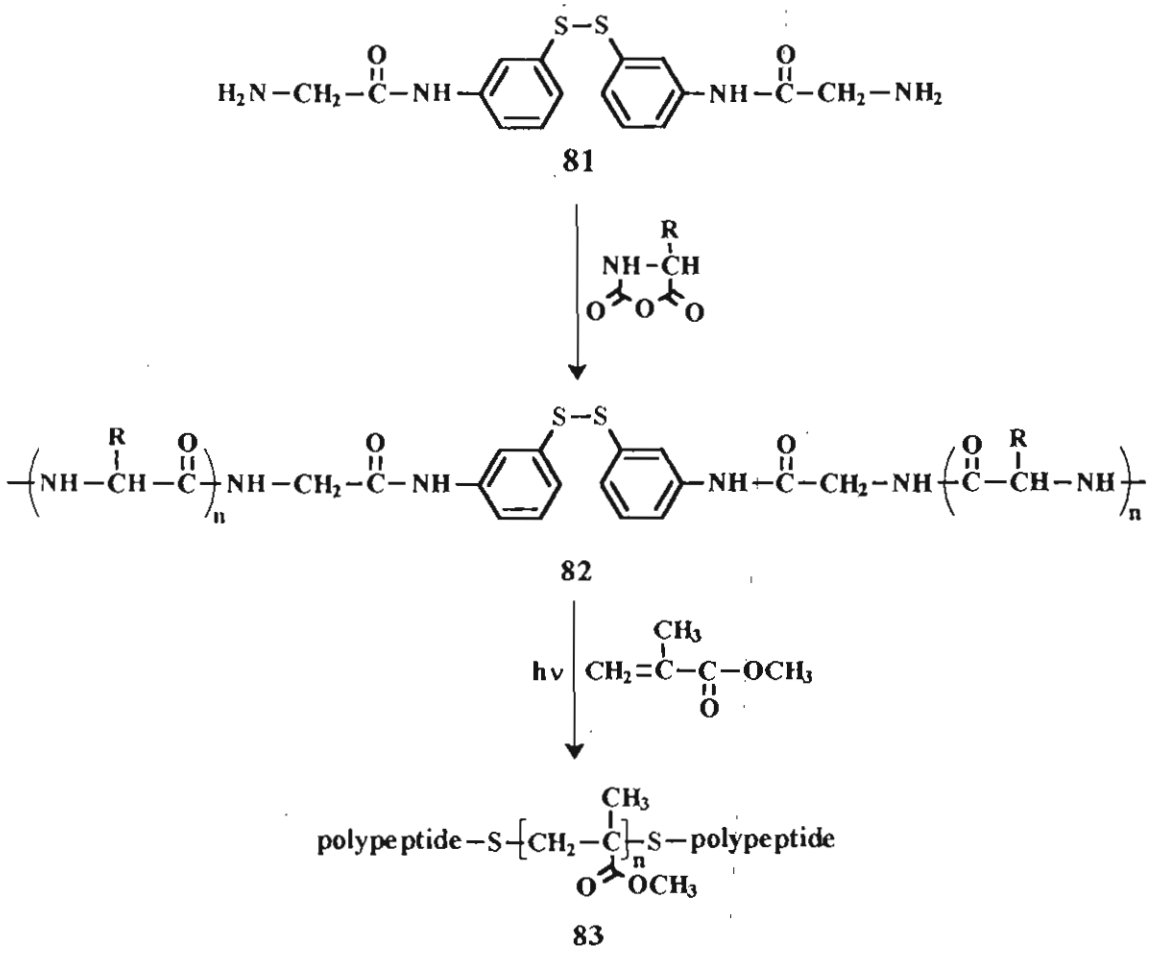

Scheme 16

polymer chain is that the resultant block copolymers in such cases show broad polydispersity. This could be primarily due to the uncontrolled termination processes involved in the polymerization. As illustrated earlier in Scheme 12, if two unsymmetrical macroradicals are formed during photodissociation, both can initiate polymerization leading to the formation of polymers with different types of blocks having different chain length and polydispersity. Since various modes of terminations such as combination, disproportionation or hydrogen abstraction are possible, highly inhomogeneous block copolymers will be formed. However, this

method has the advantage of suppressing the homopolymer formation since photodissociation leads to the formation of two polymeric radicals, both can lead to block copolymers.

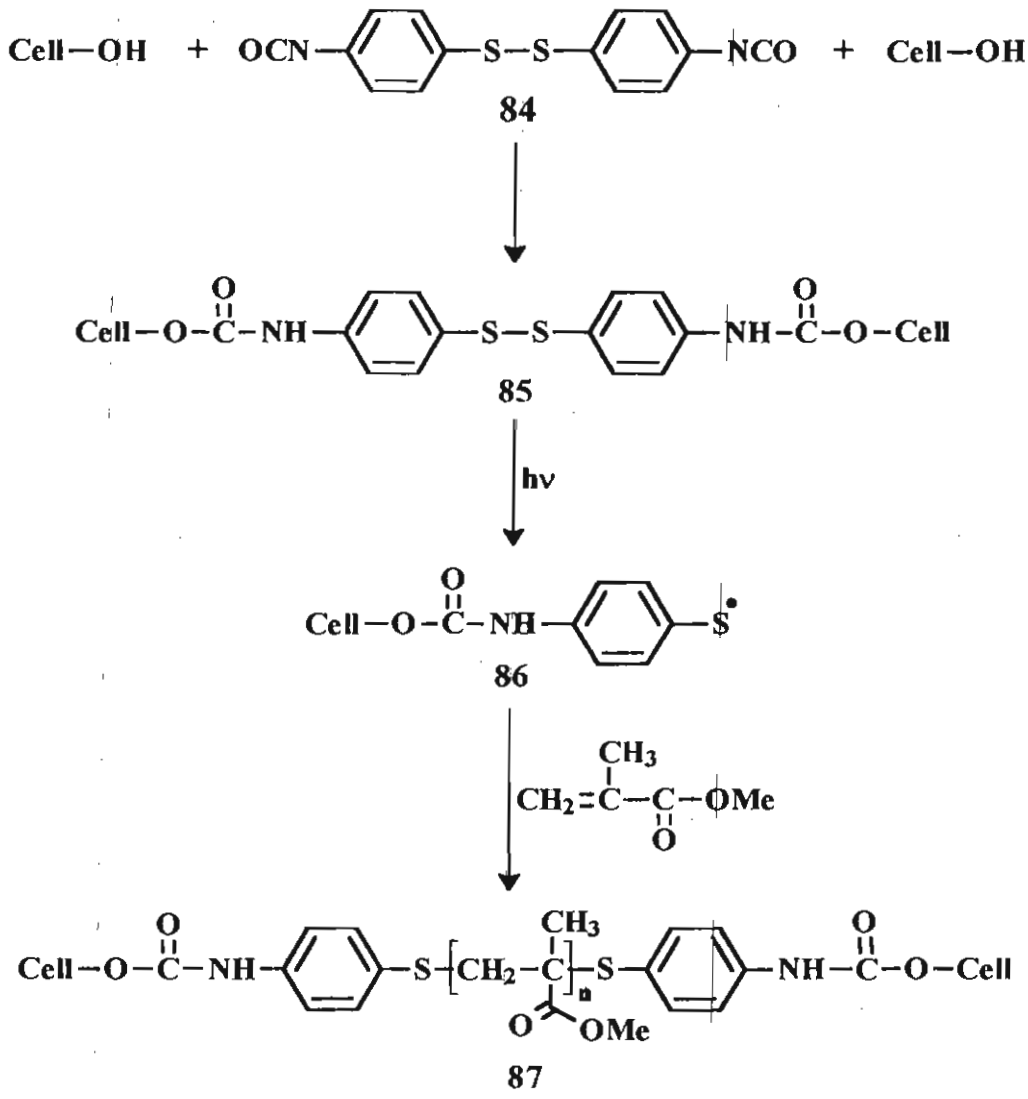

Scheme 17

1.4.2.2. Polymeric photoinitiators having photolabile groups at chain ends

Polymers carrying photolabile end groups produce two free radical centres out of which only one is a macroradical. The second radical which is a low molecular weight initiator fragment will initiate homopolymerization of the monomers. Consequently, the formation of both blockcopolymers and homopolymers will be followed by this method. Therefore, special efforts to control the homopolymer formation are required for enhancing the block copolymer yield. In this respect, Banford's metal carbonyl initiating method is a novel approach towards block copolymer synthesis.[98-100] This method is based on the fact that transition metal carbonyls such as $Mn_2(CO)_{10}$, $Re_2(CO)_{10}$ and $Os_3(CO)_{12}$ react with polymers having $-CX_3$, $-CHX_2$ or $-CH_2X$ end groups (X = halogen atom) to form terminal carbon centered macroradicals (Scheme 18). The principal radical generating reaction is an electron transfer process from transition metal to halide, the former assuming a low oxidation state.

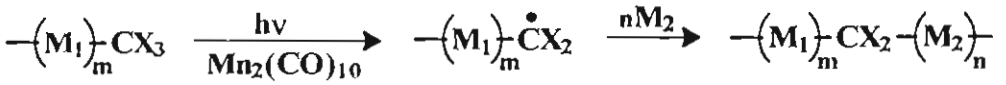

88 89 90

Scheme 18

1.4.2.3. Macroiniferters for block copolymer synthesis

As described earlier in this Chapter (Section 1.3), the use of certain sulfur containing molecules such as tetraethylthiuram disulfide and N,N-dialkyldithiocarbamates as photoinitiators can give polymers with photoactive dithiocarbamate end groups. For example, thermal or photochemical polymerization of styrene in the presence of tetraethylthiuram disulfide gives a telechelic polymer **91** with two photoreactive end groups. Photopolymerization of

vinyl acetate in the presence of the macroinitiator **91** yields a block copolymer, which contains nearly 80% of the vinyl acetate.[101]

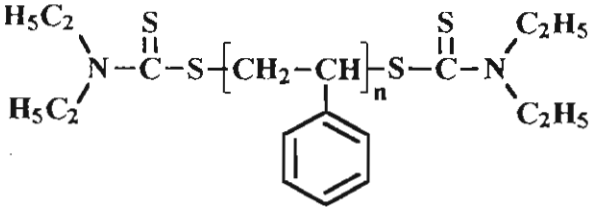

91

Niwa et al. have used bis(isopropyl xanthogen) disulfide (**92**) for the designing of block copolymers (Scheme 19).[102,103] The mechanism of block copolymerization is same as in the case of the disulfide **91**. Upon absorption of light, C-S bond cleavage occurs to form a carbon centered macroradical and a sulfur centered dithiocarbamate radical. The macroradical initiate the block copolymerization whereas the sulfur centered radical is much less reactive and acts as the terminator. Otsu et al. have extensively studied the use of dithiocarbamates for the designing of block copolymers.[104-107] In an attempt to synthesize extremely pure homopolymer free block copolymer, they have used the solid-phase synthetic strategy along with their *iniferter* method.[107] The block copolymer was synthesized on to crosslinked chloromethylated polystyrene containing dithiocarbamate groups through an anchoring linkage and subsequently detached the block copolymer from the polymer support by using an appropriate cleaving agent. Turner and Blevins and Lambrinos et al. have reinvestigated the block copolymer synthesis using dithiocarbamate photochemistry and revealed the occurrence of a side reaction during photolysis (Scheme 20).[108,109] They proposed a photochemical cleavage of the thiocarbonyl nitrogen bond and subsequent elimination of carbon disulfide, which limits the living nature of the polymerization.

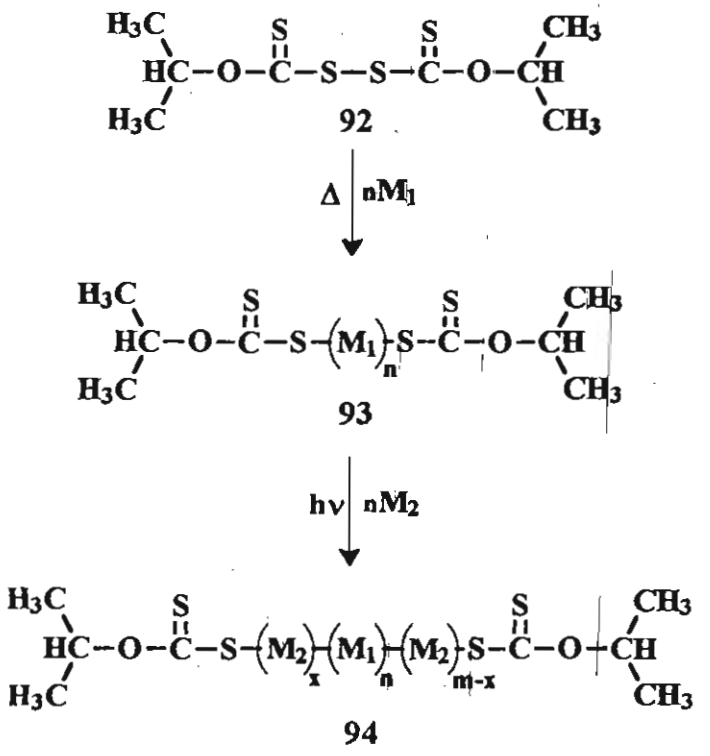

Scheme 19

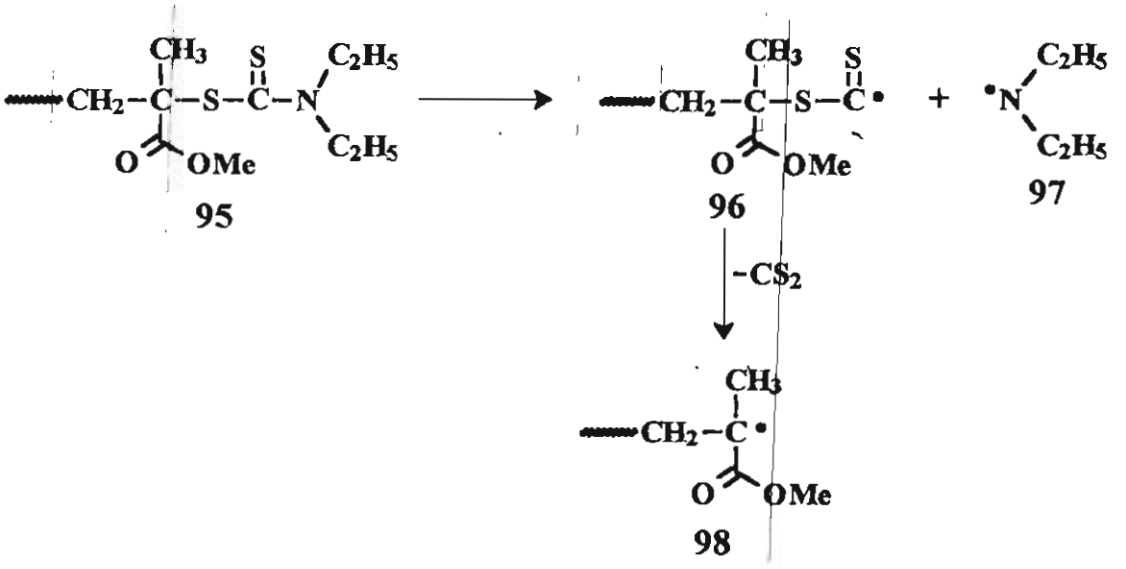

Scheme 20

Detailed studies on the photochemical and thermal block copolymerizations using tetraalkylthiuram disulfide (TD) and benzyl N,N-diethyldithiocarbamate as initiator was reported by van Kerckhoven et al..[110] According to these authors the thermal block copolymer synthesis is preferred over the photochemical method because of the low quantum yield of the photodissociation of TD. Even though the photoiniferter apporach is widely used for block copolymer synthesis, its main drawback is the broad polydispersity of the resultant block copolymers. The main reason for such broad dispersity could be due to the uncontrolled self polymerization of the monomer under the low wavelength irradiation condition employed for the iniferter method ($\leq$ 300 nm).

1.5. Conclusions

The brief review of the role of monomeric and polymeric photoinitiators presented here reveals both fundamental and technological importance of the research in this area of polymer (photo) chemistry. The recent advances in printing and coating technologies have demanded the need for designing novel polymerizable and polymeric photoinitiators. Synthesis of polymerizable monomers carrying photosensitive chromophore that can undergo homolytic bond scission to form reactive radical centers have great significance in the designing of polymeric photoinitiators and photocrosslinkable copolymers. Similarly, designing of photoinitiators for controlled synthesis of macromolecular architectures particularly for the synthesis of graft and block copolymers with narrow polydispersity and minimum homopolymer formation is an area, which is gaining the attention of polymer chemists.

1.6. References

1. Pappas, S. P. (Ed.) *UV Curing: Science and Technology* Vol. 2 Technology Marketing Corporation, Norwalk, CT, **1984**.
2. Roffey, C. G. *Photopolymerization of Surface Coatings*, Wiley, New York, **1982**.
3. Fouassier, J.-P *Photopolymerization Science and Technology*, Allen, N.S. (Ed)., Elsevier, London, **1989**.
4. Pappas, S.P. *Handbook of Organic Photochemistry*, Vol. II, Scaiano, J. C. (Ed)., CRC press, Inc. Boca Raton, Florida, **1989**.
5. Hageman, H. J. in *Photopolymerization and Photoimaging Science and Technology*, Allen, N. S. (Ed)., Elsevier Applied Science, London, **1989**.
6. Holman, R. *UV and EB Curing Formulations for Printing Inks, Coatings and Paints*, Sita Technology, **1984**.
7. Wentink, S. G.; Koch, S. D. (Eds.)., *UV Curing in Screen Printing for Printed Circuits and the Graphic Arts*, Technology Marketing Corp., Norwalk, CT, **1981**.
8. Thompson, L. F.; Willson, C. G.; Bowden, M. J. (Eds.)., *Introduction to Microlithography, ACS Symp. Ser. 219*, American Chemical Society, Washington, D. C. **1983**.
9. Ito, H.; Willson, C. G. *Application of photoinitiators to the design of resists for semicondutor manufacturing*, in *Polymers in Electronics*, Davidson, T. (Ed)., *ACS Symp. Ser. 242,* American Chemical Society, Washington, D. C., **1984**.
10. Monroe, B. M.; Weed, G. C. *Chem. Rev.* **1993**, *93*, 435.
11. Carlblom, L. H.; Pappas, S. P. *J. Polym. Sci. Polym. Chem. Ed.* **1977**, *15*, 1381.
12. Pappas, S. P.; Asmus, R. A. *J. Polym. Sci. Polym. Chem. Ed.* **1982**, *20*, 2643.

13. Lewis, F. D.; Lauterbach, R. T.; Heine, A.-G.; Hartmann, W.; Rudolph, H. *J. Am. Chem. Soc.* **1975**, *97*, 1519.
14. Pappas, S. P.; Chattopadhyay, A. K. *J. Am. Chem. Soc.* **1973**, *95*, 6484.
15. Delzenne, G. A.; Laridon, U.; Peeters, H. *Eur. Polym. J.* **1970**, *6*, 933.
16. Hong, S. L.; Kurasaki, T.; Okawara, M. *J. Polym. Sci. Polym. Chem. Ed.* **1974**, *12*, 2553.
17. Mc Ginniss, V. D. *J. Radiat. Curing* **1975**, *2*, 3.
18. Jacobi, M.; Henne, A. *J. Radiat. Curing* **1983**, *10*, 16.
19. Sumiyoshi, T.; Schnabel, W.; Henne, A.; Lechtken, P. *Polymer* **1985**, *26*, 141.
20. Sumiyoshi, T.; Schnabel, W. *Makromol. Chem.* **1985**, *186*, 1811.
21. Kuhlmann, R.; Schnabel, W. *Polymer* **1976**, *17*, 419.
22. Sengupta, P. K.; Modak, S. K. *Makromol. Chem.* **1985**, *186*, 1593.
23. Mc Gimpsey, W. G.; Scaiano, J. C. *J. Am. Chem. Soc.* **1987**, *109*, 2179.
24. Ledwith, A.; Nadalio, G.; Taylor, A. R. *Macromolecules* **1975**, *8*, 1.
25. Amirzadeh, G.; Schnabel, W. *Makromol. Chem.* **1981**, *182*, 2821.
26. Allen, N. S.; Catalina, F.; Green, P. N.; Green, W. A. *Eur. Polym. J.* **1986**, *22*, 793.
27. Wamser, C. C.; Hammond, G. S.; Chang, C. T.; Baylor, C. Jr. *J. Am. Chem. Soc.* **1970**, *92*, 6362.
28. Inaki, Y.; Takahashi, M.; Kameo, Y.; Takemoto, K. *J. Polym. Sci., A1* **1978**, *16*, 399.
29. Specht, D. P.; Martic, P. A.; Farid, S. *Tetrahedron* **1982**, *38*, 1203.
30. Williams, J. L. R.; Specht, D. P.; Farid, S. *Polym. Eng. Sci.* **1983**, *23*, 1022.
31. Kinstle, J. F.; Watson, S. L. Jr. *J. Radiat. Curing* **1975**, *2*, 7.
32. Huchison, J.; Lambert, M. C.; Ledwith, A. *Polymer* **1973**, *14*, 250.
33. Martens, J.; Praefcke, K. *Chem. Ber.* **1974**, *107*, 2319.

34. Ogata, Y.; Tagaki, K.; Takayanagi, Y. *J. Chem. Soc. Perkin Trans. 2* **1973,** 1244.

35. Bak, C.; Praefcke, K.; Muszkat, K. A.; Weinstein, M. *Naturforsch* **1977,** *326*, 674.

36. Schönberg, A.; Fateen, A. K.; Omran, S. M. A. R. *J. Am. Chem. Soc.* **1956,** *78*, 1224.

37. Tsunooka, M.; Tanaka, S.; Tanaka, M. *Makromol. Chem. Rapid Commun.* **1983**, *4*, 539.

38. Tsuda, K.; Otsu, T. *Bull. Chem. Soc. Japan* **1966**, *39*, 2206.

39. Tsuda, K.; Kosegaki, K. *Makromol. Chem.* **1972**, *161*, 267.

40. Fcrington, T. E.; Tobolsky, A.V. *J. Am. Chem. Soc.* **1955,** 77, 4510.

41. Otsu, T. *J. Polym. Sci.* **1956**, 21, 559.

42. Otsu, T.; Nayatani, K.; Muto, I.; Imai, M. *Makromol. Chem.* **1958,** *27*, 142.

43. Otsu, T.; Nayatani, K. *Makromol. Chem.* **1958,** *27*, 149.

44. Otsu, T. *J. Polym. Sci.* **1957**, *26*, 236.

45. Barton, A. F.; Bevington, J. C. *Makromol. Chem.* **1963,** *68*, 216.

46. Barton, A. F.; Bevington, *J. C. Trans. Faraday Soc.* **1966**, *62*, 433.

47. Otsu, T.; Yoshida, M. *Makromol. Chem., Rapid Commun.* **1982,** *3*, 127.

48. Otsu, T.; Yoshida, M.; Tanaki, T. *Makromol. Chem., Rapid Commun.* **1982,** *3*, 133.

49. Otsu, T.; Yoshida, M.; Kuriyama, A. *Polym. Bull.* **1982**, *7*, 45.

50. Otsu, T.; Matsunaga, T.; Kuriyama, A.; Yoshioka, M. *Eur. Polym. J.* **1989,** *25*, 643.

51. Ajayaghosh, A.; Das, S.; George, M. V. *J. Polym. Sci. A. Polym. Chem.* **1993**, *31*, 653.

52. Weir, D.; Ajayaghosh, A.; Muneer, M.; George, M. V. *J. Photochem. Photobiol. A: Chem.* **1990**, *52*, 425.

53. Muneer, M.; Ajayaghosh, A.; Das, S.; George, M. V. *J. Photochem. Photobiol. A: Chem.* **1995**, *86*, 155.

54. Smets, G.; Doi, T. *New Trends in Photochemistry of Polymers*, Allen. N. S.; Rabek, J. F. Eds., Elsevier Applied Science Publishers, London, **1985**.

55. Arthur, Jr. J. C. *Developments in Polymer Photochemistry 2*, Allen, N. S. Ed., Applied Science Publishers, London, **1985**.

56. Fouassier, J. P. *Graft Copolymerization of Lignocellulosic Fibers*, David, N.; Hohn, S. Eds., *ACS Symp. Ser. 187*, American Chemical Society, New York, **1982**.

57. Yagei, Y.; Schnabel, W. *Prog. Polym. Sci.* **1990**, *15*, 551.

58. Davidson, R. S. *J. Photochem. Photobiol. A: Chem.* **1993**, *69*, 263.

59. Gupta, S. N.; Thijs, L.; Neckers, D. C. *J. Polym. Sci., Polym. Chem. Ed.* **1981**, *19*, 855.

60. Gupta, I.; Gupta, S. N.; Neckers, D. C. *J. Polym. Sci., Polym. Chem. Ed.* **1982**, *20*, 147.

61. Ahn, K. D.; Ihn, C. J.; Kwon, I. C. *J. Macromol. Sci. Chem. A*, **1986**, *23*, 355.

62. Ahn, K. D.; Kwon, I. C.; Choi, H. S. *J. Photopolym. Sci. Technol.* **1990**, *3*, 137.

63. Davidson, R. S.; Hageman, H. J.; Lewis, S. *Radtech. Europe '91*, Conf. Proc., Radtech, Fribourg, **1991**, 691.

64. Angiolini, L.; Carlini, C. *Chem. Ind.* (Milan), **1990**, *72*, 124.

65. Angiolini, L.; Carlini, C.; Tramontini, M.; Altomare, A. *Polymer* **1990**, *31*, 212.

66. Kurusu, Y.; Nishiyama, H.; Okawara, M. *J. Chem. Soc. Jap. Ind. Chem. Sec.* **1967**, *70*, 593.

67. Rudolph, H.; Rosenkranz, H. J.; Heine, H. G. *Appl. Polym. Symp.* **1975**, *26*, 157.

68. Klos, R.; Gruber, H.; Greber, G. *J. Macromol. Sci. Chem. A.* **1991**, *28*, 925.

69. Fouassier, J. P.; Lougnot, D. J.; Li Bassi, G.; Nicora, C. *Polymer* **1989**, *30*, 245.

70. Fouassier, J. P.; Ruhlmann, D.; Zahouily, K.; Angiolini, L.; Carlini, C.; Lelli, N. *Polymer* **1992**, *33*, 3569.

71. Okawara, M.; Yamashita, N.; Ishiyama, K.; Imoto, E. *Kogyo Kagaku Zasshi* **1963**, *66*, 1383.

72. Okawara, M.; Morishita, K.; Imoto, E. *Kogyo Kagaku Zasshi* **1966**, *69*, 761.

73. Inoue, H.; Kohama, S. *J. Appl. Polym. Sci.* **1984**, *29*, 877.

74. Nishizawa, E. E.; Wynalda, D. J.; Lednicer, D. *Trans. Am. Soc. Artif. Int. Organs*, XIX, **1973**, 13.

75. Miyama, H.; Sato, T. *J. Polym. Sci. A-1*, **1972**, *10*, 2469.

76. Otsu, T.; Yamashita, K.; Tsuda, K. *Macromolecules* **1986**, *19*, 287.

77. Nakayama, Y.; Matsuda, T. *Macromolecules* **1996**, *29*, 8622.

78. Kinstle, J. F.; Watson, S. L. Jr. *J. Radiat. Curing* **1975**, *2*, 7.

79. Carlini, C. *Br. Polym. J.* **1986**, *18*, 236.

80. Carlini, C.; Ciardelli, F.; Donati, C.; Gurzoni, F. *Polymer* **1983**, *24*, 599.

81. Carlini, C.; Toniolo, L.; Rolla, P. A.; Barigelletti, F.; Bortolus, P.; Flamigni, *New Polym. Mater.* **1987**, *1*, 63.

82. Flamigni, L.; Barigelletti, F.; Bortolus, P.; Carlini, C. *Eur. Polym. J.* **1984**, *20*, 171.

83. Mateo, J. L.; Manzarbeita, J. A. *J. Photochem. Photobiol. A: Chem.* **1987**, *40*, 169.

84. Catalina, F.; Peinado, C.; Sastre, R.; Mateo, J. L.; Allen, N. S. *J. Photochem. Photobiol. A: Chem.* **1989**, *47*, 365.

85. Catalina, F.; Peinado, C.; Madruga, E. L.; Sastre, R.; Mateo, J. L. *J. Polym. Sci. A: Polym. Chem.* **1990**, *28*, 967.

86. Allen, N. S.; Peinado, C.; Lam, E.; Kotecha, J. L.; Catalina, F.; Navarathnam, S.; Parsons, B. J. *Eur. Polym. J.* **1990**, *26*, 1237.

87. Bamford, C. H. *New Trends in the Photochemistry of Polymers*, Allen, N. S.; Rabek, J. F. Eds., Elsevier Applied Science Publishers, London, **1985**.

88. Burrows, H. D.; Eliseu, P. J. S. C.; Gil, M. H.; Freire, R. M. S. *J. Photochem. Photobiol. A: Chem.* **1991**, *59*, 81.

89. Smets, G. J.; Doi, T. *New Trends in the Photochemistry of Polymers*, Allen, N. S.; Rabek, J. F. Eds., Elsevier Applied Science Publishers, London, **1986**.

90. Yagchi, Y.; Schnabel, W. *Prog. Polym. Sci.* **1990**, *15*, 551.

91. Lanza, E.; Bergmans, H.; Smets, G. *Polym. Sci. Polym. Phys. Ed.* **1973**, *11*, 95.

92. Smets, G. *Polym. J.* **1985**, *17*, 153.

93. Doi, T.; Smets, G. *Macromolecules* **1989**, *22*, 25.

94. Craubner, H. *J. Polym. Sci. Polym. Chem. Ed.* **1980**, *18*, 2011.

95. Vlasov, G. P.; Rudkovskaya, G. D.; Ovsyannikova, L. A. *Makromol. Chem.* **1982**, *183*, 2635.

96. Mezger, T.; Cantow, H. J. *Makromol. Chem. Rapid Commun.* **1983**, *4*, 313.

97. Mezger, T.; Cantow, H. J. *Angew. Makromol. Chem.* **1983**, *116*, 13.

98. Bamford, C. H.; Mullick, S. U. *J. Chem. Soc. Faraday I*, **1977**, *47*, 1260.

99. Bamford, C. H.; Mullick, S. U. *J. Chem. Soc. Faraday I*, **1978**, *48*, 1634.

100. Bamford, C. H.; Han, X. Z. *Polymer* **1981**, *22*, 1299.

101. Imoto, M.; Otsu, T.; Yonezawa, *J. Makromol. Chem.* **1960**, *36*, 93.

102. Niwa, M.; Matsumoto, T. *Polym. Prep. Jpn.* **1985**, *34*, 291.

103. Niwa, M.; Matsumoto, T.; Izumi, H. *J. Macromol. Sci. Chem.* **1987**, A24, 567.

104. Otsu, T.; Kuriyama, A. *Polym. Bull.* **1984**, *11*, 135.

105. Otsu, T.; Kuriyama, A. *Polym. J.* **1985**, *17*, 97.

106. Otsu, T.; Kuriyama, A. *J. Macromol. Sci. Chem.* **1984**, A21, 961.

107. Otsu, T.; Ogawa, T.; Yamamoto, T. *Macromolecules* **1986**, *19*, 2087.

108. Turner, R. S.; Blevins, R. W. *Macromolecules* **1990**, *23*, 1856.

109. Lambrinos, P.; Tardi, M.; Polton, A.; Sigwalt, P. *Eur. Polym. J.* **1990**, *26*, 1125.

110. Van Kerckhoven, C.; den Broeck, C. V.; Smets, G.; Huybrechts, J. *Makromol. Chem.* **1991**, *192*, 101.

CHAPTER 2

SYNTHESIS, CHARACTERIZATION AND COPOLYMERIZATION BEHAVIOUR OF A FEW XANTHATE DERIVED PHOTOACTIVE MONOMERS

2.1. Introduction

Free radical induced copolymerization of various monomers is a widely accepted procedure in the designing of novel polymeric materials with specific physical and chemical properties. In this way it is even possible to prepare polymers of those monomers which are reluctant to undergo homopolymerization. Thermally induced free radical copolymerization of two or more monomers are extensively used in the preparation of polymers with improved physical properties for specific technological applications. Synthesis of copolymers bearing photosensitive pendant functional groups is an important area of research due to their wide-ranging use in microelectronics, printing and photocurable coating applications.[1-6] Synthesis of new photosensitive monomers and knowledge about their copolymerization behaviour with other monomers are therefore essential for designing copolymers with optimum performance.

Thermally induced radical copolymerization behaviour of a variety of monomers is known in the literature. Out of these, one of the most interesting system consists of maleic anhydride and styrene.[7-12] Due to the donor-acceptor interaction, the existence of a 1:1 charge-transfer complex has been established in this system which gives an alternating copolymer. Subsequently, the synthesis and copolymerization of a variety of new monomers leading to the formation of water soluble[13], thermally stable[14,15] and optically[16,17] active copolymers have been reported.

Despite the large volume of publications in the thermal copolymerization behaviour of a variety of monomers, analogous studies pertaining to monomers carrying photodissociable chromophores are very few. Typical examples of this kind represent monomers such as **1** and **2** containing photodissociable benzoin ethers[18-20] and substituted perester group **3**.[21,22] Copolymerization of these monomers with other acrylic and vinylic monomers provides copolymers carrying pendant photoinitiator moieties. These copolymers can be used as polymeric photoinitiators for the preparation of photoinduced graft copolymers. A major problem of using these copolymers for graft copolymer synthesis is the formation of homopolymers. This problem can be solved to a great extent using a vinyl monomer **4** containing a photoactive dithiocarbamate group.[23] Copolymerization of **4** with other monomers provides photosensitive copolymers which can be used for graft and block copolymer synthesis. Apart from that copolymers of the monomer **4** can be used as negative photoresist materials.[24]

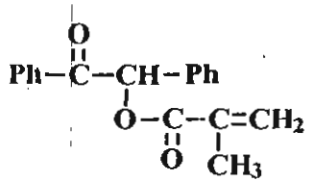

1

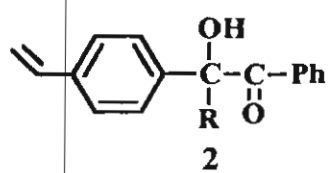

2

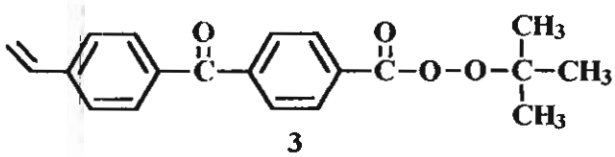

3

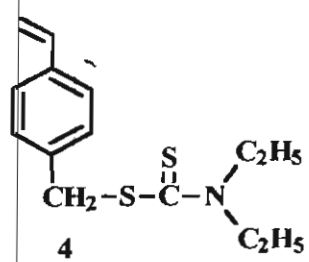

4

Chart 1

Acyl and aroyl xanthates are known to undergo homolytic bond scission on photolysis.[25,26] This photoreaction has already been used in the designing of photoinitiators.[27] Polymeric photoinitiators having pendant xanthate chromophore are known to show better efficiency for the photopolymerization

of acrylic monomers.[28,29] In addition, polymers containing xanthate group have added significance due to their affinity to form metal ion complexes. Because of the possibility of wide ranging application of polymers bearing pendant xanthate chromophore, synthesis of copolymers with appropriate xanthate compositions is important from both practical and theoretical points of view. In the present study, the synthesis, characterization and copolymerization behaviour of a few monomers containing photoactive xanthate chromophore is described.[30]

2.2. Results and Discussion

2.2.1. Preparation of monomers

The sulfur-containing monomers S-acryloyl O-ethyl xanthate (AX, **6**) and S-methacryloyl O-ethyl xanthate (MAX, **7**) were prepared by the reaction of the corresponding acid chlorides with potassium O-ethyl xanthate as per Scheme 1. AX was formed in a very low yield (24%). The major product obtained in this case was a solid, melting at 69-70 °C which is identified as S-(3-hydroxypropionyl) O-ethyl xanthate **8**. The infrared spectrum of **8** showed a characteristic absorption due to a strongly hydrogen bonded OH group at 3400-2800 cm^{-1}. The ^1H NMR spectrum showed the presence of highly deshielded proton at δ 11.3, which could be assigned to an intramolecularly hydrogen bonded proton (Figure 1). The ^{13}C NMR spectrum of **8** was in agreement with the proposed structure (Figure 2). The mass spectrum of **8** showed the molecular ion peak at 194, in agreement with the assigned structure. It is inferred that **8** is formed from **6** and its formation can be understood in terms of the Michael type addition of water to **6**, during work-up (room temperature) as shown in Scheme 1. However, under identical work-up conditions we could not obtain the water added product of **7**, probably because MAX is a weak Michael acceptor. The ^1H NMR spectrum of MAX showed the expected peaks at δ 6.5-5.9 as a multiplet corresponding to the methacrylic protons, a quartet at δ 4.7 corresponding to the OCH_2 protons and a singlet and

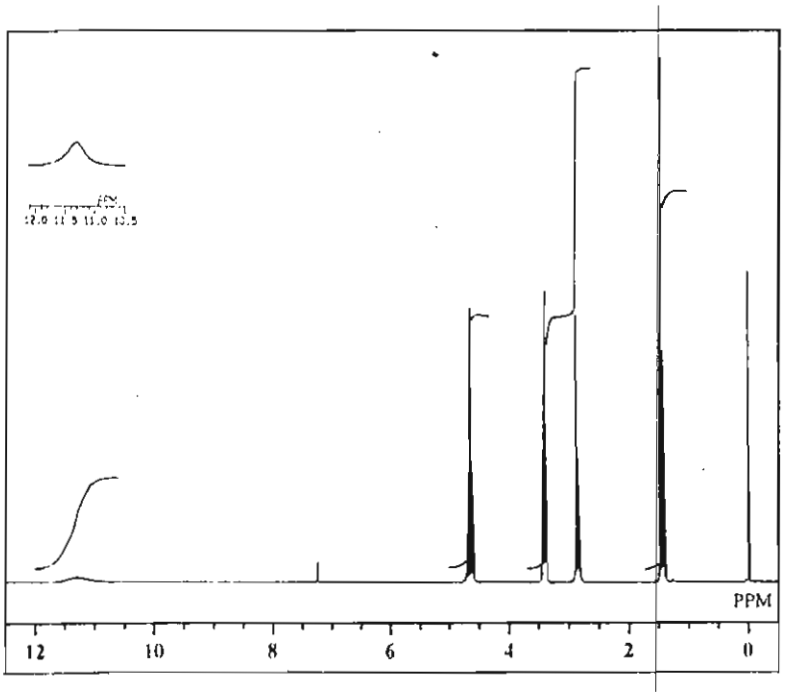

Figure 1. ^{1}H NMR spectrum of **8**

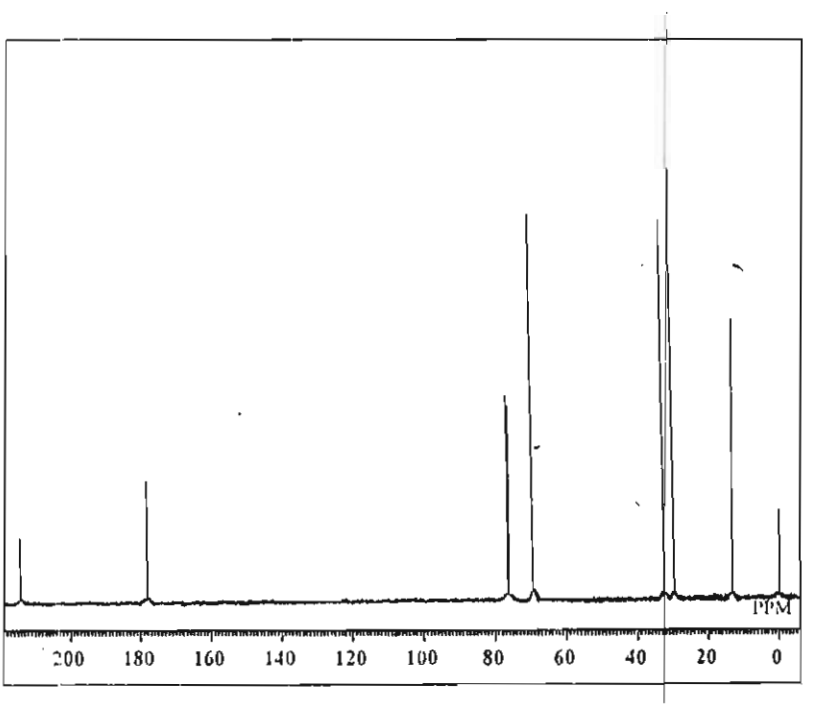

Figure 2. ^{13}C NMR spectrum of **8**

a triplet around δ 2.0 and 1.45 respectively, corresponding to the two methyl groups (Figure 3). The ^{13}C NMR spectrum showed seven carbon signals at δ 204, 186, 144, 126, 71, 18 and 14 in accordance with its structure (Figure 4). The mass spectrum of **8** showed a molecular ion peak at 191 (M^++1).

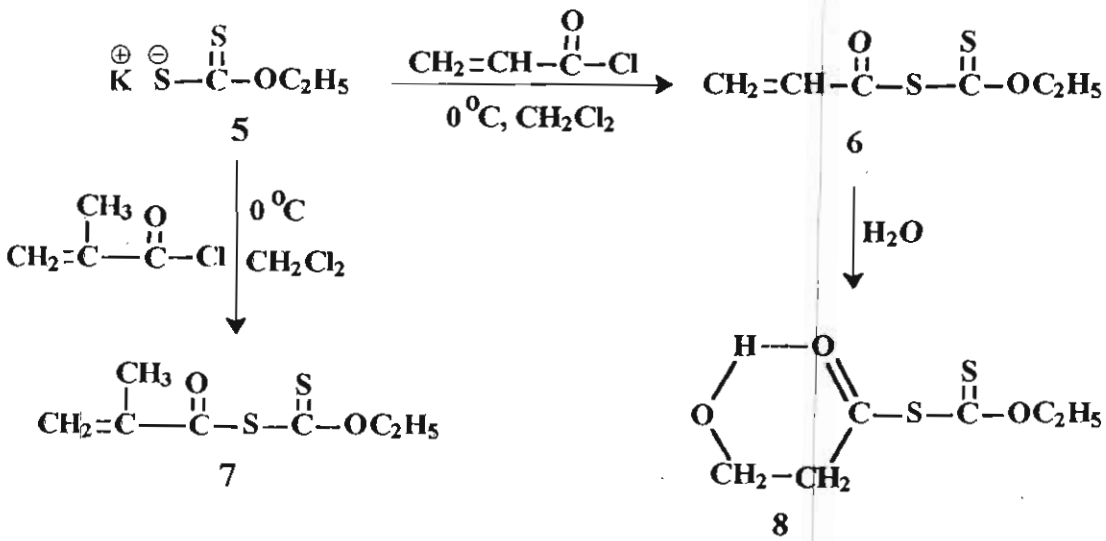

Scheme 1

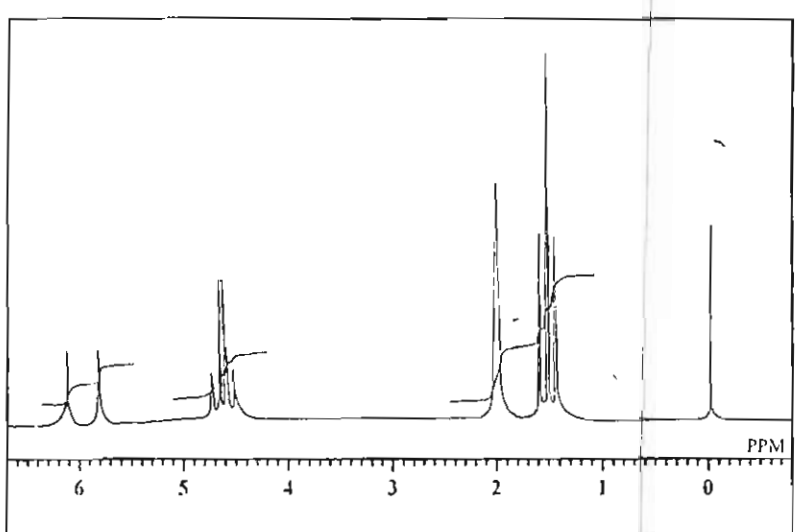

Figure 3. 1H NMR spectrum of 7

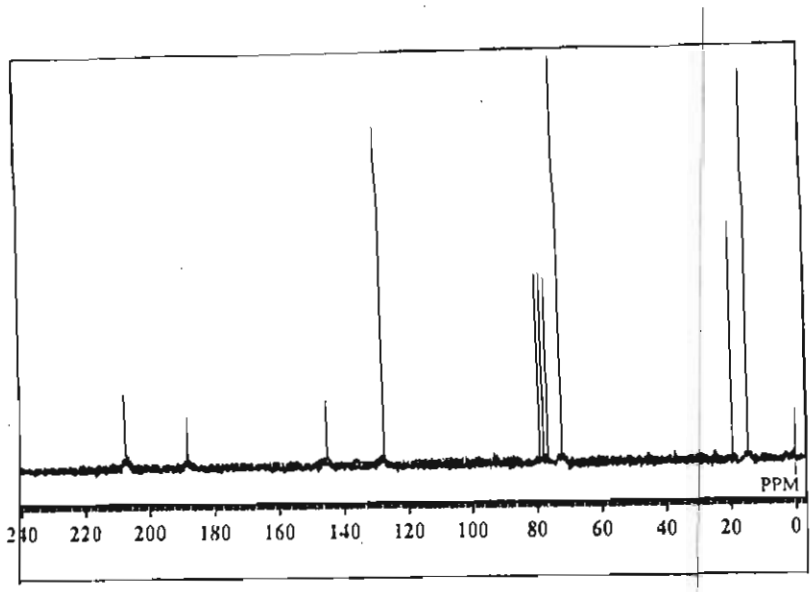

Figure 4. ^{13}C NMR spectrum of **7**

S-(4-Maleimidobenzoyl O-ethyl xanthate (MBX, **13**) was prepared as per Scheme 2. 4-Maleimidobenzoic acid obtained by the reaction of maleic anhydride and 4-aminobenzoic acid was converted to the corresponding acid chloride **12**, which on subsequent reaction with potassium O-ethyl xanthate *afforded MBX in 90% yield. The ^{1}H NMR spectrum of MBX (Figure 5)* showed a multiplet at δ 8-7.6 corresponding to the four aromatic protons. The two protons of the double bond appeared as a singlet at δ 6.9. The O-ethyl group showed a quartet and triplet at δ 4.7 and δ 1.5 respectively. The ^{13}C NMR spectrum of **13** (Figure 6) showed signals at δ 184.2, 168.6 and 125 corresponding to the carbonyl carbons and the unsaturated carbons of the maleimido group. Similarly, the signals at δ 136, 134, 128, 126 could be assigned to the aromatic carbon atoms. High resolution mass spectrometry showed the exact mass of **13** as 322.0202 corresponding to the assigned structure of MBX.

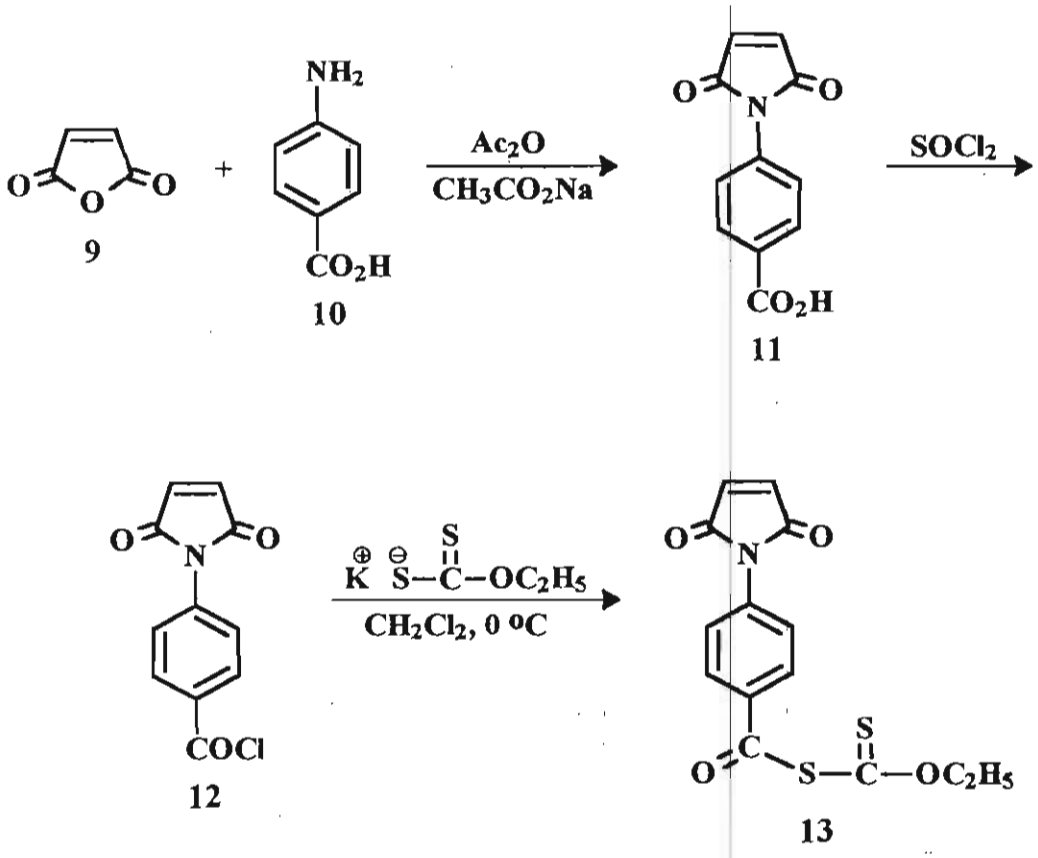

Scheme 2

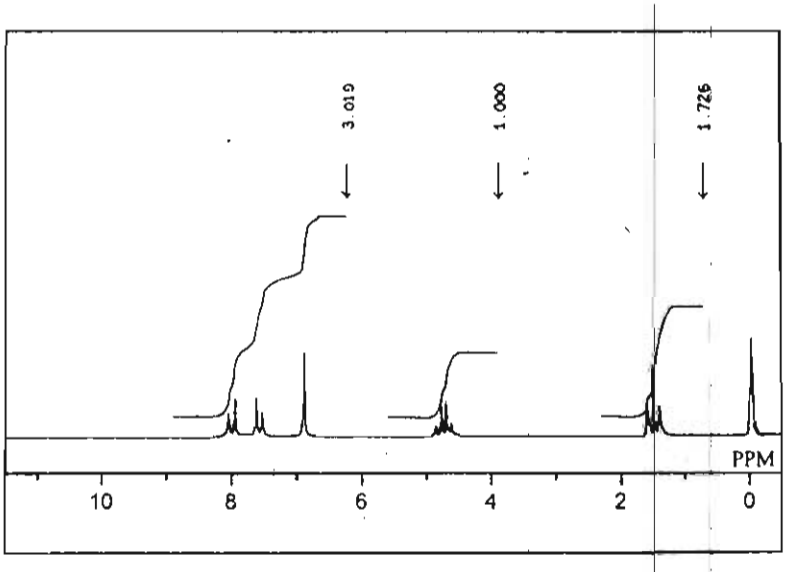

Figure 5 . ^{1}H NMR spectrum of **13**

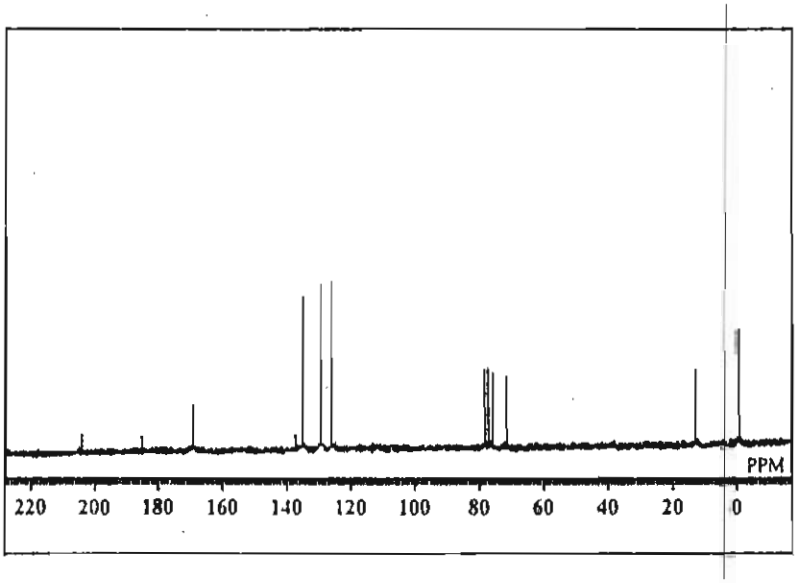

Figure 6. ^{13}C NMR spectrum of **13**

S-(4-Vinylbenzoyl) O-ethyl xanthate (VBX, **19**) was synthesized as shown in Scheme 3. Reaction of *p*-toluic acid with N-bromosuccinimide in boiling CCl_4 afforded the 4-bromomethylbenzoic acid **15**, which is converted, to 4-vinylbenzoic acid **17**, by Wittig reaction. Reaction of the acid chloride **18** with potassium O-ethyl xanthate gave VBX in 95% yield. The ^1H NMR spectrum of VBX (Figure 7) showed a multiplet around δ 7.8-7.4 corresponding to the four aromatic protons. A multiplet at δ 6.7 and two doublets at δ 5.4 and δ 5.9 were assigned to the three vinylic protons. The O-ethyl protons appeared as a quartet and triplet at δ 4.8 and δ 1.4, respectively. The ^{13}C NMR spectrum of VBX was in agreement with its structure (Figure 8). The exact molecular mass was found to be 253.0357 by high-resolution mass spectrometry, in agreement with the assigned structure.

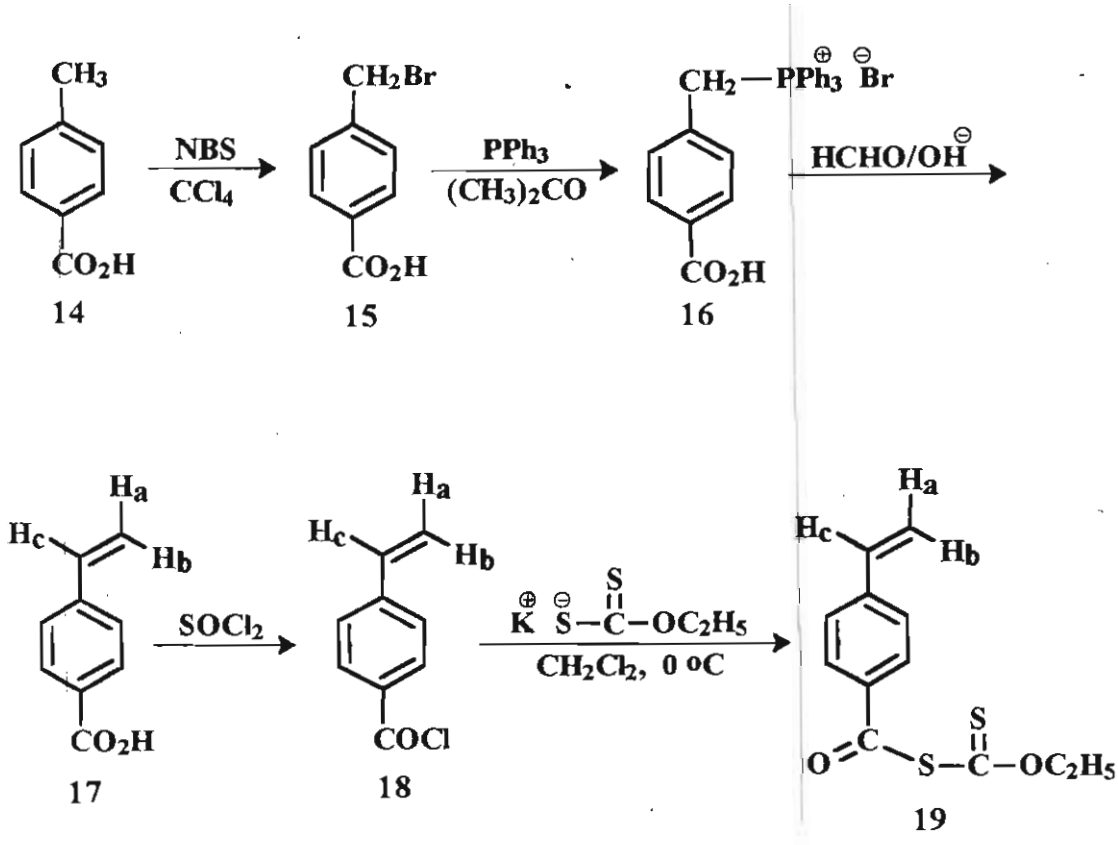

Scheme 3

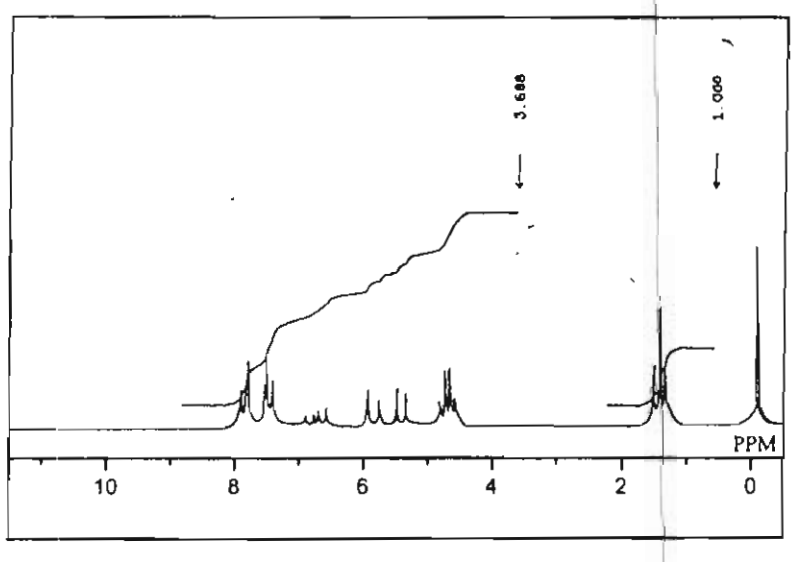

Figure 7. ^{1}H NMR spectrum of **19**

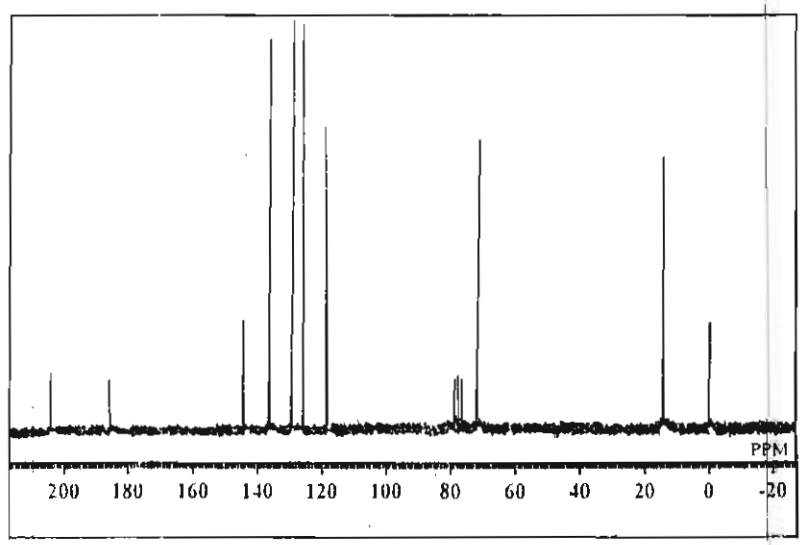

Figure 8. ^{13}C NMR spectrum of **19**

2.2.2. Copolymerization of MAX with MMA and styrene (St)

Copolymers of MAX with MMA and St were prepared according to Scheme 4. All copolymerizations of MAX were carried out in toluene using AIBN as initiator, which gave pale yellow polymers. All copolymers were characterized by their spectral analysis. The ^{1}H NMR spectra of two representative copolymers, MAX-co-MMA and MAX-co-St are shown in Figures 9 and 10, respectively. Attempts to prepare a homopolymer of MAX were not successful probably due to the strong chain transfer termination, immediately after the initiation of polymerization (Scheme 5). This leads to the formation of a mixture of extremely low molecular weight oligomers, which is confirmed from the GPC analysis of the reaction mixture. Results of the copolymerization of MAX with MMA and St in toluene using AIBN at 60 °C are shown in Tables 1 and 2, respectively. In all the cases the conversion of the monomers was kept below 20% for the purpose of evaluating the copolymerization parameters.

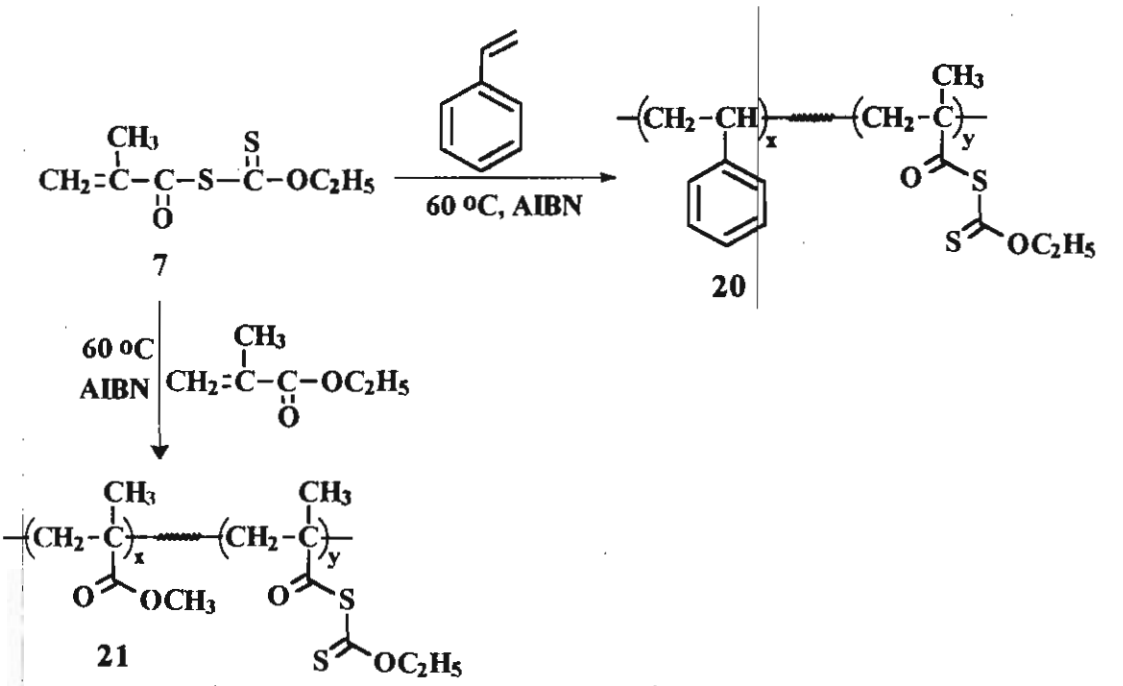

Scheme 4

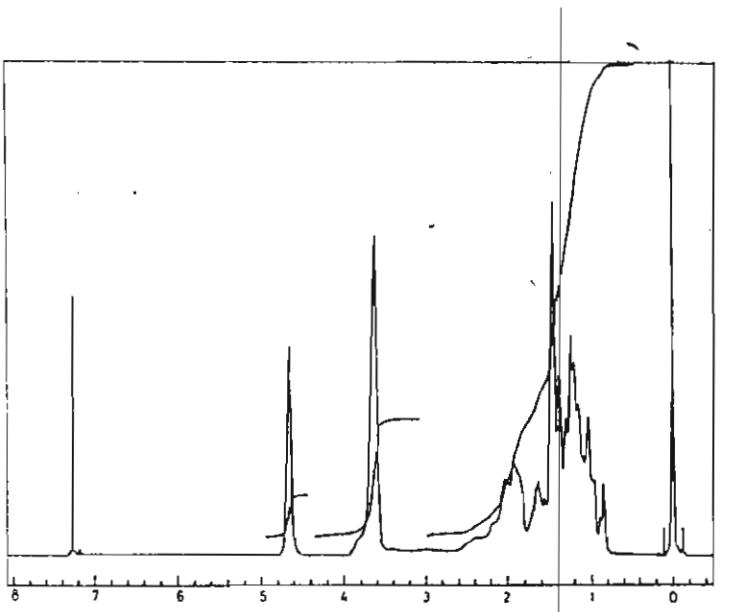

Figure 9. ^{1}H NMR spectrum of MAX-co-MMA

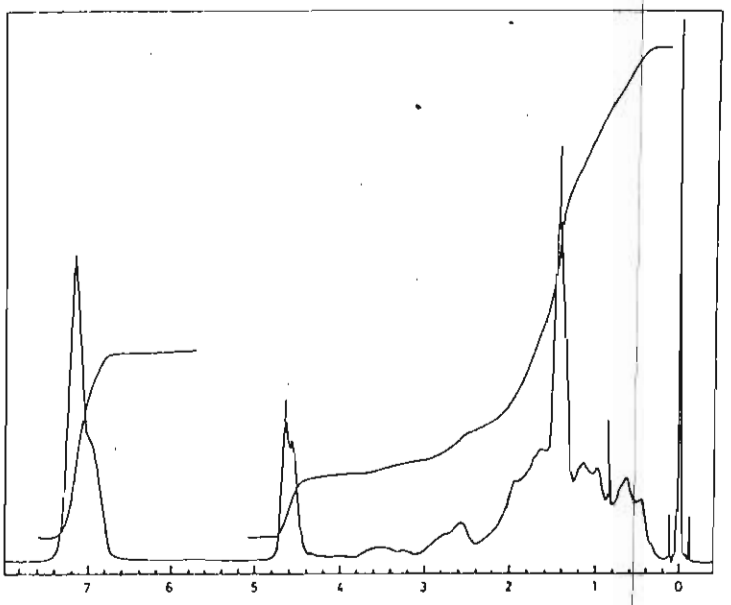

Figure 10. ^{1}H NMR spectrum of MAX-co-St

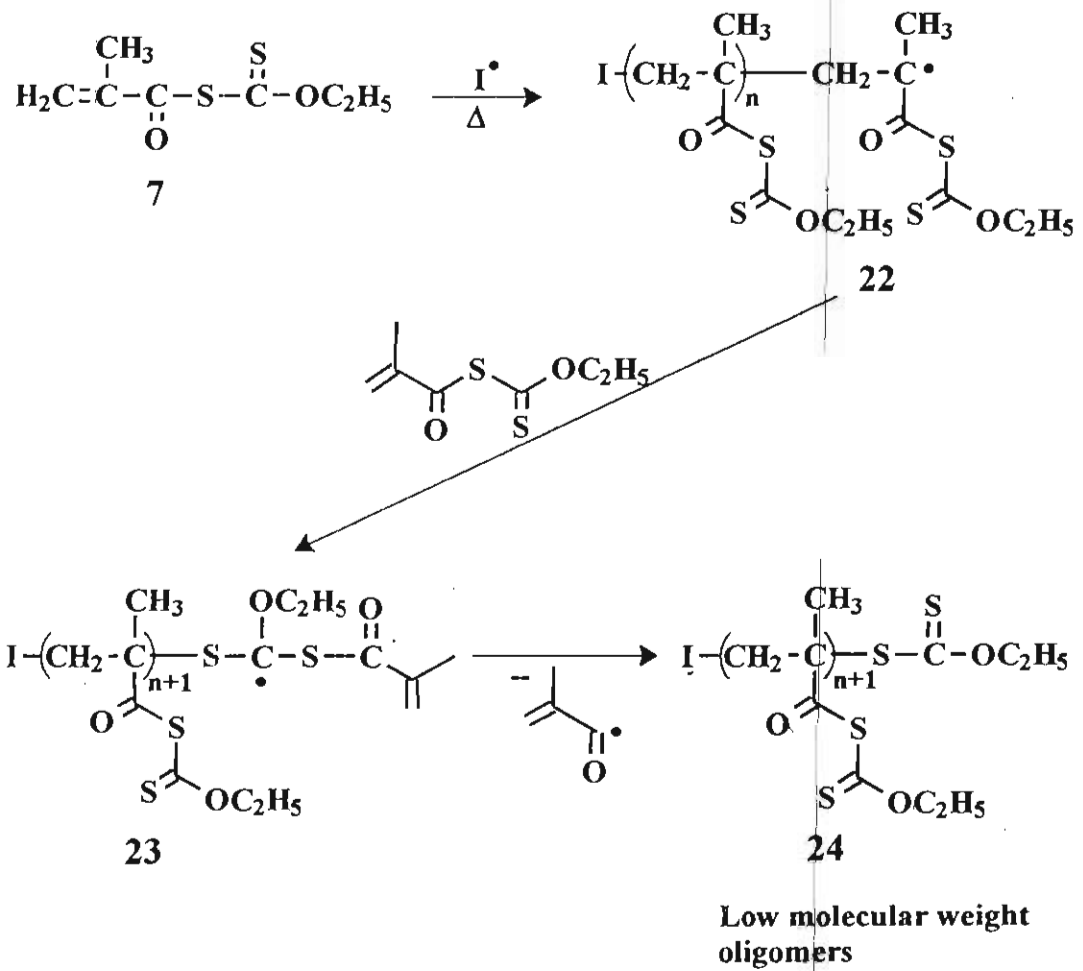

Scheme 5

As shown in Tables 1 and 2 the percentage yields of isolated copolymers, rate of polymerization and molecular weights of all copolymers decreased with increase in the mole percentage of MAX in the monomer feed. The yields and molecular weights of copolymers above 70 mol percentage of MAX in the monomer feed were extremely low. This observation indicates that MAX has a retardation effect during copolymerization. This could be explained on the basis of the chain transfer reaction between the growing polymer radicals with MAX as shown in Scheme 6. The probable mechanism of chain transfer can be explained on the basis of the addition of MAX to the growing polymer radical **25** to form a new carbon centered polymer radical **26**. This radical on fragmentation gives the xanthate terminated copolymer **27** and the methacryloyl radical **28**. This reaction becomes more predominant when the mole fraction of MAX in the feed composition becomes high. The drastic reduction in the rate of polymerization with increase in the mole fraction of MAX further reveals that the double bond in MAX is not reactive as in other acrylic monomers.

Table 1. Radical copolymerization* of MAX (M_1) with MMA (M_2)

M_1 in the feed (mol %)	Time (h)	Copolymer yield (%)	$R_p \times 10^6$ (gs^{-1})	M_1 in copolymer (mol %)		$M_n \times 10^{-3}$	D (M_w/M_n)
				^{1}H NMR	S Anal		
10	1.5	13	27.0	12	14	10.5	1.8
20	2.0	7	8.6	21	20	4.4	1.7
30	6.0	13	3.9	31	31	1.9	1.5
40	10.0	17	2.7	39	37	1.4	1.3
50	12.0	10	1.6	46	45	1.2	1.3
60	15.0	8	1.0	55	54	-	-

* [AIBN] = 0.16 mol L^{-1}, $M_1 + M_2$ = 4.5 M in toluene

Table 2. Radical copolymerization* of MAX (M_1) with styrene (M_2)

M_1 in the feed (mol %)	Time (h)	Copolymer yield (%)	$R_p \times 10^6$ (gs^{-1})	M_1 in copolymer (mol %)		$M_n \times 10^{-3}$	D (M_w/M_n)
				^{1}H NMR	S Anal		
10	1.5	19	4.2	21	21	6.7	2.0
20	1.5	16	3.6	28	30	5.6	1.8
30	4.0	20	2.8	33	35	5.1	1.8
40	5.0	18	1.8	43	43	4.6	1.5
50	5.0	13	1.1	48	48	4.0	1.5
60	8.0	15	0.84	57	56	3.5	1.4

* [AIBN] = 0.16 mol L^{-1}, $M_1 + M_2 = 4.5$ M in toluene

The copolymer composition of various copolymers of MAX was calculated independently through ^{1}H NMR and elemental sulfur analyses. The NMR analyses of the MAX-MMA copolymers were carried out by comparing the integrated intensity of the resonance signal at δ 4.6 which is assigned to the O-CH_2 protons of the xanthate group with that at δ 3.6 of the O-CH_3 protons of the methacrylate group. In the case of the MAX-St copolymers the intensity of the resonance signal at δ 4.6 was compared with that of the aromatic protons at δ 7.1. Information on the copolymer compositions based on NMR analysis was in good agreement with that obtained from the elemental sulfur analysis using equation (1), where $W_{(s)}$ and m_1 represent the weight percentage of sulfur and the mole fraction of MAX in the copolymer, and M_1 and M_2 are the molecular weights of monomers, which are used for the copolymerization.

$$(s) = \frac{64.14\ m_1}{M_1 m_1 + M_2 (1-m_1)} \times 100 \qquad (1)$$

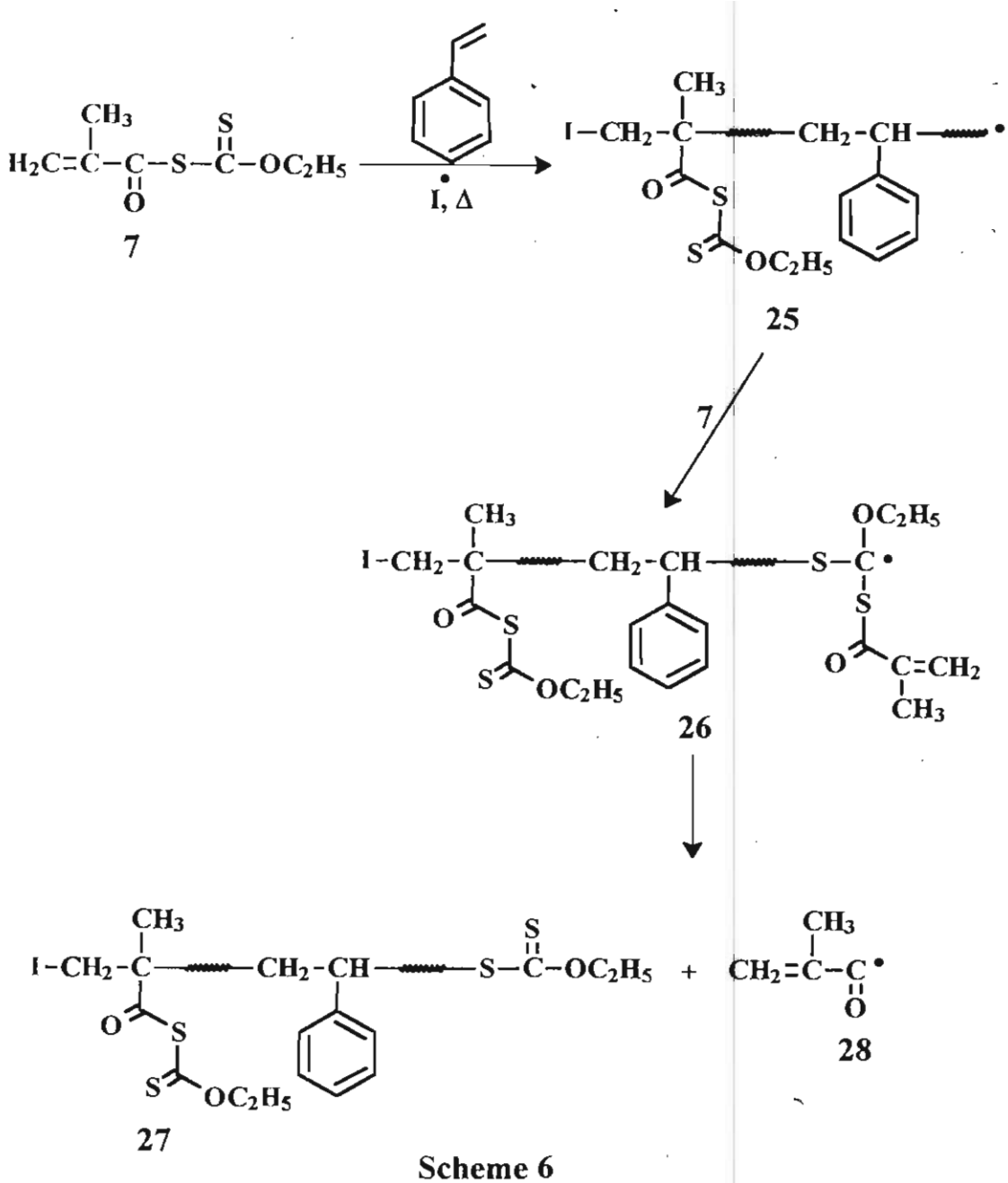

Scheme 6

In order to compare the reactivity of MAX with MMA and St, the mole fraction of MAX in each copolymer obtained by the ^{1}H NMR analysis was plotted against the mole fraction of MAX in the monomer feed. The copolymer composition curve obtained for the MAX-MMA and MAX-St monomer systems are shown in Figures 11 and 12, respectively. Figure 11 reveals that

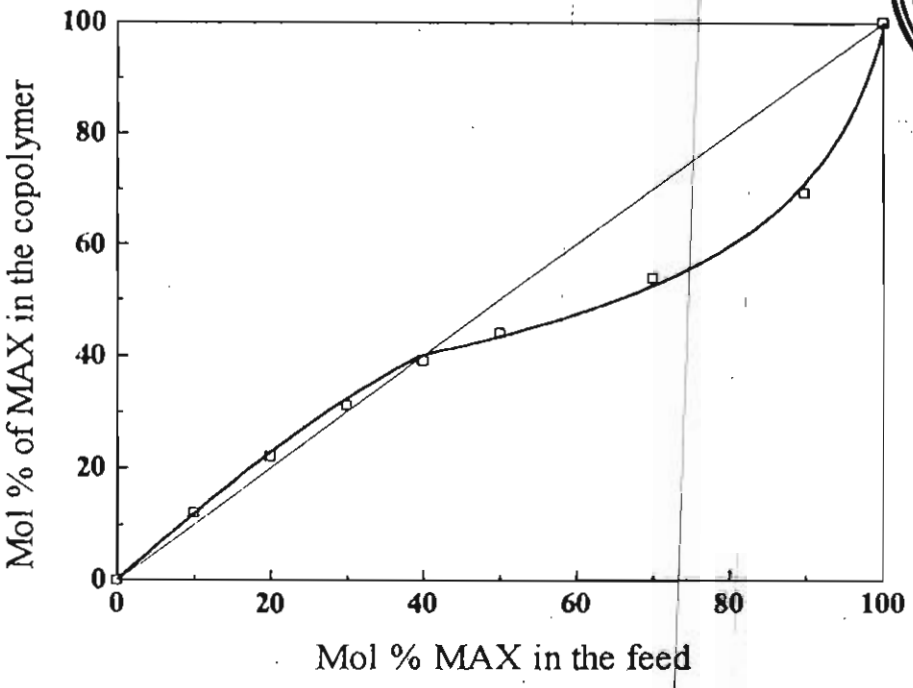

Figure 11. Copolymer composition curve for MAX-co-MMA

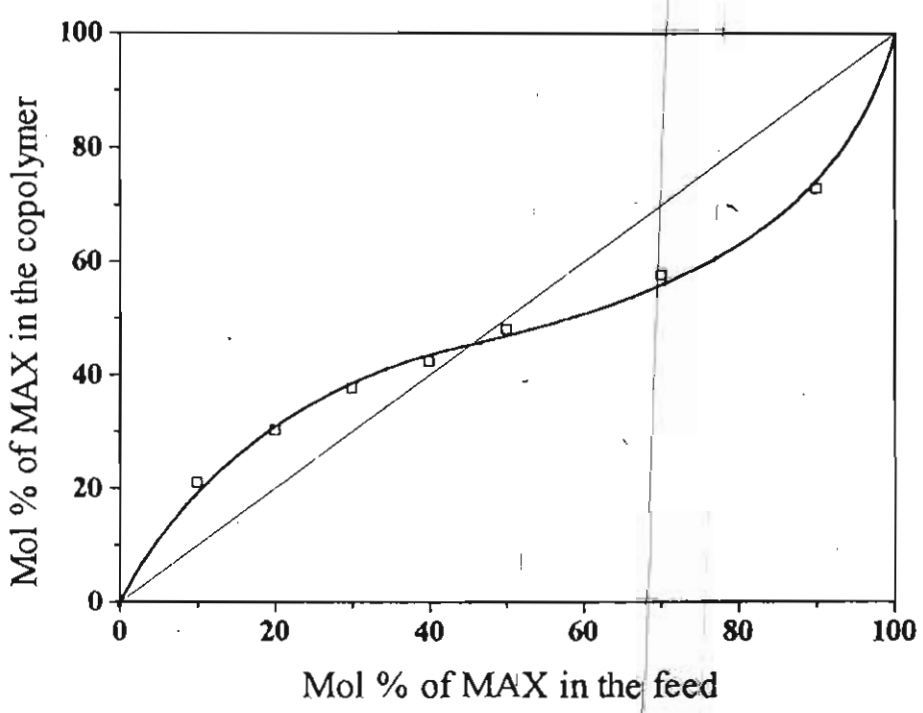

Figure 12. Copolymer composition curve for MAX-co-St

under low MAX concentration most of it is incorporated into the copolymer whereas, under higher MAX concentration its percentage incorporation is very low. This could be associated with the chain transfer reaction by excess of MAX to the copolymer radicals. On the other hand, the MAX-St monomer system showed a weak alternation tendency as shown in Figure 12. This could be due to a weak interaction between the electron deficient MAX and electron rich St that facilitates the close proximity of these monomers during their copolymerization.

2.2.3. Copolymerization of MBX with MMA and St

Attempts to prepare homopolymers of MBX using thermal free radical initiation method were not successful as in the case of MAX. Maleimides in general, are difficult to undergo homopolymerization due to the weak reactivity of their double bond towards propagation. However, they can be easily copolymerized with a variety of monomers. Maleimides are electron deficient monomers and are known to form alternate copolymers with electron rich monomers such as styrene. MBX is expected to be a more electron deficient monomer when compared to MAX and hence thermal copolymerization behaviour of MBX may be different from that of MAX. Moreover the presence of the maleimido group in MBX is expected to enhance the thermal stability of the resultant copolymers. In order to study these aspects, several copolymers of MBX with monomers such as MMA and St were prepared using AIBN as initiator (Scheme 7). The ^{1}H NMR spectra of two representative copolymers of MBX with MMA and St are shown in Figures 13 and 14, respectively. The copolymerization data for the MBX-MMA and MBX-St monomer systems are presented in Tables 3 and 4, respectively. When the copolymerizations were carried out using concentrated solutions of monomers (3M), the copolymers were formed in high yields. However, considerable gelation and crosslinking were also observed. Therefore, solutions of low monomer concentration (0.25 M in toluene) were used for copolymerization in order to prevent any

unwanted crosslinking of polymers. The increase in the mole fraction of MBX in the monomer feed is found to have significant influence on the rate of polymerization as well as the molecular weights of the resultant copolymers as

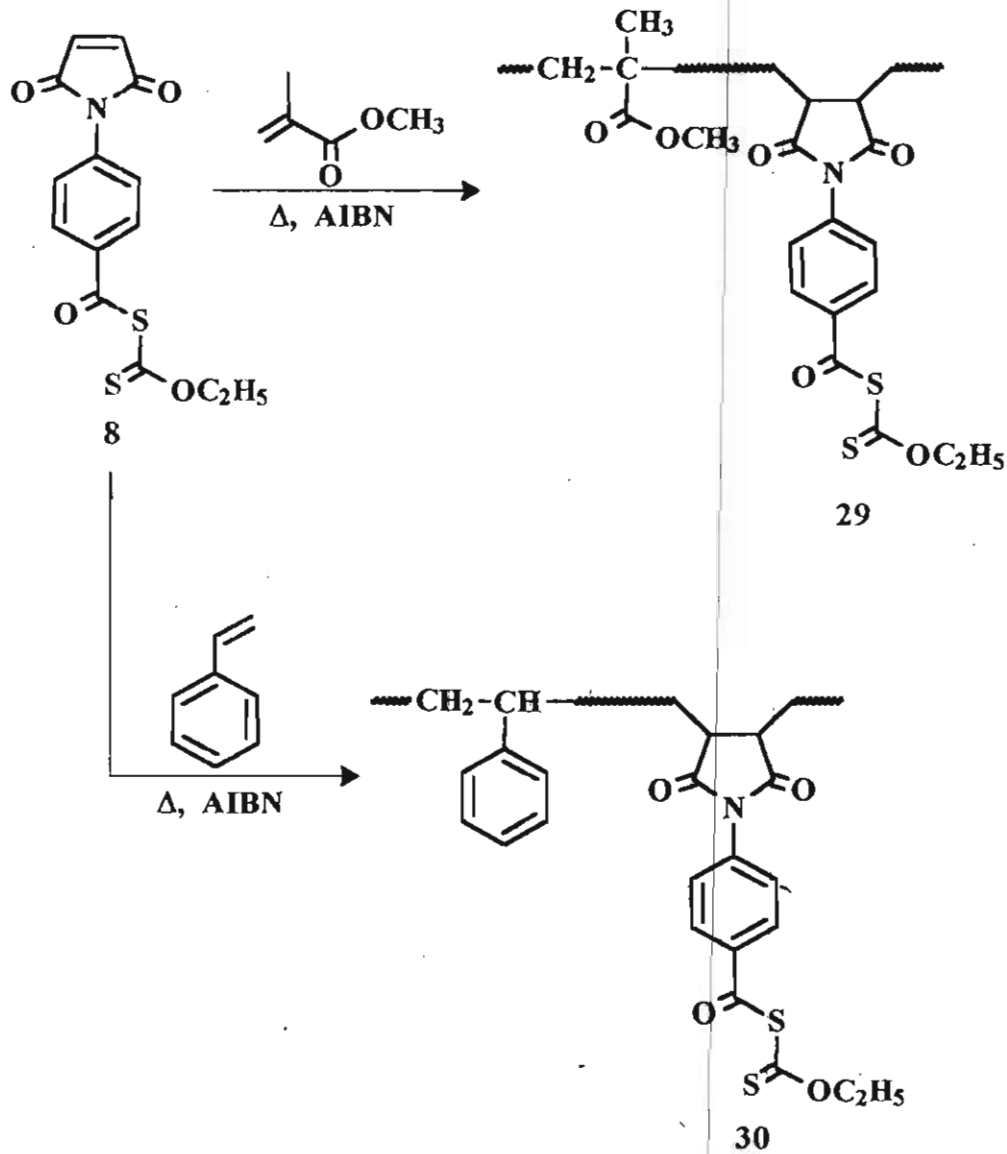

Scheme 7

noticed in the case of the MAX-MMA monomer system. The copolymer composition of all the copolymers were determined by the ^{1}H NMR method as described in the case of MAX-co-MMA copolymers. The copolymer

composition curve shown in Figure 15 indicates extremely low incorporation of MBX monomers in all monomer feed compositions. This observation reveals that, MBX is a less reactive monomer than MMA and during the propagation of the polymer chain, the polymer radicals have the tendency to preferably add onto the MMA monomer rather than the MBX monomer.

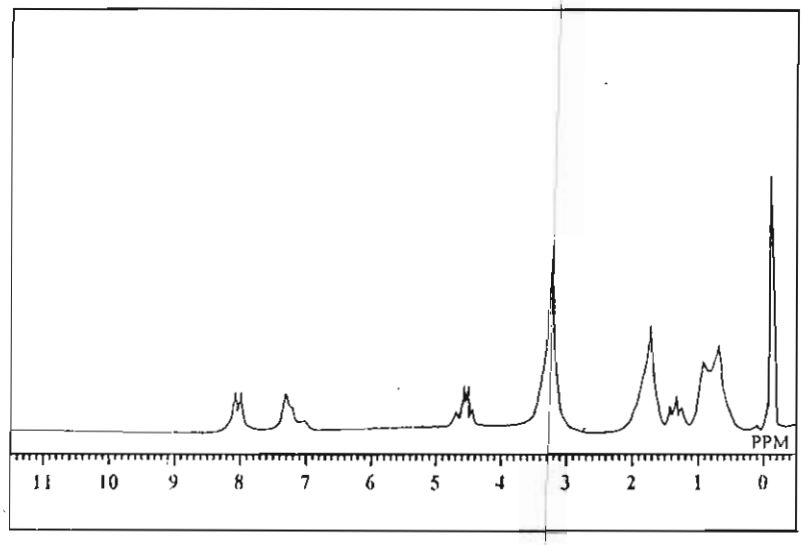

Figure 13. ^{1}H NMR spectrum of MBX-co-MMA

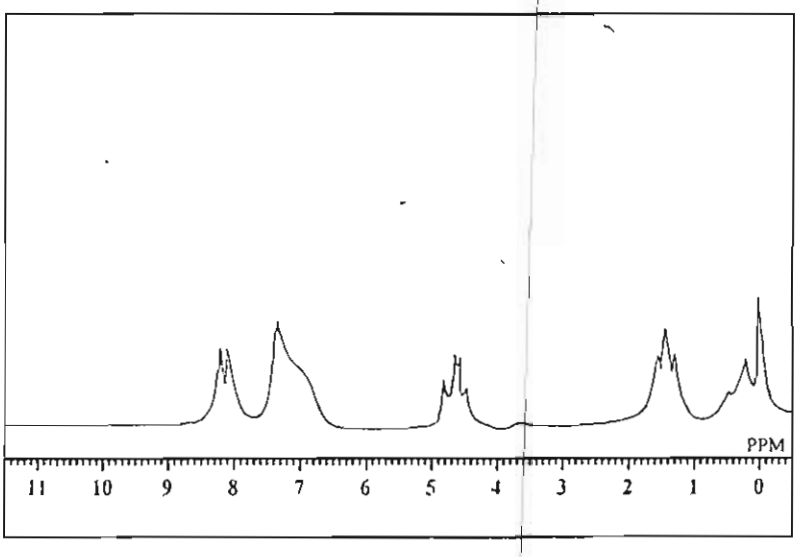

Figure 14. ^{1}H NMR spectrum of MBX-co-St

Table 3. Radical copolymerization* of MBX (M_1) with MMA (M_2)

M_1 in the feed (mol %)	Time (h)	Copolymer yield (%)	$R_p \times 10^6$ (gs^{-1})	M_1 in copolymer ^{1}H NMR (mol %)	$M_n \times 10^{-3}$	D (M_w/M_n)
10	1.0	10	8.3	3	16.0	1.2
20	2.0	12	5.9	7	14.0	1.1
30	2.0	10	5.8	11	11.0	1.1
40	3.0	13	5.6	19	10.0	1.1
50	6.0	21	5.0	25	8.0	1.2
70	12.0	19	2.7	37	6.0	1.1
80	14.0	14	1.9	45	5.0	1.1

* [AIBN] = 0.012 mol L^{-1}, M_1+M_2 = 0.25 M in toluene

The results obtained from the copolymerization of MBX with St are shown in Table 4. In this case also, increase in the MBX mole fraction has drastically reduced the rate of copolymerization as well as the molecular weights of copolymers. However, under identical conditions, the rate of copolymerization of MBX-St monomer system is higher than that of MBX–MMA monomer system. This means that the overall reactivity and hence the copolymer yields are higher.

A plot of the MBX feed composition against the copolymer composition determined by the ^{1}H NMR analysis is shown in Figure 16, which shows a reasonably good alternation tendency during copolymerization. This is presumably due to a donor-acceptor interaction between the electron deficient MBX and the electron rich St. This interaction seems to be stronger in this system when compared to that between the MAX-St monomer system indicating that MBX is more electron deficient than MAX.

Table 4. Radical copolymerization* of MBX (M_1) with styrene (M_2)

M_1 in the feed (mol %)	Time (h)	Copolymer yield (%)	$R_p \times 10^5$ (gs^{-1})	M_1 in copolymer ---------- ^1H NMR (mol %)	$M_n \times 10^{-3}$	D (M_w/M_n)
10	0.5	15	2.8	23	14.0	1.4
20	0.6	16	1.4	30	12.8	1.3
30	0.6	15	1.4	34	12.2	1.3
40	1.1	20	1.3	35	11.0	1.4
50	1.2	14	0.9	40	10.0	1.4
70	1.8	8	0.8	46	3.4	1.4
80	1.8	8	0.5	48	2.9	1.4

*[AIBN]=0.012 mol L^{-1}, M_1+M_2=0.25 M in toluene

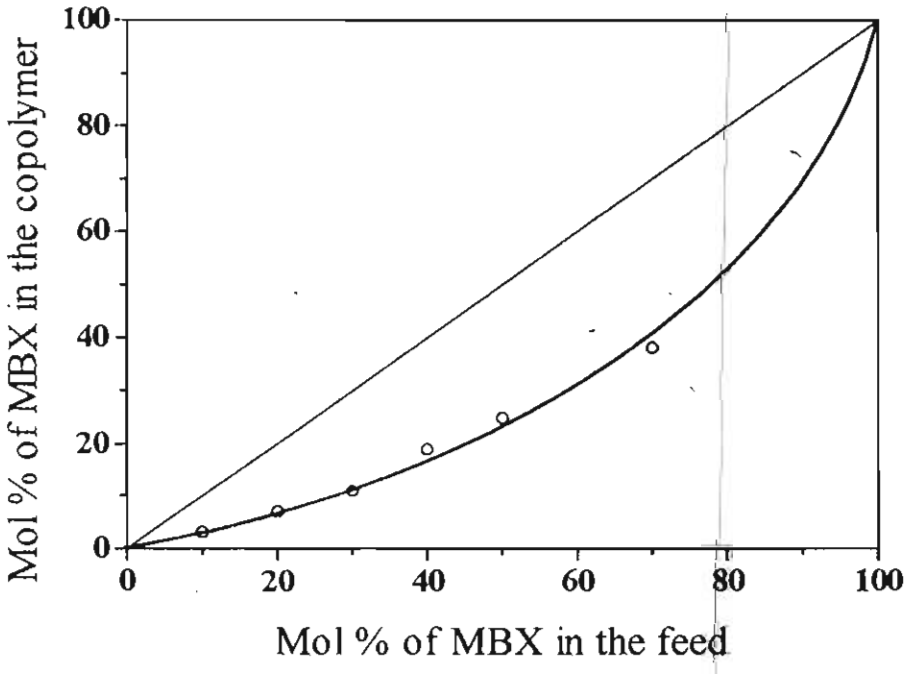

Figure 15. Copolymer composition curve for MBX-co-MMA

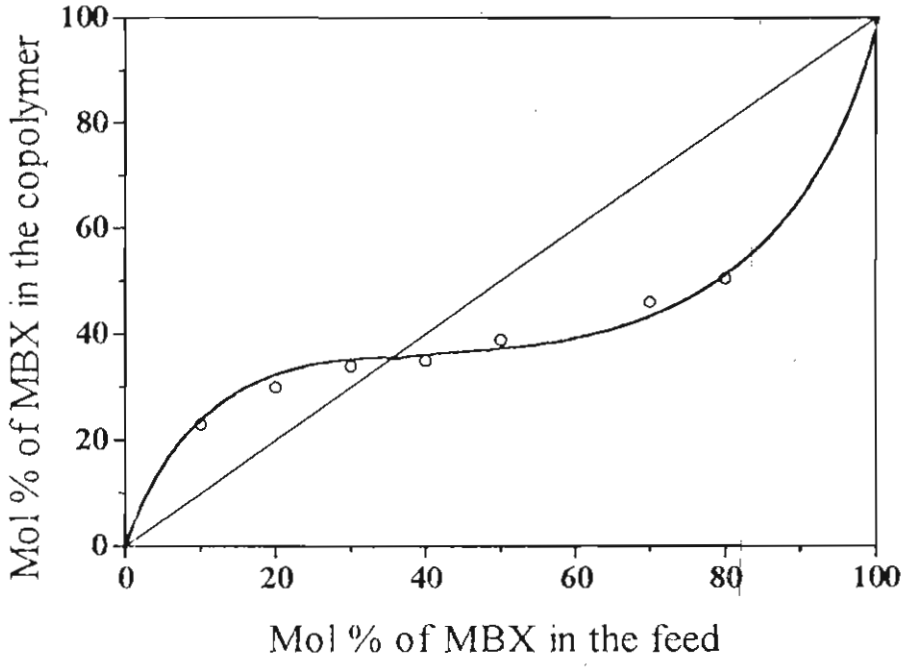

Figure 16. Copolymer composition curve for MBX-co-St

2.2.4. Thermal copolymerization behaviour of VBX with MMA and St

Styrene and its derivatives such as *p*-chloromethylstyrene, *p*-methylstyrene and *p*-methoxystyrene are known to be electron rich monomers. Sulfur-containing monomers such as *p*-[((benzothiazolyl)thio)methyl]styrene and N,N-diethyldithiocarbamate are also known to behave as electron rich monomers during copolymerization with other monomers.[23] Therefore, it is anticipated that VBX may behave as an electron rich monomer during copolymerization. In such cases the copolymerization characteristics of VBX should be significantly different from those of MAX and MBX. In order to study this, self polymerization of VBX and its copolymerization with MMA and St under various monomer feed compositions were carried out (Scheme 8). The ^{1}H NMR spectra of two representative copolymers of VBX with MMA and St are shown in Figures 17 and 18, respectively.

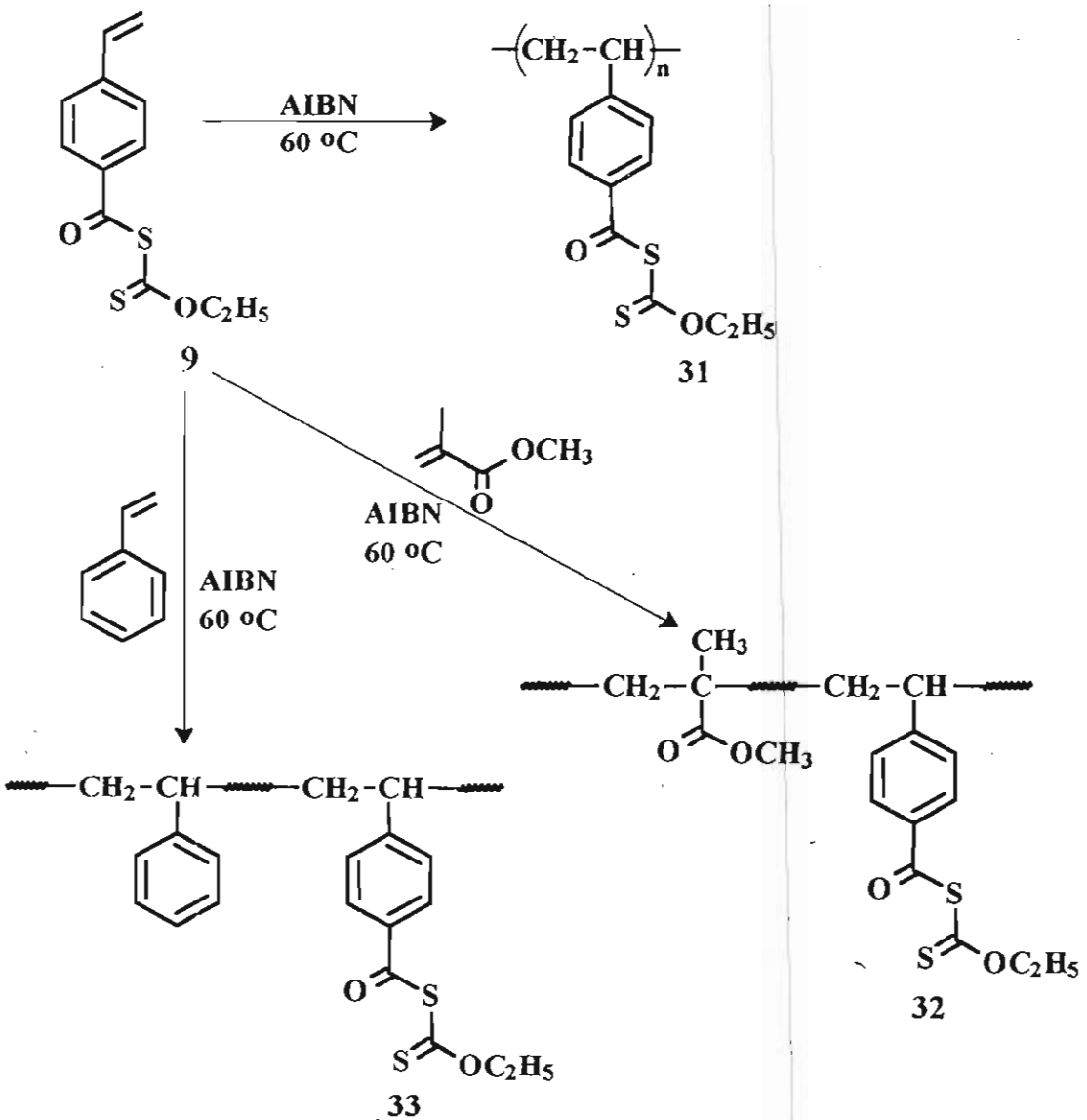

Scheme 8

Interestingly, VBX is found to homopolymerize in the presence of AIBN under dark, in contrast to MAX and MBX. This observation reveals that VBX is a highly reactive monomer when compared to MAX and MBX. In this case the rate of chain transfer may presumably be lower than that of the rate of propagation. The time-conversion relationship for the homopolymerization of

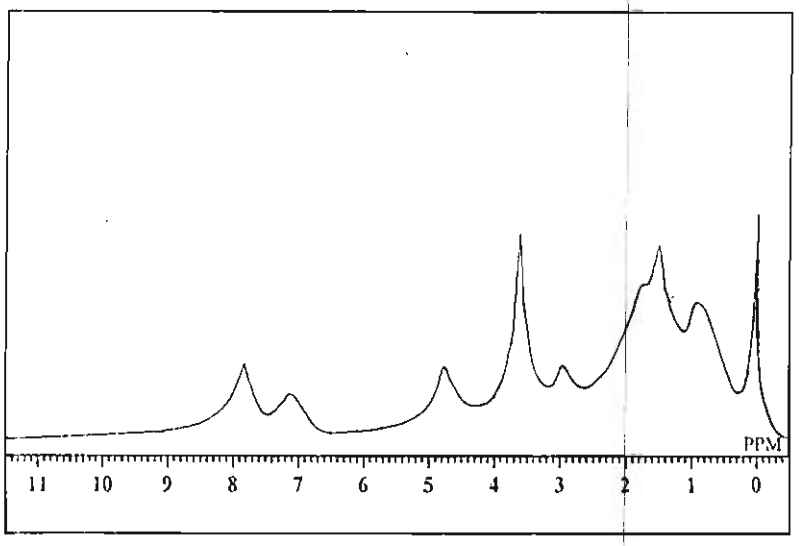

Figure 17. ^{1}H NMR spectrum of VBX-co-MMA

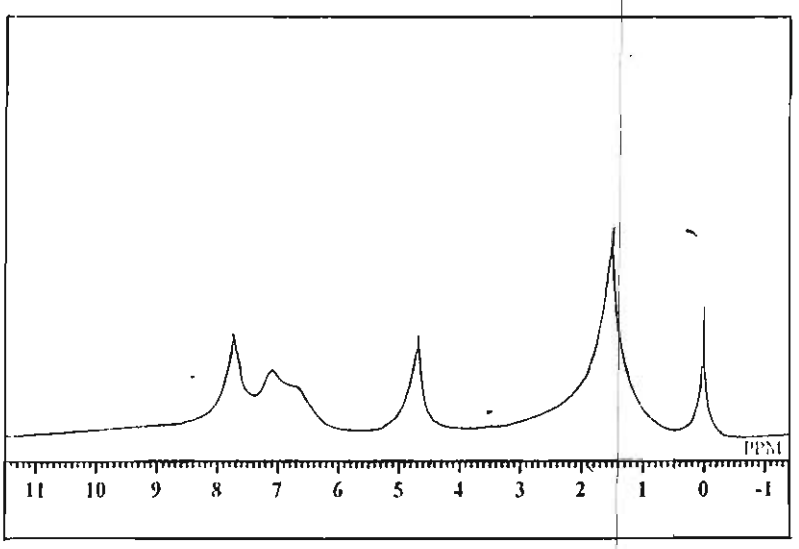

Figure 18. ^{1}H NMR spectrum of VBX-co-St

VBX at 60 °C using AIBN as the initiator is shown in Figure 19. Under higher monomer conversions considerable amount of crosslinked polymer was also

obtained. This may be due to the chain transfer between the growing polymer radical and the pendant xanthate chromophore, as shown in Scheme 9. This will lead to the formation of polymeric radical 38 with pendant benzoyl group, which on combination results in the formation of crosslinked polymer.

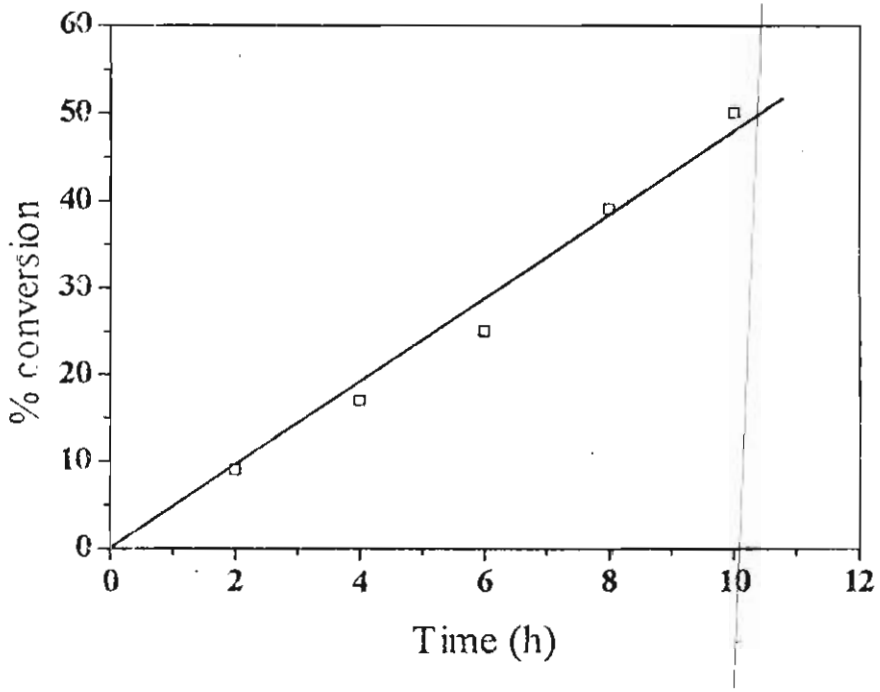

Figure 19. Effect of polymerization time on % conversion for the homopolymerization of VBX

The results of the copolymerization of VBX with MMA are listed in Table 5. The rate of polymerization is found to increase with the increase in the mole fraction of VBX in the monomer feed. This is in contrast to our earlier observation of the decrease in the rate of polymerization with the increase in the mole fraction of MAX or MBX during their copolymerization with MMA and St. The copolymer compositions determined by the ^{1}H NMR spectral analysis indicate a high percentage incorporation of VBX. A plot of the VBX mole percentage in the monomer feed versus the mole percentage of VBX in the copolymer is shown in Figure 20. The polymer composition curve in Figure

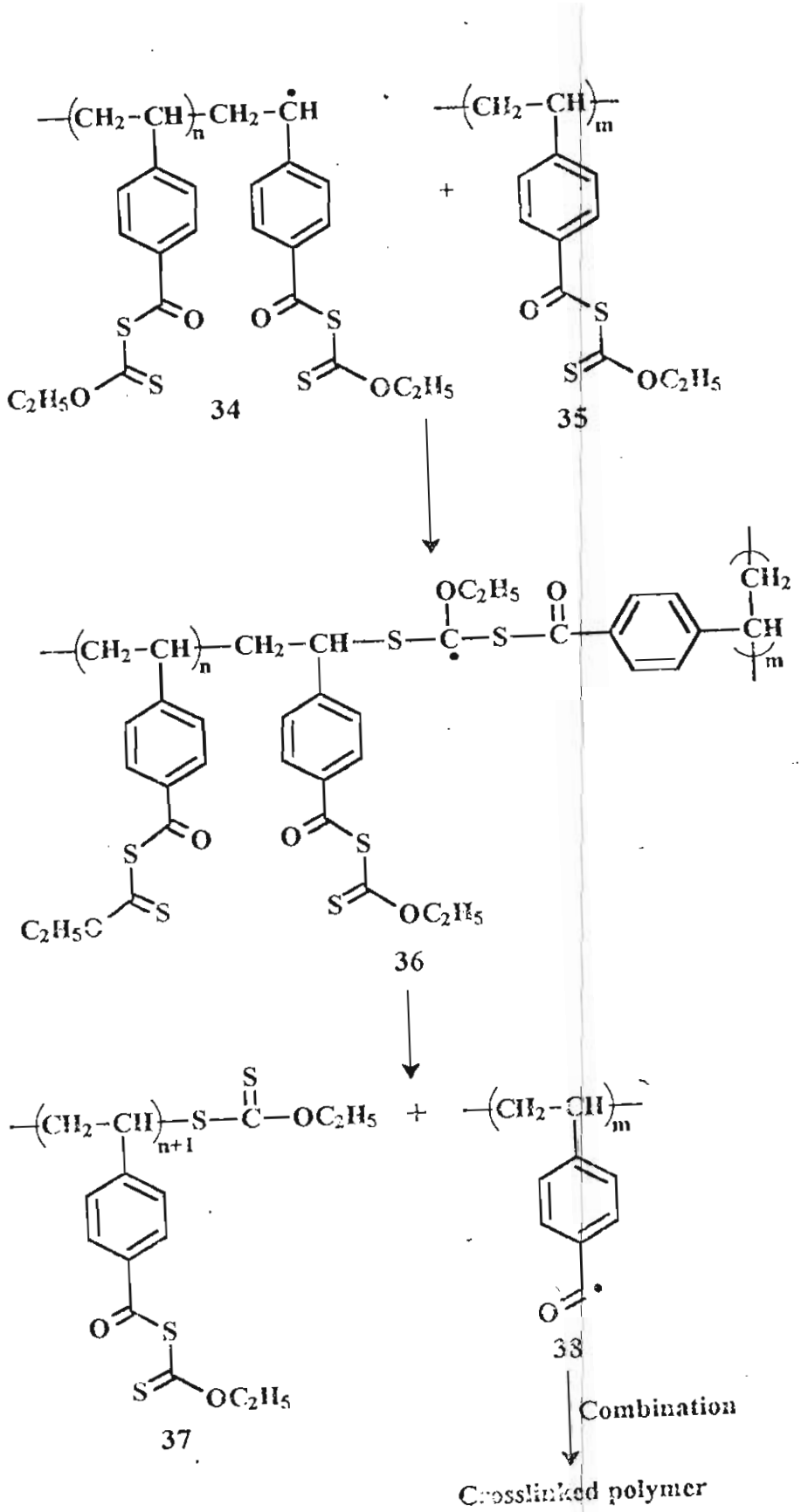

Scheme 9

20 reveals that VBX has a strong tendency for homopolymerization during its copolymerization with MMA. In other words, a growing polymer chain with terminal VBX radical or MMA radical prefers to add to another VBX monomer instead of adding to MMA. In this case also considerable amounts of crosslinked polymer was formed under higher monomer conversion as observed in the case of the homopolymerization of VBX. Results of copolymerization of the VBX-St monomer system are shown in Table 6. The rate of copolymerization is found to increase with increase in VBX mole percentage as observed in the case of VBX-MMA monomer system. However, the copolymer composition curve shown in Figure 21 reveals a low incorporation of VBX in the copolymer in contrast to the observation in the case of the copolymerization of VBX with MMA. This observation reveals that St is more reactive than VBX. In this case a growing polymer radical has the tendency to react with St rather than with VBX.

Table 5. Radical copolymerization* of VBX (M_1) with MMA (M_2)

M_1 in the feed (mol %)	Time (h)	Copolymer yield (%)	$R_p \times 10^6$ (gs^{-1})	M_1 in copolymer ^{1}H NMR (mol %)	$M_n \times 10^{-3}$	D (M_w/M_n)
10	20	10	0.4	13	5.1	1.4
20	16	12	0.6	24	5.6	1.8
30	10	12	1.2	42	7.7	1.8
40	8	13	1.8	68	9.0	2.0
50	6	10	2.0	73	13.0	1.8
70	3	8	3.8	95	13.1	1.8
80	2	6	4.6	96	14.0	2.0

*[AIBN] = 0.02 mol L^{-1}, $M_1 + M_2 = 0.5$ M in toluene

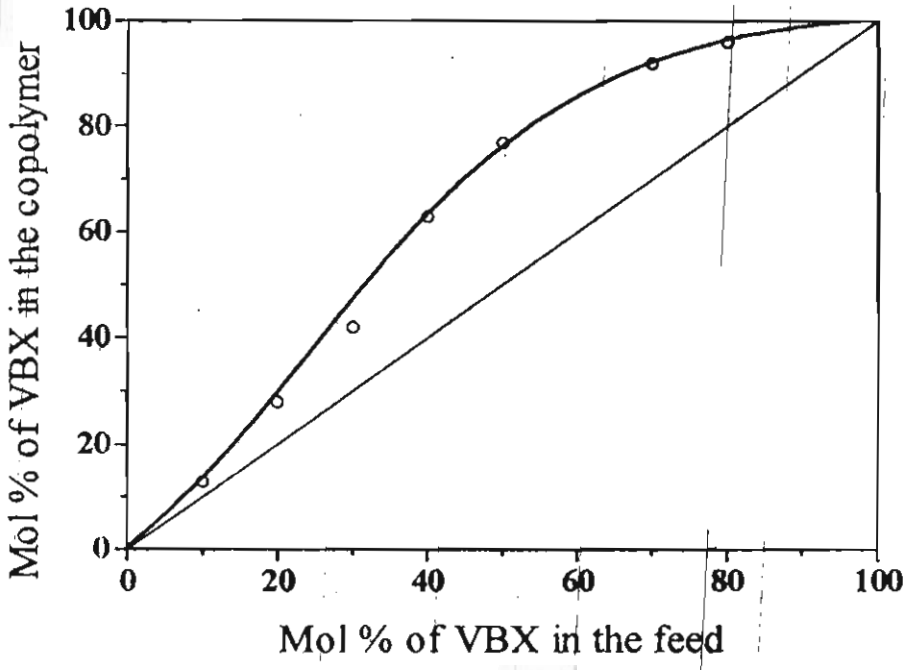

Figure 20. Copolymer composition curve for VBX-co-MMA

Table 6. Radical copolymerization* of VBX (M_1) with styrene (M_2)

M_1 in the feed (mol %)	Time (h)	Copolymer yield (%)	$R_p \times 10^6$ (gs^{-1})	M_1 in copolymer ^1H NMR (mol %)	$M_n \times 10^{-3}$	D (M_w/M_n)
10	20	15	0.5	5	9.3	1.3
20	16	17	1.0	8	10.3	1.5
30	10	20	1.9	10	10.9	2.0
40	8	15	2.0	17	11.1	2.6
50	6	18	3.7	25	13.3	3.5
70	4	20	6.9	36	14.6	3.4
80	2	13	9.7	42	15.5	3.5

*[AIBN] = 0.02 mol L^{-1}, $M_1 + M_2$ = 0.5 M in toluene

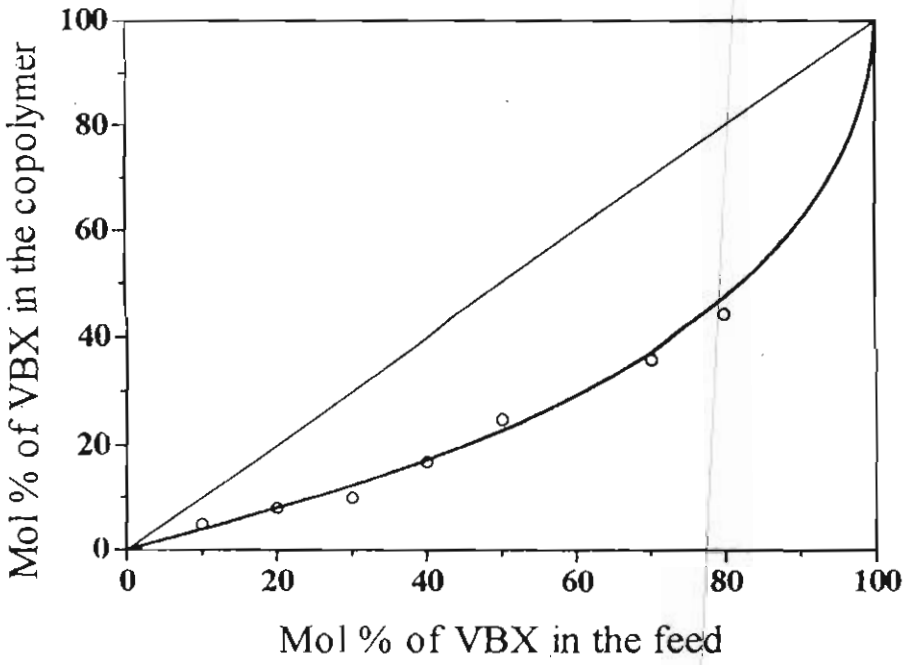

Figure 21. Copolymer composition curve for VBX-co-St

2.2.5. Determination of reactivity ratios

The reactivity ratios of MAX, MBX and VBX were calculated from the copolymer compositions by using the graphical methods of Finemann-Ross (FR)[31], Kelen-Tudos (KT)[32] and by a non-linear least-squares (NLLS) method.[33] The Fineman and Ross equation relating the feed and copolymer compositions can be written as,

$$\frac{F_1 (f_1 - f_2)}{F_2 f_1} = \frac{f_2 F_1^2 r_1}{f_1 F_2^2} - r_2 \qquad (2)$$

where f_1, F_1 and f_2, F_2 are the mole fractions of monomers in the polymer and the feed respectively, and r_1 and r_2 are the respective reactivity ratios. A plot of the left hand side of the equation (2) versus $f_2F_1^2/f_1F_2^2$ gives r_1 and r_2 as the

slope and the intercept, respectively. The KT method uses a modified form of the Mayo-Lewis equation,

$$\eta = r_1\xi - r_2/\alpha \qquad (3)$$

where η and ξ are functions of **f** and **F** and α is an arbitrary parameter. All calculations were based on the validity of the terminal model of copolymerizatin, which was evident from the linearity of the KT plots for both systems under study.

In Table 7, the values of the reactivity ratios of MAX, MBX and VBX, obtained by the FR and KT methods are compared. These data reveal that the reactivity ratios obtained by the two methods are in good agreement with each other. The value of r_1 for the VBX-MMA, monomer system is found to be higher than all other monomer systems under investigation, which reveals that VBX shows maximum copolymerization reactivity, when MMA is its comonomer. The product of the reactivity ratios (r_1r_2) for the MBX-St monomer system is extremely low indicating their strong tendency to form alternate copolymers.

2.2.6. Q-e values

Even though the Q-e values are empirical and have been subjected to many criticisms, they may be sometimes useful to assess the electron density and the copolymerization behaviour of a new monomer. The Q-e values of MAX, MBX and VBX were determined by the Alfrey-Price Q-e scheme using the reactivity ratios obtained experimentally by the KT method.[34] The equation relating the Q-e parameters with the reactivity ratios is given by the expression 4, which can be rewritten in the form of equation 5.

$$r_1 = \frac{Q_1}{Q_2} \exp\left[-e_1 (e_1 - e_2) \right] \qquad (4)$$

Table 7. Reactivity ratios of MAX, MBX and VBX obtained from their thermal copolymerization with MMA and styrene (St)

	FR method			KT method		
System	r_1	r_2	r_1r_2	r_1	r_2	r_1r_2
MAX-MMA	0.65±0.05	0.81±0.08	0.53	0.62±0.06	0.82±0.04	0.5
MAX-St	0.37±0.03	0.47±0.02	0.17	0.37±0.05	0.46±0.06	0.17
MBX-MMA	0.52±0.05	3.60±0.1	1.9	0.57±0.05	3.6±0.1	2.05
MBX-St	0.01±0.0	0.5±0.03	0.005	0.01±0.0	0.51±0.01	0.005
VBX-MMA	8.4±0.3	1.2±0.1	10.08	8.5±0.3	1.16±0.1	9.86
VBX-S t	0.03±0.01	2.3±0.1	0.07	0.03±0.01	2.4±0.1	0.07

$$\ln (Q_1/r_1)-e_1^2 = \ln Q_2-e_1e_2 \qquad (5)$$

From the known values of Q_2 = 1.0 and e_2 = 0.8 for St and Q_2 = 0.75 and e_2 = 0.38 for MMA, the Q-e values of MAX, MBX and VBX were calculated. The Q values for MAX, MBX and VBX are 0.91, 0.29 and 0.16 and the 'e' values are 0.29, 0.41 and –0.55 respectively. The negative 'e' value of VBX indicates that this monomer has an electron-rich double bond. However, this value is higher than the 'e' value of styrene and some of its derivatives indicating that VBX is electron deficient when compared to styrene. The high 'e' value of MBX reveals that it is the most electron deficient among the three monomers under investigation. This is reasonable since the copolymerization

of MBX with electron rich monomer such as St showed a strong tendency for alternation.

2.2.7. Influence of the structure and reactivity of monomers on the molecular weights and polydispersities of copolymers

The number average molecular weights (M_n) and the polydispersities of copolymers obtained by the copolymerization of MAX with MMA and St are shown in Tables 1 and 2, respectively of the Section 2.2.2. These data reveal that in both cases the molecular weights and polydispersities of copolymer decrease with increase in the mole fractions of MAX in the monomer feed composition. This decrease in the molecular weights is more significant in the case of MAX-MMA monomer system. The effect of MAX concentration on the molecular weights and polydispersities are clear from Figures 22 and 23 for MAX-co-MMA and MAX-co-St, respectively. Both molecular weights and polydispersities are comparatively high at lower concentration of MAX. In the case of MAX-MMA monomer system the molecular weight showed a sharp decrease between 0-30 mole percentage of MAX in the monomer feed composition. Further increase in the MAX mole percentage showed only a marginal decrease in the molecular weight. On the other hand, a linear decrease in the molecular weight was observed for the copolymers of MAX-St monomer system as shown in Figure 23. The observed changes in the molecular weights and polydispersities of copolymers with increase in mole fraction of MAX are presumably due to the enhanced chain transfer property of MAX to the growing polymer radicals, as indicated earlier in Scheme 6. In this way MAX plays a key role in controlling the molecular weights of the resultant copolymers.

Effect of MBX concentration on the molecular weights and polydispersities of its copolymers with MMA and styrene are shown earlier in Tables 3 and 4, respectively (Section 2.2.3). In these cases also the molecular weights showed a decreasing tendency with increase in the MBX mole

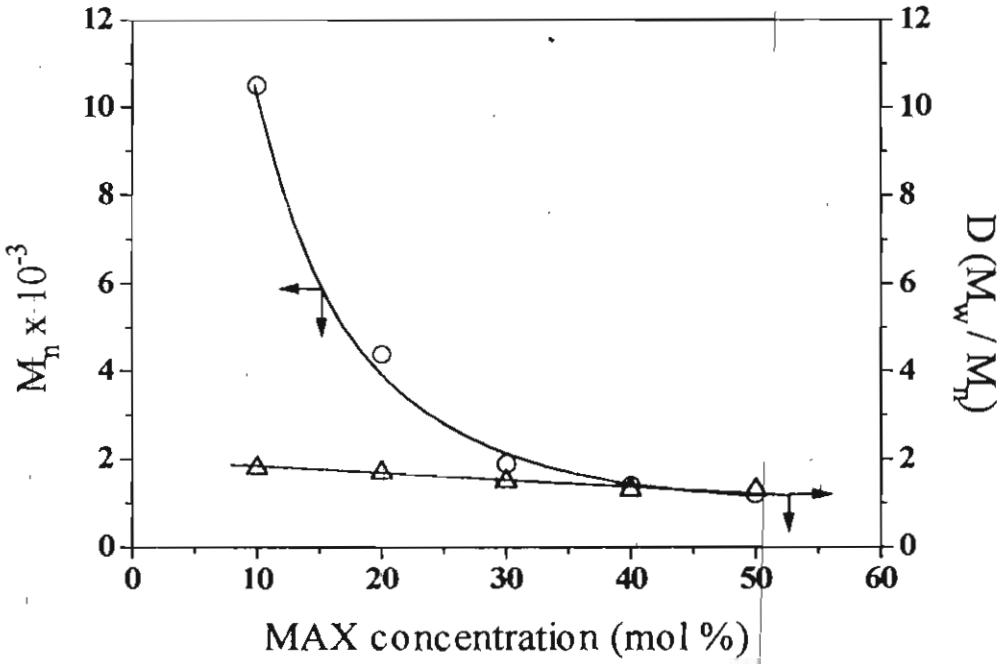

Figure 22. Effect of MAX concentration on molecular weight (M_n) and polydispersity (D) of MAX-MMA polymers

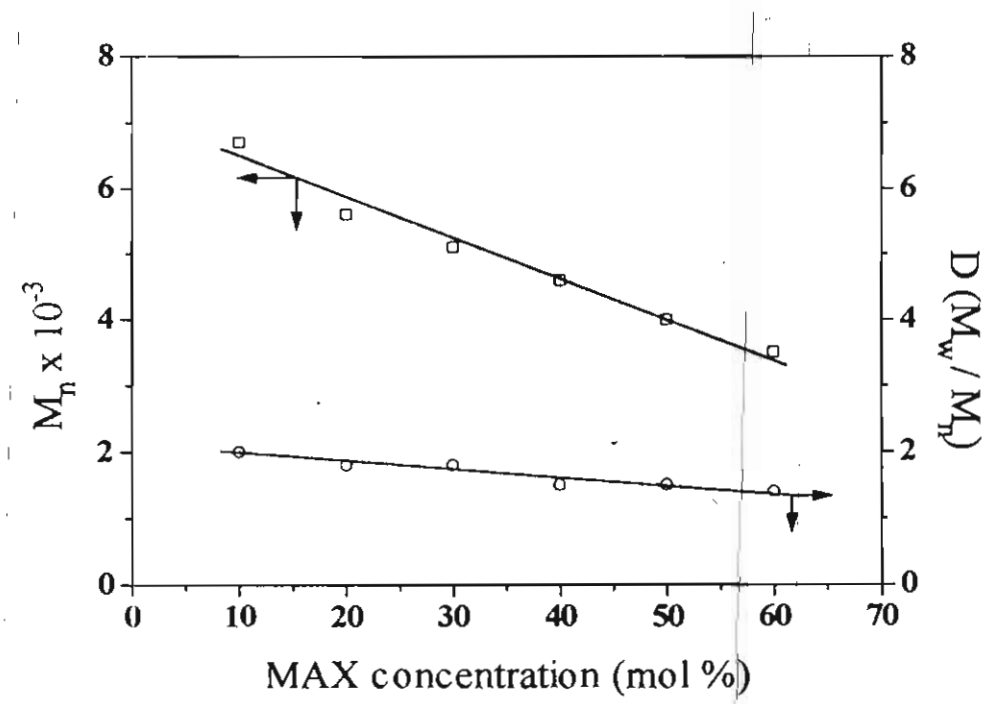

Figure 23. Effect of MAX concentration on molecular weight (Mn) and polydispersity (D) of MAX-St polymers

percentage in the monomer feed. Interestingly when concentrated solution of monomers in benzene was used, considerable amounts of crosslinked polymers are also formed. This is particularly significant in the case of MBX-St monomer system. Under higher monomer conversion the reaction mixture becomes highly viscous. Under such conditions the bimolecular combination of maleimidobenzoyl radicals, which are formed by the chain transfer reaction as shown in Scheme 10, will be facilitated leading to the formation of a crosslinked polymer. This type of crosslinking is relatively less efficient in the case of the MBX-MMA monomer system because of the poor incorporation of the MBX monomer during copolymerization. In this case the copolymerization mixture contains excess of unreacted MBX and hence the chain transfer by the pendant xanthate group of copolymer chains becomes less important. However, under low mole percentage of MBX in the monomer feed composition or under longer polymerization time, some crosslinking is observed. This is because, under these reaction conditions there is the possibility for chain transfer from the pendent xanthates to another polymer radical which leads to crosslinking as explained earlier.

Effect of monomer concentration on the molecular weights of copolymers during the copolymerization of VBX with MMA and St are shown earlier in Tables 5 and 6, respectively (Section 2.2.4). In contrast to the copolymerization of MAX and MBX, VBX showed an increase in the molecular weights with increase in concentration as shown in Figures 24 and 25. This observation reveals that the chain transfer termination of growing polymer chain is less efficient in the case of VBX. This could be due to the high reactivity of the VBX double bond and hence the rate of propagation may be higher than the rate of termination by chain transfer.

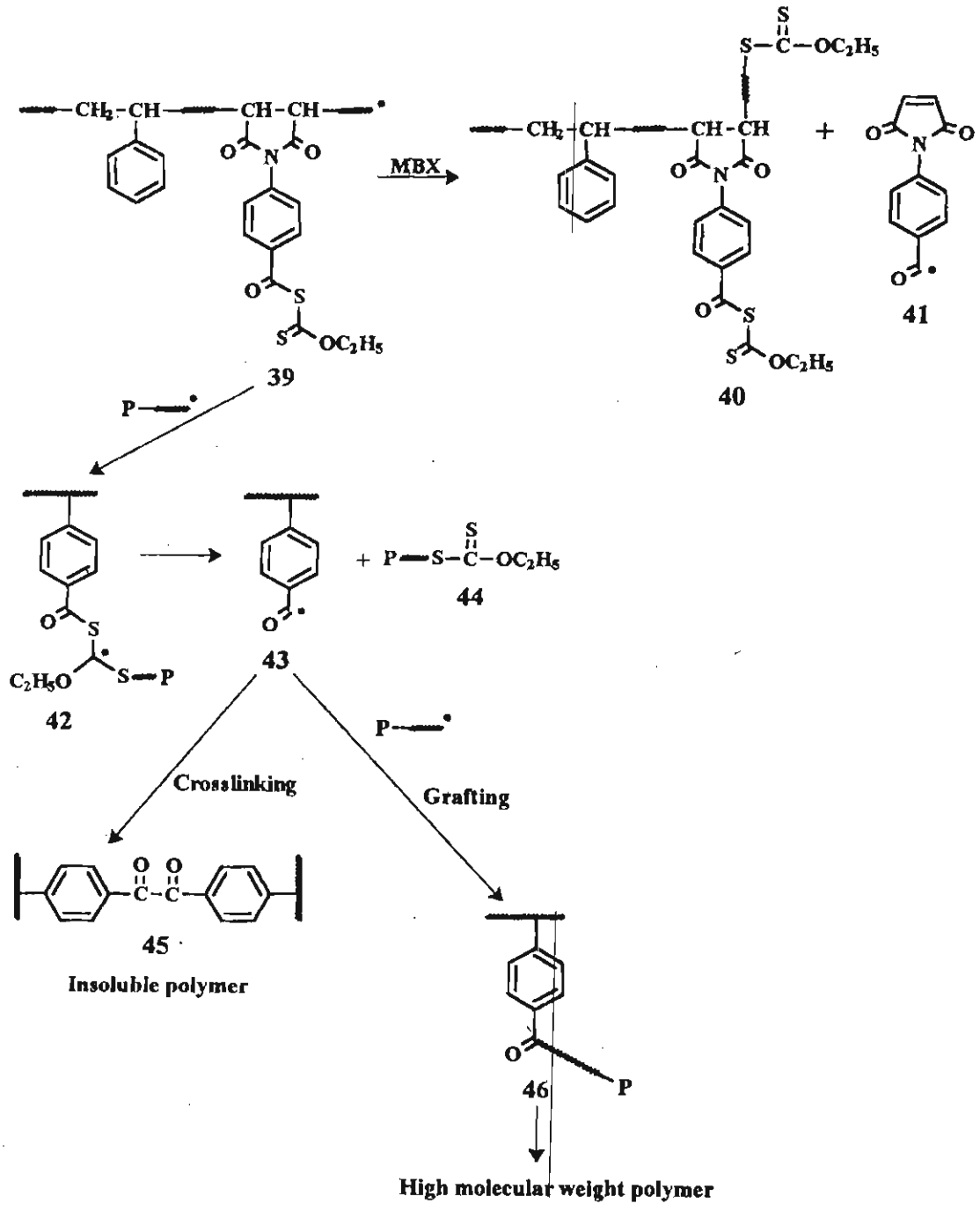
MBX
39
40
41
42
43
44
45
Insoluble polymer
46
Crosslinking
Grafting
High molecular weight polymer

Scheme 10

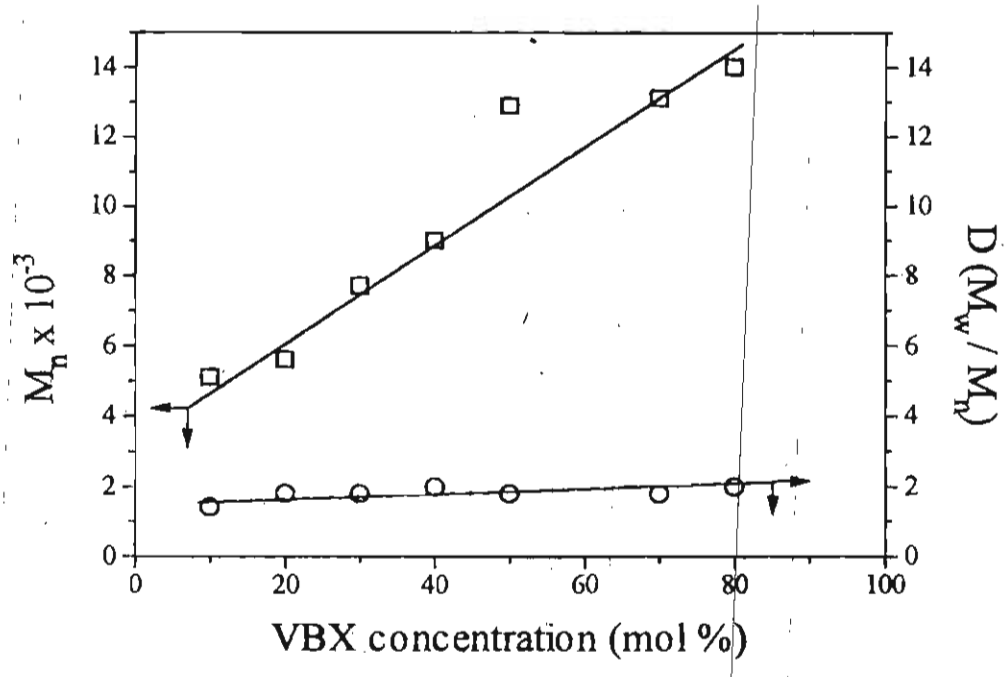

Figure 24. Effect of VBX concentration on molecular weight (M_n) and polydispersity (D) for VBX-co-MMA

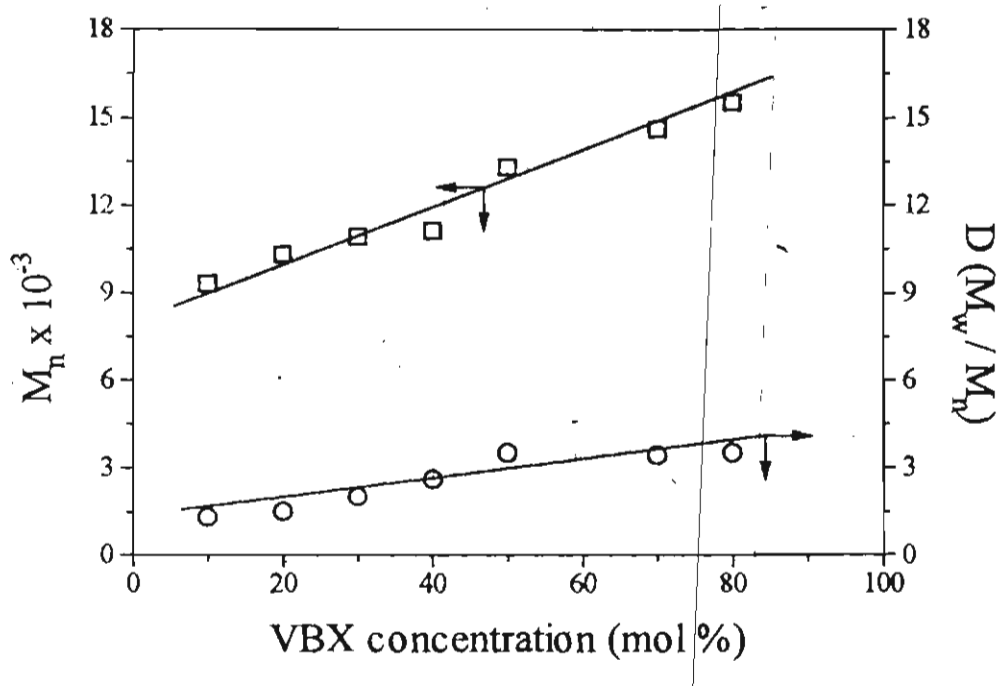

Figure 25. Effect of VBX concentration on molecular weight (M_n) and polydispersity (D) for VBX-co-St

2.2.8. Thermogravimetric Studies

Thermogravimetric analysis (TGA) of the copolymers of MAX, MBX and VBX in air showed significant differences in their pattern of decomposition. Typical thermograms of MAX-MMA and MAX-St copolymers are shown in Figures 26 and 27, respectively. They show that the overall stability of both copolymers decrease with increasing mole percentage of MAX. The thermal decomposition patterns of all the copolymers of MBX and VBX were considerably different from those of MAX copolymers. In the case of MBX and VBX copolymers three weight losses were observed. The initial weight loss, which is assigned for the decomposition of the pendant xanthate group, was found to increase with increase in xanthate group content. Considerable differences could be noticed in the second and third weight losses among the copolymers of MAX, MBX and VBX. For example, in the case of MBX-MMA copolymers (Figure 28) and VBX-MMA copolymers (Figure 29) the second weight loss which may be associated with the thermal decomposition of the main chain MMA repeat units, was found to decrease with MBX and VBX mole percentage respectively. This decrease in weight losses can be attributed to the reduction in the mol percentage of MMA units associated with increase in the mole percentage of MBX or VBX. The final weight loss may be due to the thermal degradation of the aromatic units which increases with the increase in the mol percentage of MBX or VBX units in the copolymers. The thermal studies also reveal that the overall thermal stability of the MBX copolymers are better than the VBX or MAX copolymers which is obvious due to the presence of the maleimido units.

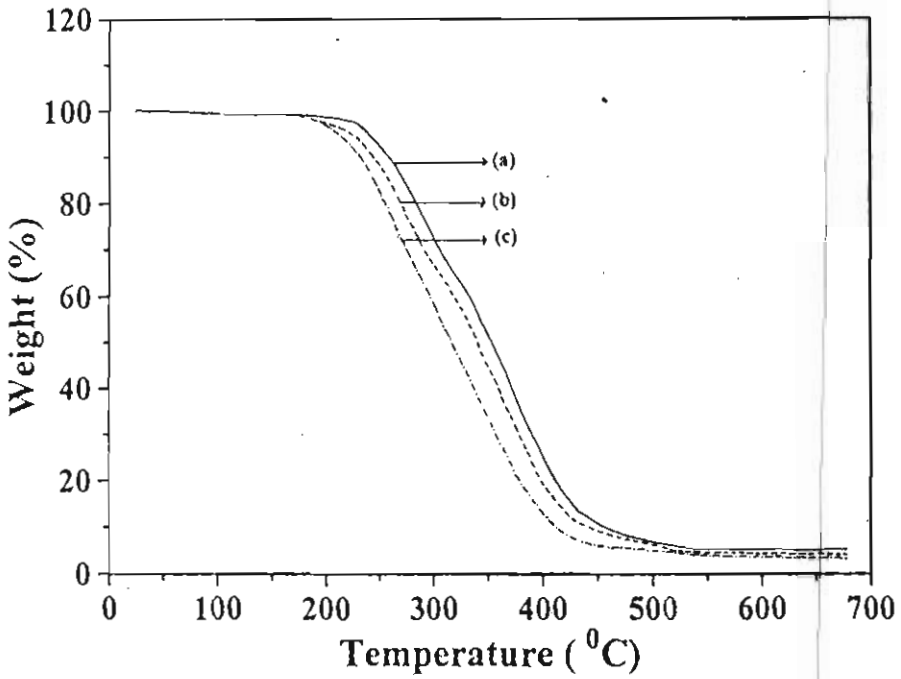

Figure 26. Thermograms of MAX-co-MMA (a) 10 mol% of MAX; (b) 30; mol% of MAX (c) 55 mol% of MAX.

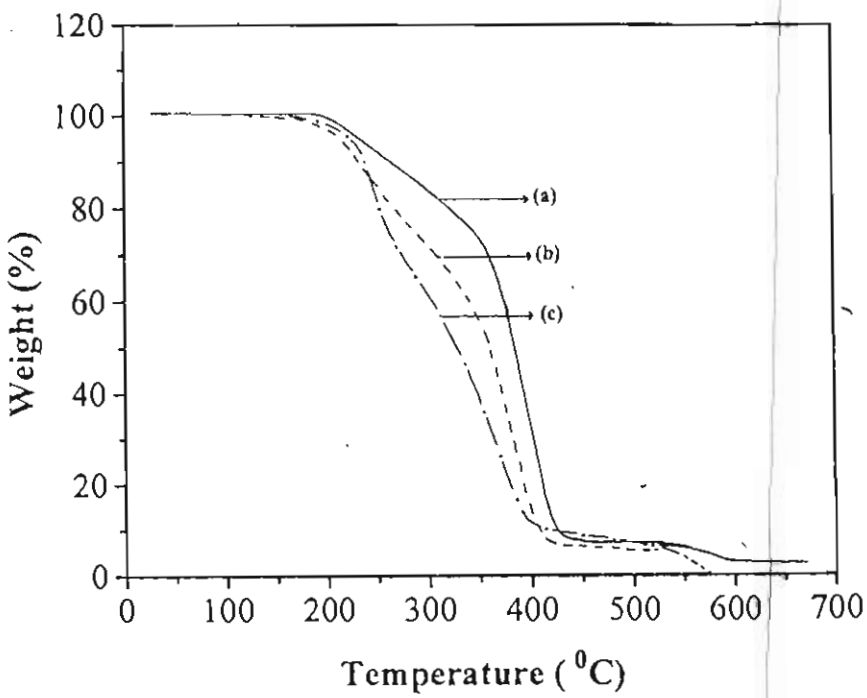

Figure 27 . Thermograms of MAX-co-St. (a) 21 mol% of MAX; (b) 33 mol% of MAX; (c) 56 mol% of MAX.

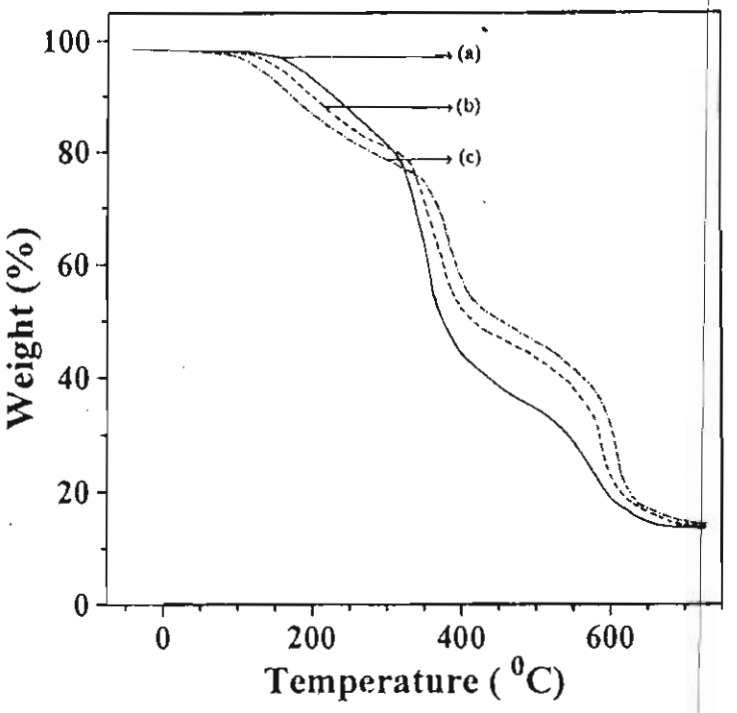

Figure 28 . Thermograms of MBX-co-MMA (a) 11 mol% of MBX; (b) 25 mol% of MBX; (c) 37 mol% of MBX.

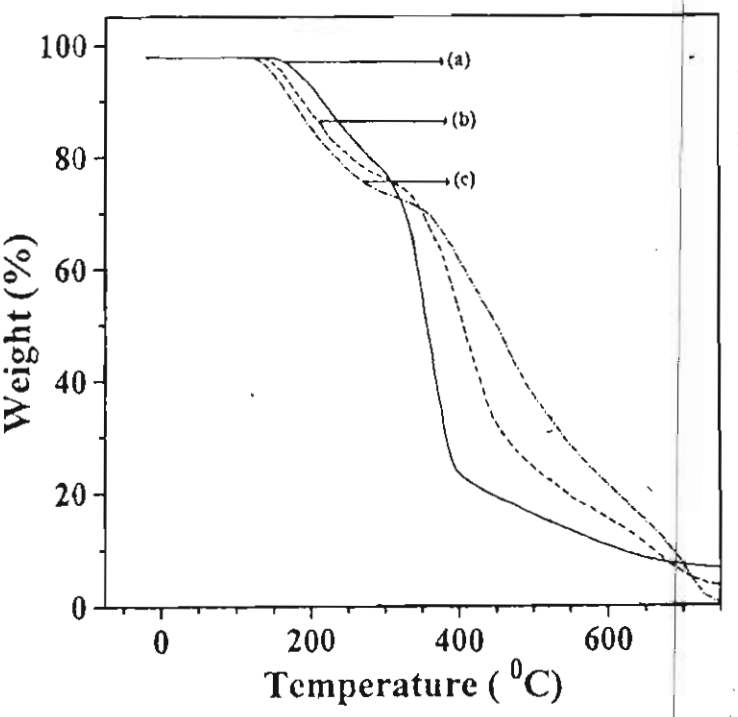

Figure 29 . Thermograms of VBX-co-MMA. (a) 42 mol% of VBX; (b) 73 mol% of VBX; (c) 95 mol% of VBX.

2.3. Conclusions

Three new monomers containing a photosensitive xanthate chromophore have been prepared and copolymerized with monomers such as MMA and St. Detailed analysis of copolymer composition and molecular weight has revealed that the new monomers show considerable differences in their copolymerization behaviour. MAX and MBX are found to be electron deficient monomers whereas VBX is an electron rich monomer. The copolymers obtained from MAX and MBX are found to have low molecular weights and low dispersity, which are formed in low yields due to strong chain transfer reaction of these monomers. On the other hand copolymers of VBX showed comparatively higher molecular weights and yields indicating that VBX is a highly reactive monomer. MAX and MBX showed an alternation tendency during copolymerization indicating a weak interaction between the electron rich St and the electron deficient MAX and/or MBX.

2.4. Experimental Section

All melting points are uncorrected and were determined using a Mel-Temp-II melting point apparatus. Infra-red (IR) spectra were recorded on a Perkin-Elmer model 880 spectrometer. The electronic spectra were recorded on a Shimadzu 2100 A spectrophotometer. ^{1}H and ^{13}C nuclear magnetic resonance (NMR) spectra were recorded on a JEOl EX 90 spectrometer using $CDCl_3$ as solvent and tetramethylsilane as internal standard. Mass spectra were recorded on a Hewlett Packard mass spectrometer model 5791, attached to 5890 series II gas chromatography setup, attached with an OV 101 (25 m long, 0.2 mm ID) or on MP-FFAP (25 m long, 0.2 mm ID) capillary column, and an FID detector or on a Finnigan MAT Model 8430 or JEOL JMSAX505HA. Gel permeation chromatography (GPC) was carried out on a Shimadzu LC-8A GPC system equipped with a refractive index detector. Calibrations were done with standard polystyrene samples. Tetrahydrofuran (THF) was used as the eluent at a flow rate of 1 mL min^{-1} at 28 °C. Thermogravimetry (TGA) curves were obtained

using a V5.1A Dupont 2000 TGA analyser at a heating rate of 10 °C min^{-1}, under air. Elemental sulphur analyses were carried out at the Mid West Micro Laboratory, Indianapolis, USA.

Absolute ethanol (Merck, 99%), methyl methacrylate (MMA) and styrene (St) (Aldrich, 99%) and 2,2'-azobis(isobutyronitrile) (AIBN) (Fluka, 99%) were used . MMA and St were purified by washing with 10% NaOH solution, followed by distillation under reduced pressure and kept in a refrigerator under nitrogen atmosphere. AIBN was recrystallized twice from methanol and kept in the refrigerator. Maleic anhydride and 4-aminobenzoic acid (s.d. fine Chemicals, India), 4-methylbenzoic acid (Spectrochem, 99%), methacrylic acid (CDH, 99%) , triphenylphosphine (SRL India, 99%) and N-bromosuccinimide (NBS) (Spectrochem, 97%) were purified according to literature procedures before use. All solvents were dried and distilled before use. Potassium O-ethyl xanthate[35] and methacryloyl chloride[36] were prepared according to reported procedures

2.4.1. Synthesis of S-methacryloyl O-ethyl xanthate (MAX) (7)

To a stirred suspension of potassium O-ethyl xanthate (16.0 g, 0.1 mol) in dichloromethane (100 mL), maintained at 0 °C, was gradually added a solution of methacryloyl chloride (10.4 g, 0.1 mol) in dichloromethane (100 mL). The reaction mixture was stirred for an additional period of 1 h and allowed to warm up gradually to room temperature. The reaction mixture was washed several times with water and the organic layer was dried over anhydrous sodium sulphate. Removal of the solvent under reduced pressure gave (17.0 g) (90%) of MAX (7) as an yellow liquid. IR ν_{max} (neat) 1720 (C=O), 1640 (C=C), 1240 (C=S), 1050 (C-O) cm^{-1}; UV λ_{max} ($CHCl_3$) 280 (ε, 10400), 395 (90) nm; ^{1}H NMR ($CDCl_3$, 90 MHz) δ 5.9-6.5 (2 H, m, CH_2), 4.7 (2 H, q, OCH_2), 2.0 (3 H, s, CH_3), 1.45 (3 H, t, CH_3); ^{13}C NMR ($CDCl_3$, 22.4 MHz) δ 204, 186, 144, 126, 71, 18, 14; Mass spectrum, m/z 191 (M^++1), 147, 122, 155, 103, 87, 73, 69.

2.4.2. Synthesis of 4-maleimidobenzoic acid[15] (11)

4-Aminobenzoic acid (27.4 g, 0.2 mol) was dissolved in 400 mL of dry THF and to this solution maleic anhydride (19.6 g, 0.2 mol) dissolved in 100 mL of THF was added dropwise over a period of 1 h at room temperature under stirring. The mixture was continually stirred for 3 h. The bath temperature was raised to 60 °C and anhydrous sodium acetate (4g) was added, followed by the dropwise addition of acetic anhydride (24.5 g, 0.24 mol). A brown solution resulted, which was continually stirred for 4 h at the same temperature. MBA was recovered by precipitation in ice-cold water. It was filtered and dried at 50 °C under vacuum. Recrystallization was done from an ethanol-THF mixture (10:1) to give 18.7g (43%) of the product (11), mp 236-238 °C. IR ν_{max} (neat) 3100 (COOH), 1780 (C=O), 1600 (C=C) cm^{-1}; ^1H NMR (DMSO, 90 MHz) δ 8.2-7.3 (4 H, m, aromatic), 6.9 (2 H, s, CH=CH).

2.4.3. Synthesis of (4-maleimido)benzoyl chloride (12)

4-Maleimidobenzoic acid (10 g, 46 mmol) was mixed with excess of thionyl chloride (20 mL) at 0 °C. The solution was slowly warmed to room temperature and stirred for 30 min. Excess of thionyl chloride was distilled off and the acid chloride was separated and purified by recrystallization from a mixture (1:4) of dichloromethane and petroleum ether to give 9.75 g (90%) of 12, mp 142-143 °C. ^1H NMR ($CDCl_3$, 90 MHz) δ 8.2-8.1 (2 H, d, aromatic, J = 9 Hz), 7.5-7.4 (2 H, d, aromatic, J = 9 Hz); ^{13}C NMR ($CDCl_3$, 22.4 MHz) δ 168.9, 166.2, 135.4, 134.4, 130.4, 129.2, 125.2; Information on the mass spectrum of 12 was derived through its methyl ester, (m/z) 231 (M^{+}), 200, 172, 146, 90.

2.4.4. Synthesis of S-(4-maleimido)benzoyl O-ethyl xanthate (MBX) (13)

4-Maleimidobenzoyl chloride (5g, 20 mmol) was dissolved in dichloromethane (50 mL) and added dropwise to a suspension of potassium O-ethyl xanthate (4 g, 25 mmol) in dichloromethane (50 mL), maintained at –5 °C. The reaction mixture was stirred for 1 h at –5 °C followed by stirring for

1 h at 10 °C. The contents were poured into water and the CH_2Cl_2 layer was separated and washed with dilute sodium bicarbonate solution, followed by distilled water. Removal of the solvent gave MBX (**13**) as a pale yellow solid (5.8 g) (90%), mp 79-80 °C (decomp). IR ν_{max} (neat) 1750, 1730 (C=O), 1640 (C=C), 1250 (C=S) cm^{-1}; UV λ_{max} ($CHCl_3$) 283 (ε, 21,000), 395 (363) nm; ^1H NMR ($CDCl_3$, 90 MHz) δ 8.05 - 7.95 (2 H, d, aromatic, J = 9 Hz), 7.63 - 7.53 (2 H, d, aromatic, J = 9 Hz), 6.9 (2 H, s, CH=CH), 4.6 (2 H, q, OCH_2), 1.48 (3 H, t, CH_3); ^{13}C NMR ($CDCl_3$, 22.4 MHz) δ 203, 184.2, 168.6, 136.7, 134.5, 128.8, 127.6, 125.4, 71.1, 13.4; exact mol wt calcd for $C_{14}H_{11}NO_4S_2$ (MH^+) 322.0208, found 322. 0202 (FAB high-resolution mass spectrometry).

2.4.5. Synthesis of 4-bromomethylbenzoic acid (15)

p-Toluic acid (13.6 g, 0.1 mol) and N-bromosuccinimide (18.5 g, 0.11 mol) were dissolved in CCl_4 (150 mL) containing a trace amount of benzoyl peroxide and the reaction mixture was refluxed for 3 h. After 90 min of reaction, the brown colour faded and it became colourless, at the end of the reaction. The hot solution was filtered and washed with hot water (3 times). The crude product was recrystallized from methanol to give 15 g (70%), mp 224-225 °C of **15**.

2.4.6. Synthesis of (4-carboxy)benzyltriphenylphosphonium bromide (16)

A solution of 4-bromomethylbenzoic acid (4.3g, 20 mmol) and triphenylphosphine (5.25 g, 20 mmol) in 150 mL of dry acetone was stirred at 70 °C. The solution, which was clear in the beginning, became milky. After cooling in an ice-bath the solution was filtered and washed with dry ether (2 x 50 mL). The mother liquor was concentrated to 1/3 its volume and the crystallized product was collected to give 8.54 g (89%) of **16**, mp 298-300 °C.

2.4.7. Synthesis of 4-vinylbenzoic acid (17)

To a stirred suspension of (4-carboxy)benzyltriphenylphosphonium bromide (**16**) (4.77 g, 10 mmol) in 50 mL of 30% of aqueous formaldehyde

solution and 15 mL of water, was added dropwise sodium hydroxide solution (3 g in 15 mL of water, 80 mmol) at room temperature. The solution was continually stirred for 1 h and was filtered. To the filtrate was added dropwise 10 mL of 6 M HCl (pH 1). The precipitated 4-vinylbenzoic acid (17) was collected and washed with water (3 x 50 mL) and was vacuum dried at 40 °C. The product was recrystallized from a mixture (7:3) of methanol and water to give 1.13 g (76%) of 4-vinylbenzoic acid (17), mp 142-145 °C. ^{1}H NMR ($CDCl_3$, 90 MHz) δ 12.33 (1 H, s, COOH), 8.06, 7.44 (2 H, d, J = 9 Hz, aromatic), 6.76 (1 H, J_{ac} = 17 Hz, J_{bc}= 11 Hz, H_c), 5.82 (1 H, d, J=17 Hz, H_b), 5.36 (1 H, d, J = 11 Hz, H_a).

2.4.8. Synthesis of 4-vinylbenzoyl chloride (18)

To an ice-cold dry mixture of 4-vinylbenzoic acid (17) (2 g, 13.5 mmol) and 4-t-butylcatechol (3 mg), was added thionyl chloride (4.5 mL, 62 mmol) dropwise with stirring. The suspension was allowed to gradually (15 min) warm to room temperature, controlling the evolution of HCl gas, followed by maintaining at 40-50 °C for 3.5 h. The final clear solution was distilled to remove excess of thionylchloride and the fraction collected at 90 °C (1 mm) gave 1.35 g (60 %) of (18). ^{1}H NMR ($CDCl_3$, 90 MHz) δ 8.06, 7.44 (2 H, d, J = 9 Hz, aromatic), 6.76 (1 H, dd, J_{ac}=17 Hz, J_{bc}=11 Hz, H_c), 5.82 (1 H, d, J=17 Hz, H_b), 5.36 (1 H, d, J=11 Hz, H_a); ^{13}C NMR ($CDCl_3$, 22.4 MHz) δ 167.5, 144.2, 135.2, 131.9, 131.6, 126.4, 118.3; Treatment of a small quantity of 18 with methanol gave the methyl ester; m/z 162 (M^{+}), 144, 135, 131, 117, 103, 77.

2.4.9. Synthesis of S-(*p*-vinyl)benzoyl O-ethyl xanthate (VBX) (19)

To a suspension of potassium O-ethyl xanthate (1.3 g, 8.3 mmol) in dichloromethane (25 mL) maintained at 0 °C, a dichloromethane solution of 4-vinylbenzoyl chloride (18) (1.5 g, 8.3 mmol) was added, dropwise. The solution was stirred for 1 h at this temperature, followed by stirring for 30 min at room temperature. The contents were poured into water and the

dichloromethane layer was washed with dilute sodium bicarbonate solution, followed by water and dried over anhydrous sodium sulphate. Removal of the solvent gave VBX (**19**) as a pale yellow liquid (95%). IR ν_{max} (neat) 1701 (C=O), 1543 (C=C), 1257 (C=S), 1040 (C-O) cm^{-1}. UV λ_{max} ($CHCl_3$): 283 (ε, 16, 000), 395 (150) nm. ^1H NMR ($CDCl_3$, 90 MHz) δ 7.8, 7.4 (2 H, d, J = 9 Hz, aromatic), 6.7 (1 H, dd, J_{ac}. 17 Hz, J_{bc} = 11 Hz, H_c), 5.8 (1 H, d, J = 17 Hz, H_b), 5.4 (1 H, d, J = 11 Hz, H_a), 4.6 (2 H, q, OCH_2), 1.47 (3 H, t, CH_3). ^{13}C NMR ($CDCl_3$, 22.4 MHz) δ 203.4, 184.1, 143.3, 135.4, 134.6, 128.2, 126.5, 117.5, 70.9, 13.3; exact mol wt calcd for $C_{12}H_{12}O_2S_2$ (MH^+) 253.0357, found 253.0373 (FAB high-resolution mass spectrometry).

2.4.10. Thermal copolymerization. General procedure

The required amount of monomers, solvent and initiator (AIBN) were taken in glass tubes (1.4 cm diameter and 10 cm long), stoppered with rubber septa. The polymerization mixture was deoxygenated for 15 min by purging with dry nitrogen and heated at 60 °C for known periods of time. The copolymers (Schemes 4, 7 and 8) were precipitated by pouring the reaction mixtures into excess of methanol. After two reprecipitations by pouring a chloroform solution in to methanol, the copolymers were dried in a vacuum oven at 40 °C.

2.5. References

1. Thompson, L. F.; Willson, C. G.; Bowden, M. J. (Eds)., *Introduction to Microlithography*, ACS Symp Ser. 219 American Chemical Society, Washington, D.C. **1983**.
2. Ito, H.; Willson, C. G. *Polymers in Electronics*, Davidson, T. (Ed)., ACS Symp. Ser. 242, American Chemical Society, Washington, D. C. **1984**.
3. Wentink, S. G.; Koch, S. D. Eds., UV. Curing in Screen Printing for Printed Circuits and Graphic Arts, Technology Marketing Corp., Norwalk, CT, **1981**.
4. Pappas, S. P. Ed., *UV. Curing : Science and Technology*, Vol. 2, Technology Marketing Corporation, Norwalk, CT, **1984**.
5. Roffey, C. G. *Photopolymerization of Surface Coatings*, Wiley, New York, **1982**.
6. Fouassier, J.-P, *Photopolymerization Science and Technology*, Allen, N. S. Ed., Elsevier, London, **1989**.
7. Ebson, J.R.; Towns, C.R. *J. Macromol. Sci., Rev. Macromol. Chem. Phys.* **1986**, *C26*(4), 523.
8. Arita, K.; Ohtomo, T.; Tsurumi, Y. *J. Polym. Sci., Polym. Lett. Ed.* **1981**, *19*, 211.
9. Tsuchida, E.; Tomono, T.; Sano, H. *Makromol. Chem.* **1972**, *151*, 242.
10. Cowie, J. M. G., Ed. Alternating Copolymers; Plenum: New York, 1985.
11. Hill, D. J. T.; O'Donnell, J. H.; O'Sullivan, P. W. *Macromolecules* **1982**, *15*, 960.
12. Bevington, J. C.; Ebdon, J.R.; Huckerby, T.N. *Eur. Polym. J.* **1985**, *21*, 685.
13. Chang, Y.; McCormick, C. L. *Macromolecules* **1993**, *26*, 4814.
14. Otsu, T.; Tatsumi, A.; Matsumoto, A. *J. Polym. Sci., Polym. Lett. Ed.* **1986**, *24*, 113.
15. Nair, C. P. R. *Macromolecules* **1993**, *26*, 47.

16. Oishi, T.; Kamori, A.; Fujimoto, M. *J. Macromol. Sci.-Pure Appl. Chem.* **1992**, A29(3), 231.
17. Oishi, T.; Kagawa, K.; Fujimoto, M. *Macromolecules* **1993**, *26*, 24.
18. Kurusu, Y.; Nishiyama, H.; Okawara, M. *J. Chem. Soc. Jap. Ind. Chem. Sec.* **1967**, *70*, 593.
19. Rudolph, H.; Rosenkranz, H. J.; Heine, H. G. *Appl. Polym. Symp.* **1975**, *26*, 157.
20. Klos, R.; Gruber, H.; Greber, G. *J. Macromol. Sci. Chem. A*, **1991**, *28*, 925.
21. Gupta, S. N.; Thijs, L.; Neckers, D. C. *J. Polym. Sci., Polym. Chem. Ed.* **1981**, *19*, 855.
22. Gupta, I.; Gupta, S. N.; Neckers, D. C. *J. Polym. Sci., Polym. Chem. Ed.* **1982**, *20*, 147.
23. Otsu, T.; Yamashita, K.; Tsuda, K. *Macromolecules* **1986**, *19*, 287.
24. Yamashita, K.; Nakano, A.; Tsuda, K. *J. Appl. Polym. Sci.* **1988**, *35*, 465.
25. Barton, D.H.R.; George, M. V.; Tomoeda, M . *J. Chem. Soc.* **1962**, 1967.
26. Weir, D.; Ajayaghosh, A.; Muneer, M.; George, M. V. *J. Photochem. Photobiol. A: Chem.* **1990**, *52*, 425.
27. Ajayaghosh, A.; Das, S.; George, M. V. *J. Polym. Sci. A: Polym. Chem.* **1993**, *31*, 653.
28. Ajayaghosh, A.; Francis, R.; Das, S. *Eur. Polym. J.* **1993**, *29*, 63.
29. Ajayaghosh, A. *Polymer*, **1995**, *36*, 2049.
30. Ajayaghosh, A.; Francis, R. *Polymer*, **1995**, *36*, 1091.
31. Finemann, M.; Ross, S. *J. Polym. Sci.* **1950**, *5*, 259.
32. Kelen, T.; Tüdös, F. *J. Macromol. Sci. Chem.* **1975**, *A9*, 1.
33. Tidwell, P. W.; Mortimer, G. A. *J. Polym. Sci. Part A.* **1965**, *3*, 369.
34. Alfrey, T. Jr.; Price, C. C. *J. Polym. Sci.* **1947**, *2*, 101.
35. Shupe, I. S. *J. Assoc. Official Agr. Chem.* **1942**, *25*, 495.
36. Stempel, G. H. Jr; Cross, R. P.; Marcella, R. P. *J. Am. Chem. Soc.* **1950**, *72*, 2299.

CHAPTER 3

ROLE OF XANTHATE-DERIVED MONOMERIC INITIATORS IN CONTROLLING THE PHOTOPOLYMERIZATION PROCESSES OF METHYL METHACRYLATE AND STYRENE

3.1. Introduction

Accurate control of polymerization processes leading to the formation of polymers with well-defined end functional groups and narrow molecular weight distributions has great significance in polymer science. Traditionally, control of polymerization processes has been achieved using living polymerization techniques such as anionic[1], cationic[2], step-wise[3], group transfer[4] or co-ordination[5] processes. However, these methods suffer from rigorous synthetic requirements and incompatibility with a variety of functional monomers.[6,7] Therefore, much interest has been recently focused on the preparation of narrow polydispersed polymers having well-defined molecular weights and end functional groups by free radical mechanism due to the ease of polymerization as well as the compatibility with a wide variety of monomers.

Even though, free radical initiated polymerizations are synthetically less rigorous and in some cases offer an alternative route to chain end functionalized polymers, they in general, lack the ability to accurately control molecular weight distribution and end functional groups. This is mainly due to the uncontrollable propagation and termination processes of the growing polymer radicals. However, the contribution of termination decreases with the reduction of radical concentration because termination is a second order process with respect to growing radicals whereas propagation is first order. If a very low concentration of growing radicals is used in a conventional radical process, either dead-end polymerization or uncontrollable high polymers are formed. Therefore, the concept of "living" free radical polymerization has been

introduced in which growing polymer radicals are in dynamic equilibrium with dormant species, which facilitates step-wise incorporation of monomers.[8-10] By this approach accurate control over the molecular weight, polydispersity and end functional groups can be achieved.

"Living" free radical polymerization has undergone tremendous advancement in the past few years, particularly in the area of nitroxide mediated free radical polymerization.[11-14] The success of this approach can be related to the ability of stable nitroxide free radicals such as 2,2,6,6-tetramethylpiperidinyloxy (TEMPO) (**3**), to react at near diffusion controlled rates with the carbon-centered free radical of the growing polymer chain end in a thermally reversible process (Scheme 1). Recently, Hawker and coworkers have reported the use of a modified TEMPO-based initiator **4**, in achieving molecular weight control by a "living" free radical polymerization process (Scheme 2).[15-18]

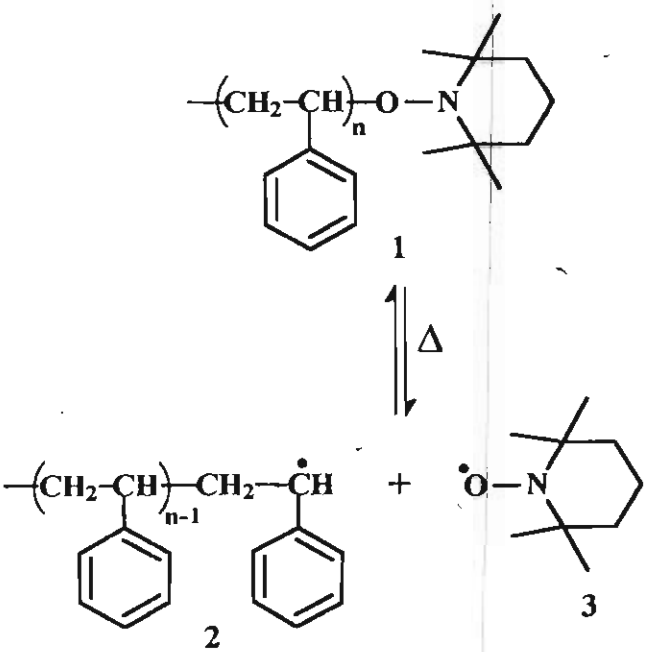

Scheme 1

Wang and Matyjaszewski have reported an alternate strategy for living radical polymerization by atom transfer method using various transition metal complexes.[19] In this method, an alkyl chloride and a CuCl/bipyridyl (bpy) complex was used as initiator and catalyst respectively, for the polymerization of styrene by repetitive atom transfer radical additions to yield well defined high molecular weight polymers with narrow molecular weight distributions.

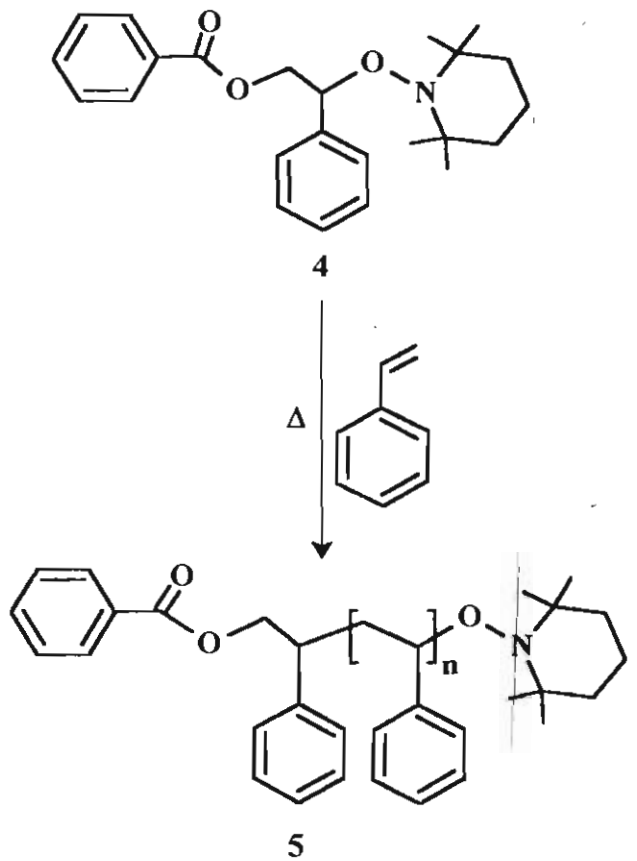

Scheme 2

Another approach towards controlled living radical polymerization involves the use of organometallic compounds such as organocobalt,[20,21] organochromium[22,23] and organoaluminium compounds[24] which reversibly release growing radicals. The synthesis of several narrow molecular weight

distribution polymers has been achieved by living radical polymerizations based on the reversible activation of carbon-halogen bonds using transition metal complexes of ruthenium[25-27] and iron.[28]

All the above described procedures are based on the reversible thermal cleavage of an end capped functional group. On the other hand, photochemical approaches towards controlled polymer synthesis is rather limited except for the photo "iniferter" concept introduced by Otsu et al. [29-32] Photoiniferters are photosensitive molecules which can act as initiator, transfer agent, and terminator. For example, benzyl N,N-diethyldithiocarbamate (6) on UV irradiation yields a pair of radicals: a reactive benzyl radical (7) and a less reactive dithiocarbamyl radical (8). The former can react with a vinyl monomer to initiate the polymerization whereas the latter is a less or non-reactive sulfur centered radical which reacts weakly or not at all with a vinyl monomer but exclusively leads to termination reaction through recombination with a growing polymer chain (Scheme 3). The mechanism is interpreted as analogous to living radical polymerization that involves photodecomposition of the end C-S bond followed by monomer insertion and termination. These processes continue leading to the growth of the polymer chain which is proportional to the monomer conversion. However, this approach is inefficient in many respects, particularly because under UV irradiation the monomers absorb light to undergo self-initiation leading to uncontrolled polymerization. As a result, the polymers obtained by the iniferter approach were found to have polydispersities similar to conventional free radical process. Moreover, several authors have questioned the validity of the living radical polymerization mechanism in the case of iniferter method due to an unavoidable side reaction which occurs during photolysis of dithiocarbamates.[33]

Even though, there are several strategies available for the synthesis of polymers with narrow polydispersities and pre-defined end functional groups, any approach towards their synthesis by conventional free radical chemistry

would be of great interest. This is due to the easy accessibility and compatibility of free radical chemistry with a variety of monomeric systems.

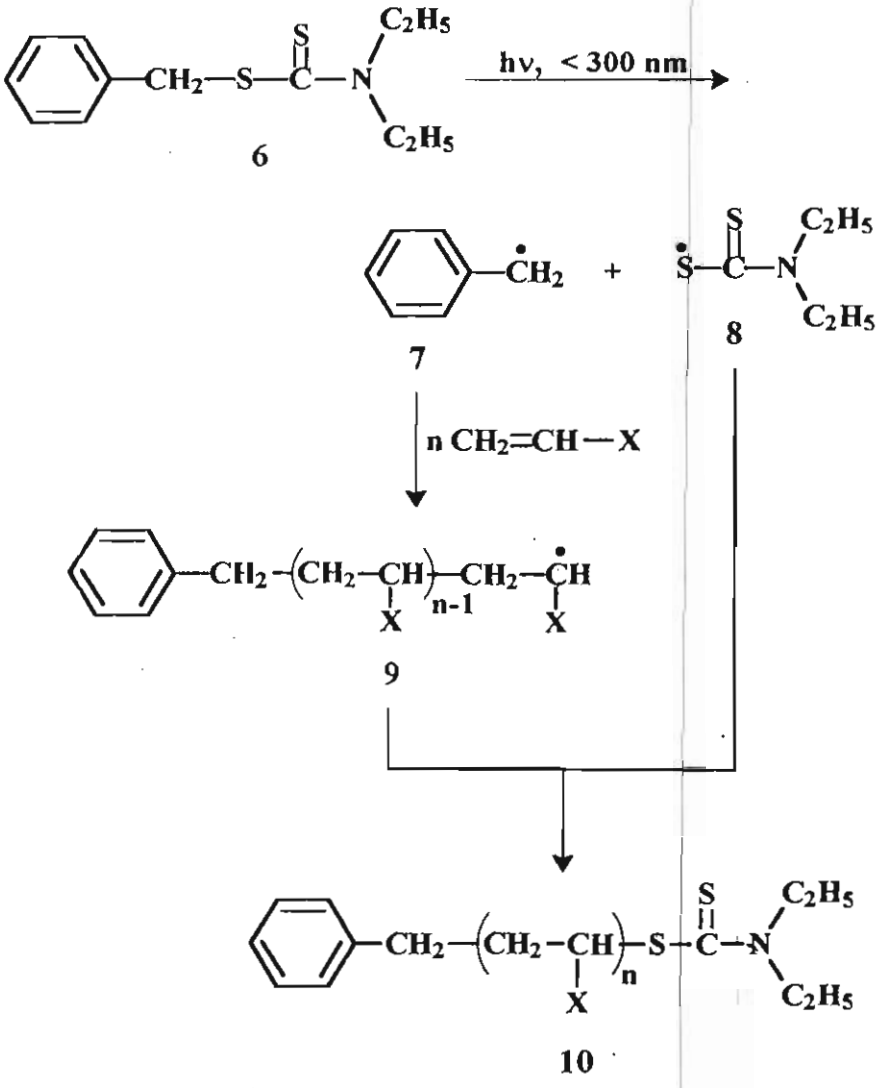

Scheme 3

In photoinitiated free radical polymerizations it would be possible to attain molecular weight and end functional group control by using a photoinitiator which decomposes to give two different free radicals with distinctly different reactivities towards polymerizable double bonds as shown in Scheme 4. In this case, one of the radicals should act as initiator while the other radical behaves as the molecular weight controlling agent. This should be

possible if one of the radicals is a stable resonance stabilized species with strong primary radical termination efficiency. In this way, the overall concentration of the reactive radicals can be controlled and the termination can be restricted to primary radical termination process. In such cases, termination by polymer radical recombination becomes less significant leading to the formation of narrow dispersity polymers.

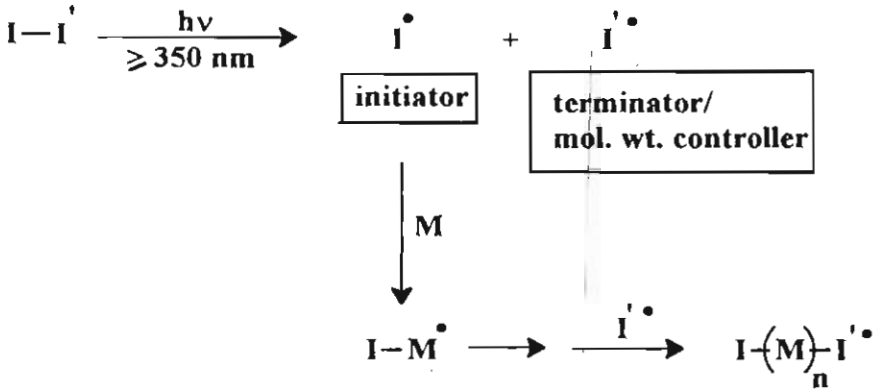

Scheme 4

In the present Chapter we describe the role of three different xanthate derived photoinitiators such as S-methacryloyl O-ethyl xanthate (MAX), S-maleimidobenzoyl O-ethyl xanthate (MBX) and S-(*p*-vinyl)benzoyl O-ethyl xanthate (VBX) in controlling the photopolymerization behaviour of monomers such as methyl methacrylate (MMA) and styrene (St). Choice of these molecules as photoinitiators is mainly based on our earlier studies pertaining to the photochemistry and photoinitiating properties of related systems.[34-36] Based on these reports, acyl and aroyl xanthates on photolysis, undergo homolytic bond cleavage at the (C=O)-S bond position leading to the formation of the corresponding ketyl radical and the thiocarbonylthiyl radical. The ketyl radicals are capable of initiating free radical polymerization of acrylic and vinylic monomers. On the other hand, the thiocarbonylthiyl radical is generally inactive towards initiation of polymerization. However, they show strong

tendency for primary radical termination of the growing polymer radicals thereby controlling the propagation of the polymer chains. The inert nature of thiocarbonylthiyl radicals towards vinyl monomers and their high affinity for termination reaction are well documented in the literature.[37-39] This can be supported by the earlier reports on the photoinduced radical reactions of xanthates and related compounds.[40-42]

3.2. Results and Discussion

The photoinitiators employed in the present study are S-methacryloyl O-ethyl xanthate (MAX), S-(4-maleimido)benzoyl O-ethyl xanthate (MBX), and S-(*p*-vinyl)benzoyl O-ethyl xanthate (VBX). The synthesis and characterization of these monomers are described in Chapter **2** of the present thesis. All the three photoinitiators under investigation showed strong absorption maxima around 285 nm and a relatively weak absorption maximum around 395 nm. All photopolymerizations were performed in Rayonet Photo Reactor (RPR) using 350 nm lamps, unless otherwise stated in order to avoid any possible light absorption by the monomers.

3.2.1. Photopolymerization of MMA and styrene using MAX

The mechanism of photopolymerization of MMA using MAX is shown in Scheme 5. Photolysis of MAX can give the methacryloyl radical **12** and the resonance stabilized sulfur centered radical **13.** In the presence of MMA, the radical **12** would initiate the polymerization, whereas the radical **13** would acts as the molecular weight controller by primary radical termination. The presence of the end functional groups in polymer **16** is clear from the spectral analysis. IR spectra of the PMMA **16** showed a strong peak at 1729 cm^{-1} due to the carbonyl absorption, weak peaks at 1606 and 1043 cm^{-1} due to C=C and C=S, respectively. ^1H NMR spectral analysis (Figure 1) revealed the presence of weak resonance peaks at δ 4.5 and 1.45 due to the O-ethyl protons of the thiocarbonylthiyl group.

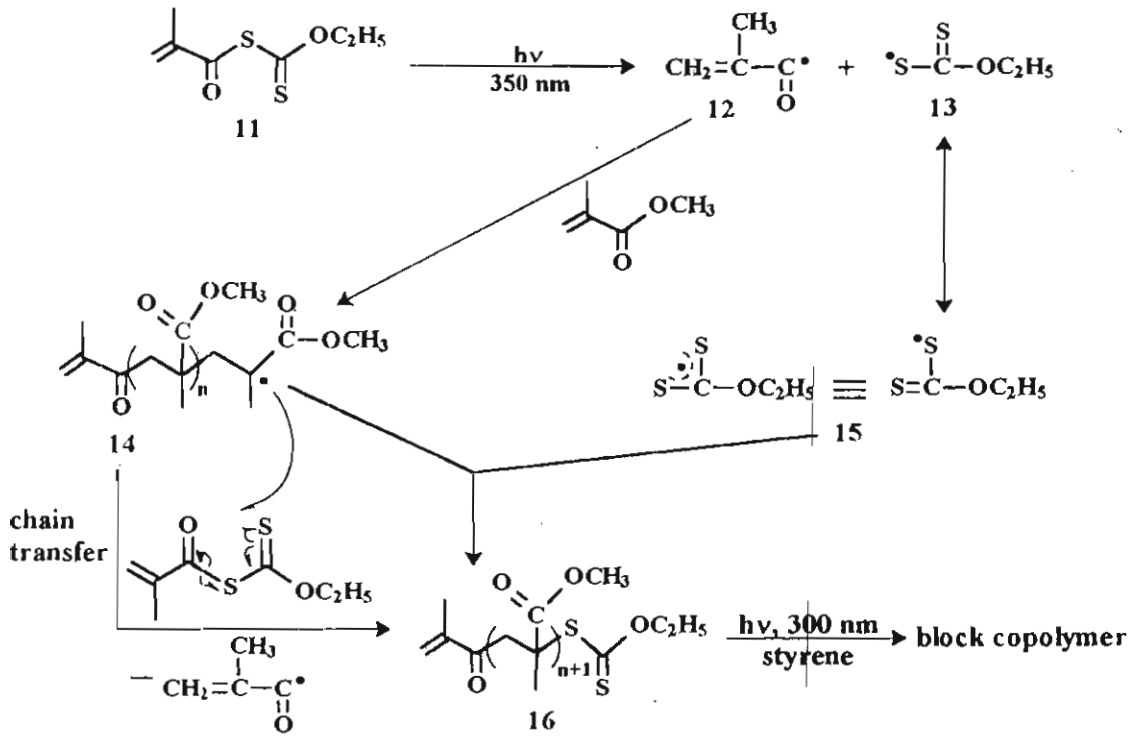

Scheme 5

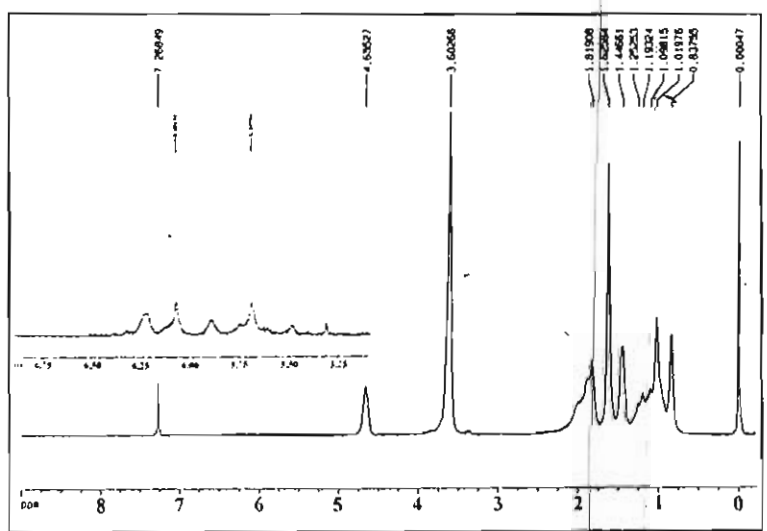

Figure 1. ^{1}H NMR spectrum of PMMA, prepared using MAX

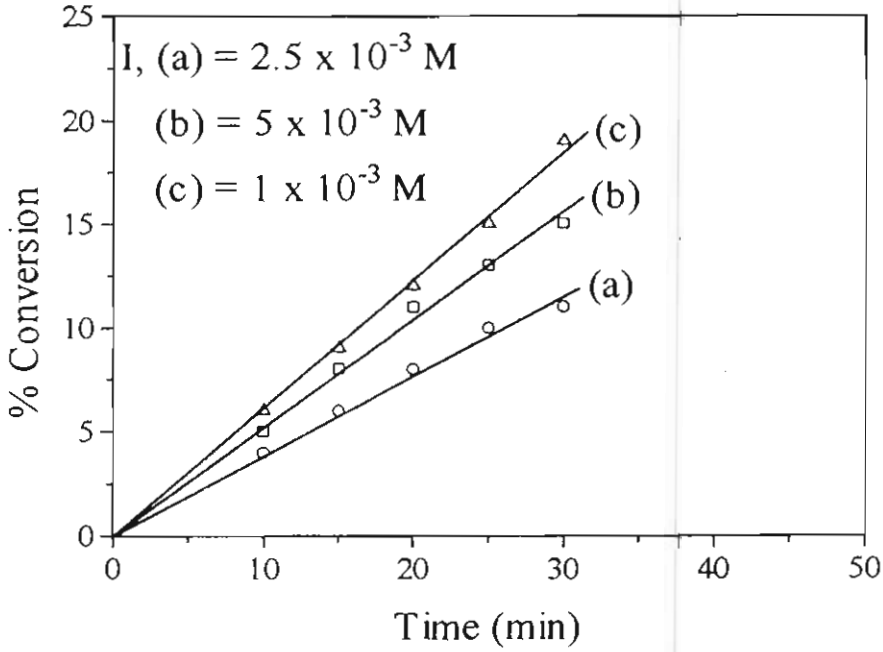

Figure 2. Time-conversion relationship for the photopolymerization of MMA using MAX as photoinitiator. [MMA] = 5 M

The time-conversion relationship for the photopolymerization of MMA at 30 °C using various concentrations of MAX is shown in Figure 2. In all cases, a good linear relationship could be noticed for lower monomer conversion whereas under higher monomer conversion (longer irradiation time) significant deviation from linearity is observed. In all polymerization rate determinations, the initial rates were taken into account since the spontaneous rate of polymerization decreases after a certain period. This may be due to the consumption of the photoinitiator during the course of polymerization. However, a good linear relationship exists between the monomer conversion and the irradiation time during the initial period of polymerization. The rate of polymerization (R_p), the percentage yield, molecular weights, and polydispersities of the polymers obtained for the photopolymerization of MMA using MAX as the photoinitiator are shown in Table 1. A steady increase in the conversion of the monomers could be noticed whereas the R_p was a constant, during the initial periods of polymerization.

Table 1. Results of the photopolymerization* of MMA using MAX as photoinitiator

Run	Time (min)	Conversion (%)	$R_p \times 10^4$ (gs^{-1})	$M_n \times 10^{-4}$	Polydispersity (D) (M_w/M_n)
1	10	5	4.5	2.1	1.4
2	15	8	4.5	2.1	1.3
3	20	11	4.6	2.2	1.4
4	25	13	4.5	2.0	1.3
5	30	15	4.4	1.9	1.2
6	40	16	4.5	1.8	1.3

*[MMA] = 5 M, [MAX] = 5×10^{-3} M, λ_{irr} = 350 nm.

Results of the photopolymerization of MMA using various concentrations of MAX are shown in Table 2. The rate of polymerization showed a linear relationship with the square root of the initiator concentration. However, under higher initiator concentrations (>2 x 10^{-2} M) considerable deviation from the linearity could be noticed. This could probably be due to the chain transfer reaction by the undissociated MAX. The molecular weights of the polymers obtained are found to decrease with increase in MAX concentration, whereas the polydispersity indices (D) remain unaffected. This is clear from Figure 3 in which the molecular weights and polydispersity indices are plotted against the MAX concentration. On the other hand, a linear increase in the molecular weights could be noticed with increase in MMA concentration as shown in Figure 4. Interestingly, the polydispersity indices in all the cases were practically unaffected by the initiator or monomer concentrations and remained lower (M_w/M_n <1.5) than the theoretical value for a conventional free radical polymerization.

Table 2. Effect of MAX concentration on R_p, M_n and Polydispersity for the photopolymerization of MMA[a)]

Run	[I] x 10^3 (M)	Conversion (%)	Rp x 10^4 (gs^{-1})	M_n x 10^{-4}	Polydispersity (M_w/M_n)
1	2.5	10	2.9	2.7	1.3
2	5.0	15	4.4	2.5	1.3
3	7.5	16	4.6	2.2	1.3
4	10	19	5.2	2.0	1.3
5	25	17	4.9	1.8	1.4
6	50	15	4.1	1.7	1.4

[a)][MMA] = 5 M, time = 30 min, I = MAX, λ_{irr} = 350 nm.

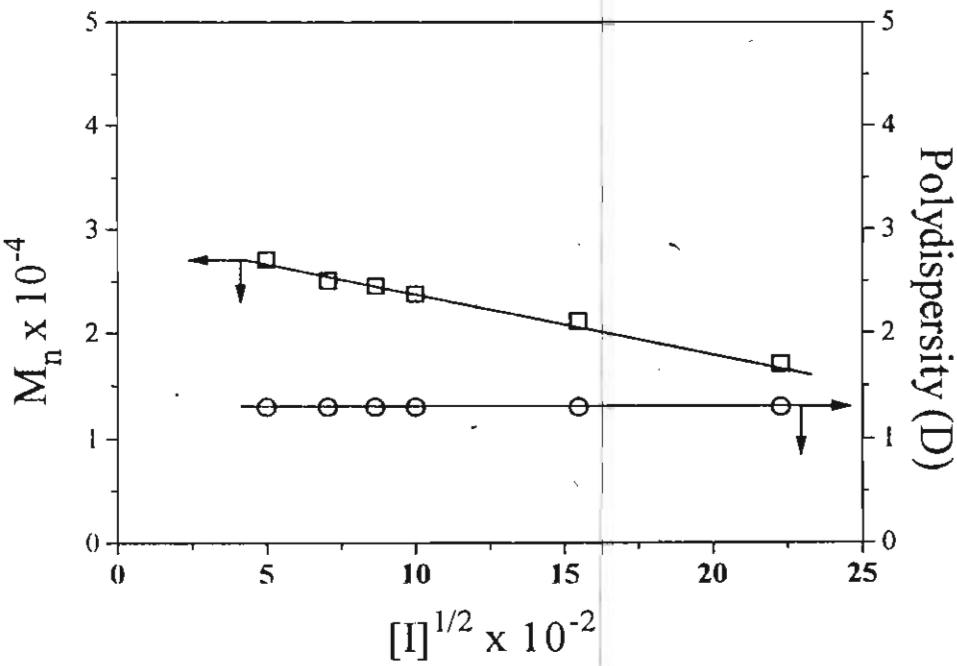

Figure 3. Effect of MAX concentration on M_n and polydispersity indices for the photopolymerization of MMA. [MMA] = 5 M.

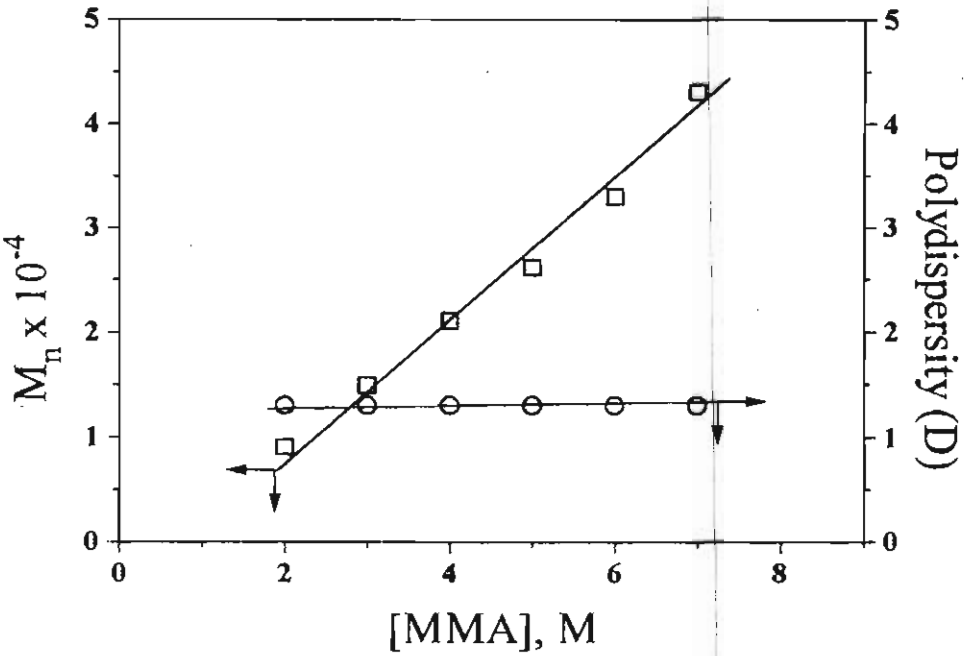

Figure 4. Effect of MMA concentration on M_n and polydispersity of PMMA. [MAX] = 5 x 10^{-3} M.

A plot of irradiation time against molecular weights and polydispersities of PMMA obtained during the photopolymerization of MMA using MAX as the photoinitiator is shown in Figure 5. It has been found that both molecular weights and polydispersities did not vary much with the polymerization time. These results reveal that even though the photopolymerization of MMA using MAX has the characteristic of a simple free radical initiated polymerization mechanism, considerable control in the polydispersity can be achieved in this case. This could be due to the control of the termination of the growing polymer radicals mainly by the bimolecular radical recombination with the thiocarbonylthiyl radical. In addition, the molecular weights of polymers can be predefined by choosing appropriate initiator and monomer concentrations.[43]

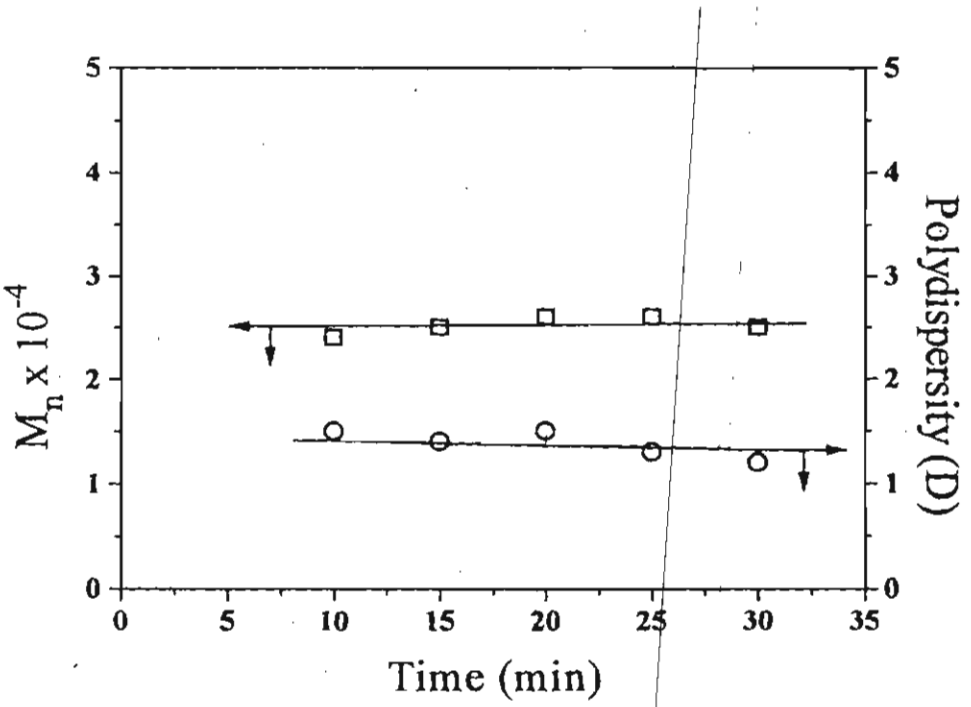

Figure 5. Effect of irradiation time on molecular weight (M_n) and polydispersity (D) for the photopolymerization of MMA (5 M) using MAX (5×10^{-3} M).

The results of the photopolymerization of styrene under various monomer and initiator concentrations are summarized in Table 3. The rate of polymerization and yield of polymer were considerably lower in the case of styrene polymerization. Even under bulk polymerization condition, the R_p for the photopolymerization of St was too low when compared to that of MMA. Surprisingly, photopolymerization of styrene showed significant increase in molecular weights as well as polydispersities with polymerization time as shown in Table 4, which is in contrast to the photopolymerization of MMA. Plots of the molecular weights and polydispersities against the time of irradiation showed linear increases as shown in Figure 6. It has been found that high concentrations of the initiator are required for obtaining reasonably good yields of polymers. Prolonged irradiation of bulk styrene using MAX resulted

in the formation of thick polymeric gels due to crosslinking. However, much better control over the molecular weights and dispersities could be obtained when the polymerizations of styrene were performed in benzene (4.5 M).

Table 3. Results of the photopolymerization* of styrene under various monomer and initiator concentrations using MAX

Styrene [M]	MAX [M]	Time (h)	Yield (%)	$M_n \times 10^{-4}$	Polydispersity (M_w/M_n)
Bulk	5×10^{-2}	1	6	2.9	1.7
Bulk	5×10^{-2}	2	12	5.6	3.4
Bulk	1×10^{-1}	4	29	gel	-
4.5 [a)]	4.5×10^{-1}	1	4	1.3	1.1
4.5 [a)]	4.5×10^{-1}	4	15	1.7	1.2
4.5 [a)]	4.5×10^{-1}	7	29	2.5	1.6

*in benzene

Table 4. Effect of irradiation time on the photopolymerization* of styrene using MAX as photoinitiator

Run	Time (min)	Conversion (%)	$R_p \times 10^4$ (gs^{-1})	$M_n \times 10^{-4}$	Polydispersity (M_w/M_n)
1	30	2	1.0	1.9	1.4
2	60	6	1.4	2.9	1.7
3	90	10	1.7	3.7	2.3
4	120	12	1.5	5.6	3.4

*Styrene = Bulk, [MAX] = 5×10^{-2} M.

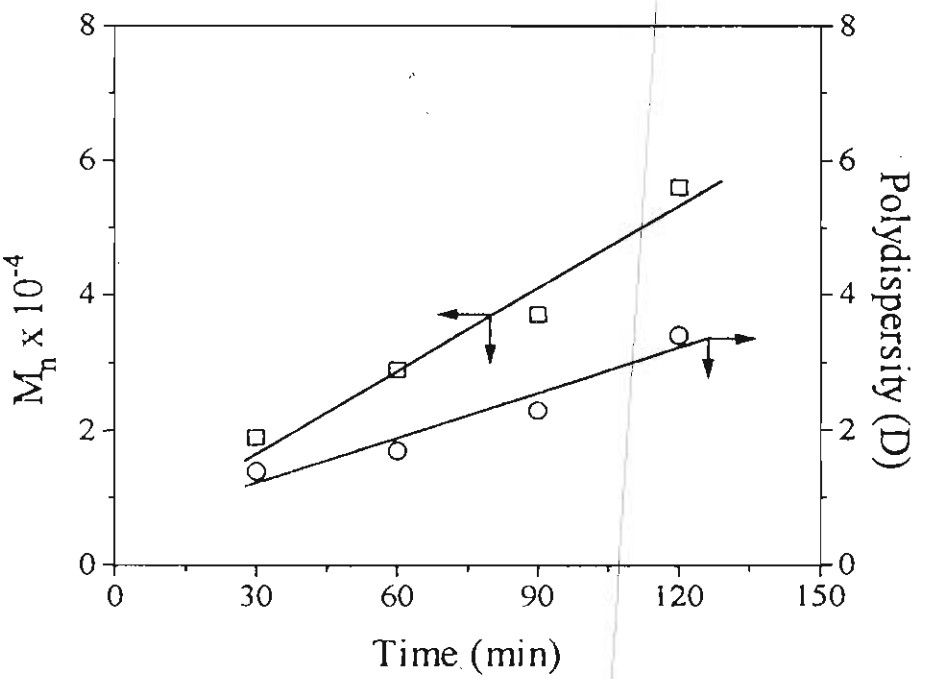

Figure 6. Effect of irradiation time on the molecular weight (M_n) and polydispersity for the photopolymerization of styrene using MAX. [MAX] = 5 x 10^{-2} M

This observation is similar to that of the 'iniferter' photopolymerization of styrene as reported earlier by Otsu et al. using 4-vinylbenzyldithiocarbamate as the photoinitiator.[31] In our case, for the 'iniferter' mechanism to operate, the end thiocarbonylthiyl group of each terminated polymer chain should be photodissociable to form a terminal radical centre on the polymer. This cannot happen in the present case because under 350 nm irradiation the C-S bond of the end thiocarbonylthiyl group is not photodissociable. This has been further confirmed by irradiating S-benzyl O-ethyl xanthate (17) at 350 nm in benzene, which revealed no change to the compound (Scheme 6).

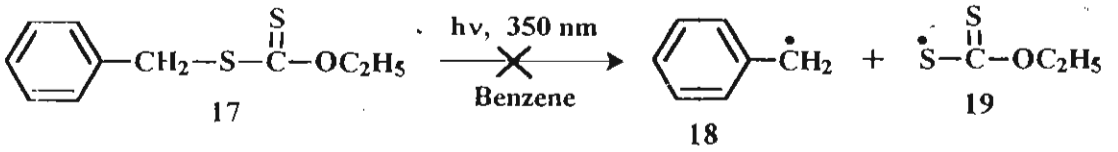

17 18 19

Scheme 6

Based on the above observations, a living radical process by the 'iniferter' mechanism can be ruled out. In this context, a possible pathway for the growth in the molecular weight and polydispersity of polystyrene can be explained on the basis of a graft polymerization mechanism as shown in Scheme 7. In this case in addition to its role as the photoinitiator, MAX is tempted to act as a comonomer by styrene (St), resulting in the incorporation of small amounts of MAX into polystyrene. This is supported by our earlier observation regarding the tendency of MAX to form alternate copolymer during its thermal copolymerization with styrene (Chapter 2). The pendant xanthate chromophore thus formed undergoes photodissociation to form free radical centres on the polystyrene chain that can initiate grafting of monomers thereby enhancing the molecular weight.

In order to support the role of the polymerizable double bond in MAX during the photopolymerization of styrene as postulated in Scheme 7, we have carried out the photopolymerization of styrene using S-benzoyl O-ethyl xanthate (BX) as the photoinitiator instead of MAX. BX was chosen because it does not posses a polymerizable double bond thereby preventing any possible copolymerization of styrene with the initiator. In this case, the polymer obtained after irradiation for 30 min and 120 min showed molecular weights of 1.81×10^4 and 1.76×10^4, respectively (Table 5) indicating no growth in the molecular weight.

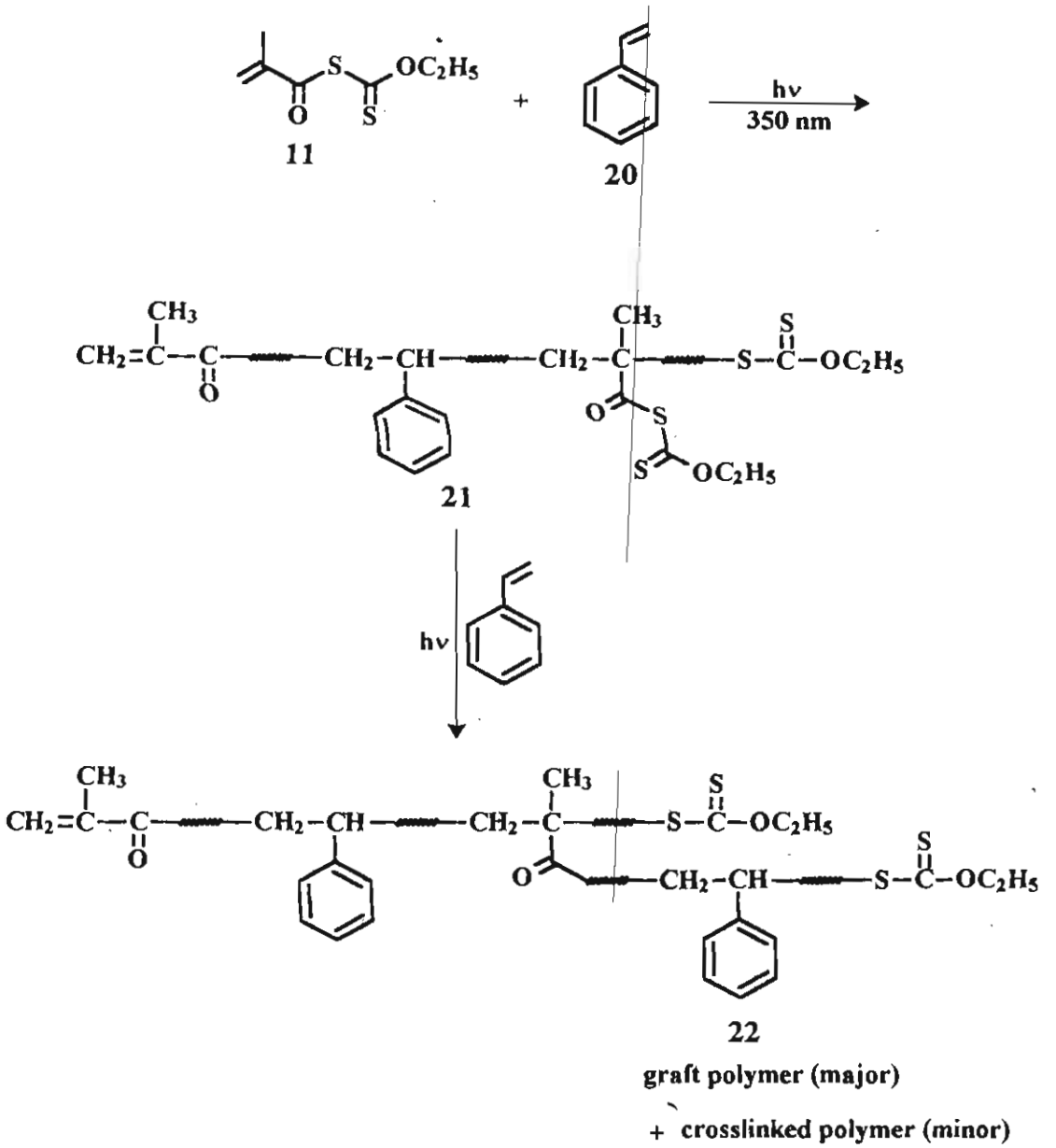

Scheme 7

A comparison of the results of photopolymerization of MMA and St using MAX as the photoinitiator clearly reveals that MAX plays the dual role of a photoinitiator as well as a comonomer during photopolymerization of styrene.

Table 5. Photopolymerization of styrene using benzoyl xanthate* (BX) at 350 nm.

Time (min)	Conversion (%)	$R_p \times 10^5$ (gs^{-1})	$M_n \times 10^{-4}$	M_w/M_n
30	2	7.2	1.81	1.4
120	8	9.2	1.76	1.4

*[BX] = 5×10^{-2} M

3.2.2. Photopolymerization of MMA and styrene using MBX

Photopolymerization of MMA using MBX was carried out under identical experimental conditions as in the case of the photopolymerization of MMA using MAX as the photoinitiator and the data obtained are shown in Table 6. Plots of the percentage yields of PMMA obtained under different initiator concentrations against the time of irradiation are shown in Figure 7. A linear relationship could be noticed during the initial periods of irradiation as in the case of MAX. Similarly, a linear decrease in the molecular weights could be noticed with the increase in the MBX concentrations whereas the dispersity values did not show much variation as shown in Figure 8. The rates of polymerizations and the yields of polymers obtained are comparable to each other except that the number average molecular weights of the PMMA obtained using MBX were nearly double than those obtained using MAX. For example, the number average molecular weights of the PMMA prepared using 5×10^{-3} M MAX and 5×10^{-3} M MBX were 25000 and 54000 amu, respectively. A possible explanation for the enhanced molecular weights can be obtained by considering the photochemical 2+2 cycloaddition of maleimides in benzene. There are several reports in the literature pertaining to the photochemical cycloaddition reactions of maleimides.[44,45] For example maleimides and N-substituted maleimides undergo photoaddition to benzene

resulting in the formation of a bis adduct (**25**) as shown in Scheme 8.[46,47] Based on this report it is reasonable to anticipate an analogous photoaddition of polymer end-capped with maleimido groups to benzene leading to high molecular weight polymeric bisadducts of the structure **29** (Scheme 9).

Table 6. Results of the photopolymerization* of MMA using MBX as photoinitiator

Run	Time (min)	Conversion (%)	$R_p \times 10^4$ (gs^{-1})	$M_n \times 10^{-4}$	Polydispersity (D) (M_w/M_n)
1	10	5	4.2	5.5	1.4
2	15	7	4.1	5.3	1.3
3	25	13	4.3	5.1	1.4
4	30	16	4.4	5.4	1.4
5	40	18	4.2	5.2	1.5

* [MMA] = 5 M, [MBX] = 5×10^{-3} M.

Supporting evidence for the molecular weight enhancement as per the mechanism suggested in Scheme 9 can be obtained from the ^{1}H NMR spectra of polymer **29** which is shown in Figure 10. The inset in Figure 9 corresponds to the zoomed portion of the spectra between δ 4-9 ppm. The resonance peaks at δ 7.9 and 7.4 corresponds to the aromatic protons and 6.6 corresponds to the vinylic protons of the bis adduct of the end maleimidobenzoyl group of the polymer **28**.

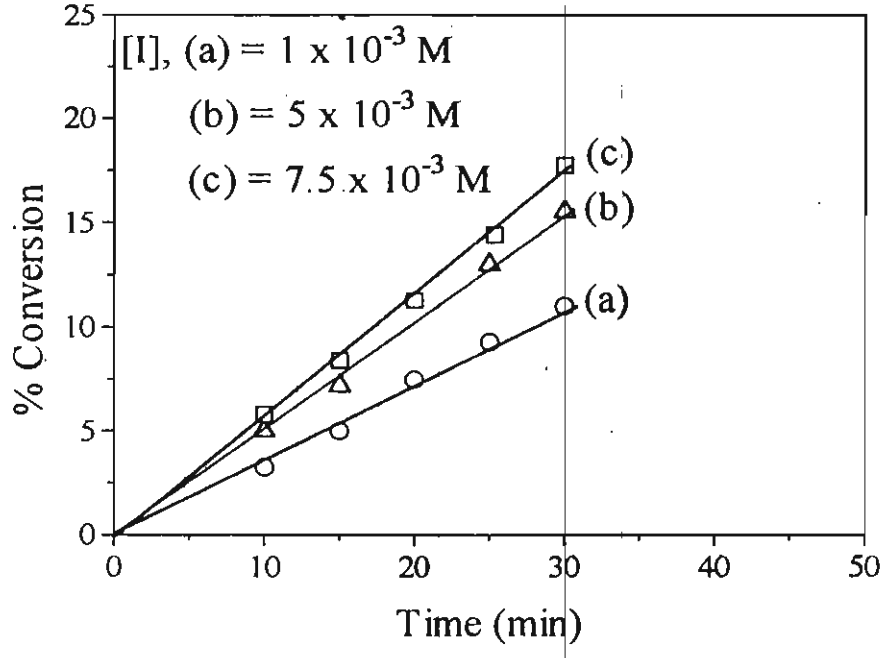

Figure 7. Plot of % yields of PMMA vs. irradiation time using MBX as photoinitiator. [MMA] = 5 M

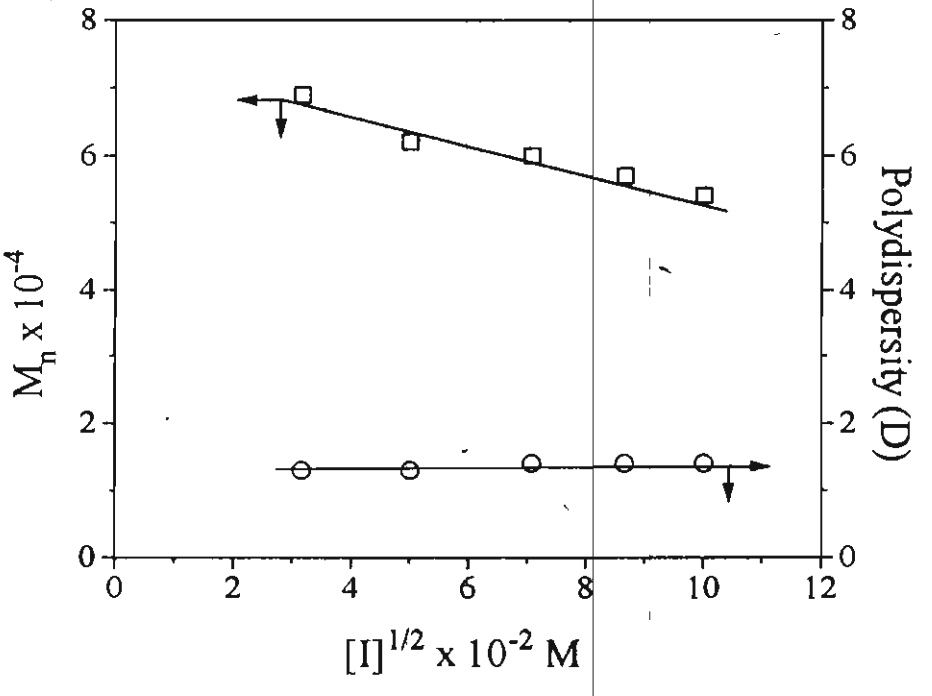

Figure 8. Effect of MBX concentration on M_n and polydispersity for the photopolymerization of MMA. [MMA] = 5 M

The resonance peak at δ 4.7 corresponds to the OCH_2 protons of the end capped thiocrbonylthiyl group. It was difficult to observe these protons in the normal NMR spectra due to their extremely low concentrations in polymer 29.

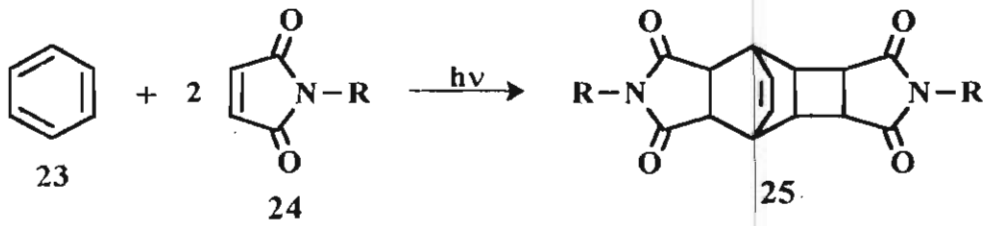

Scheme 8

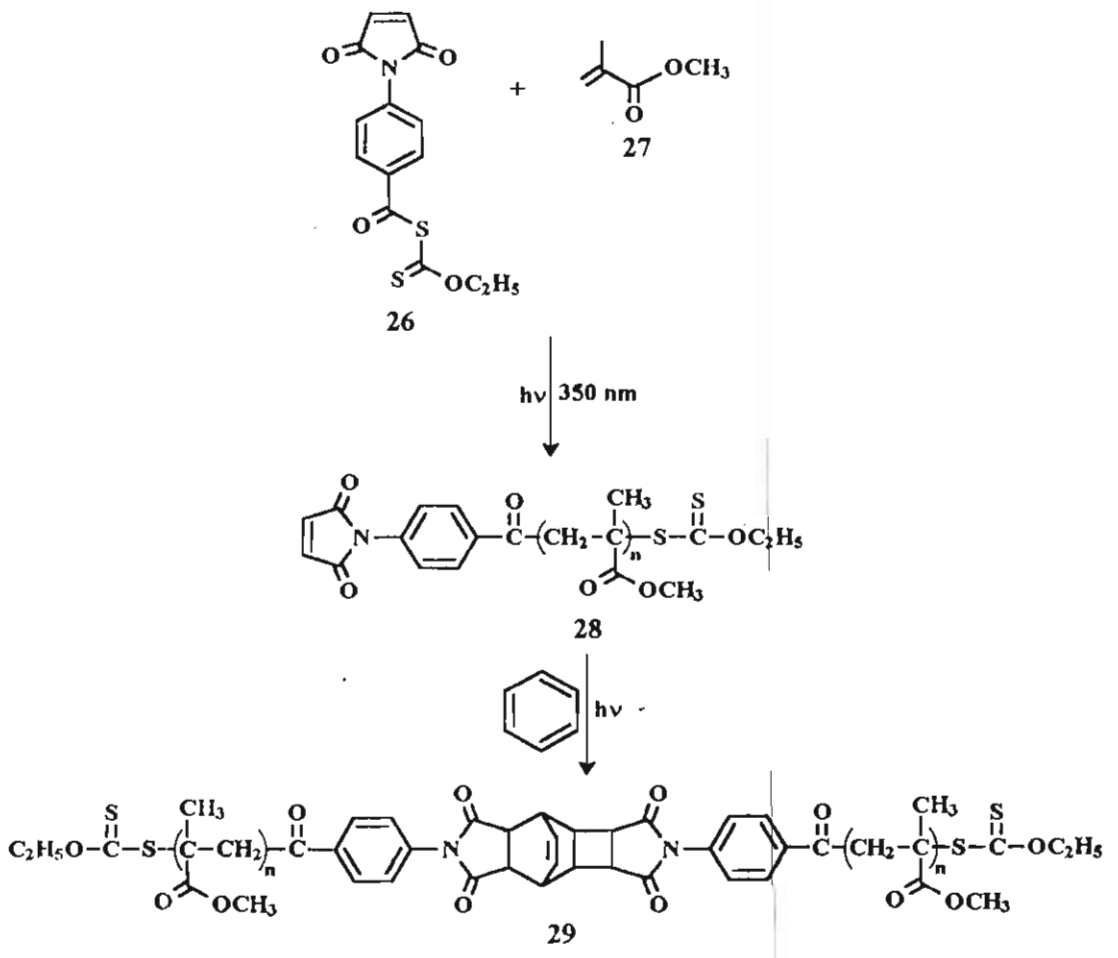

Scheme 9

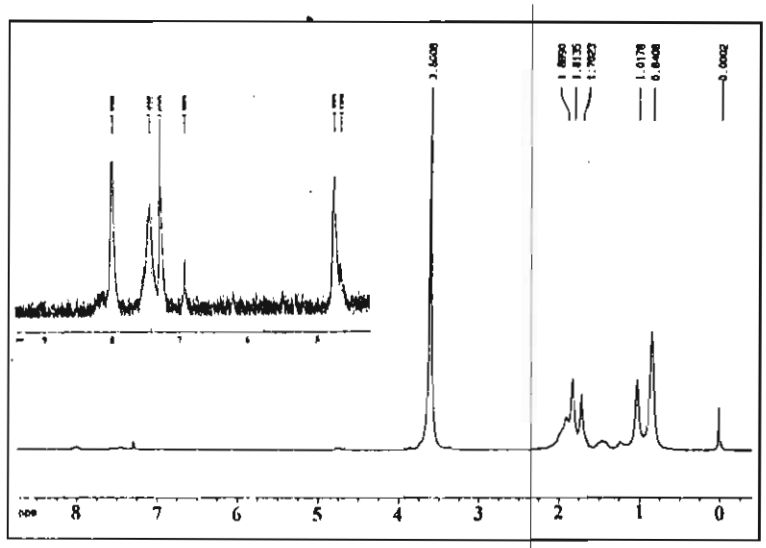

Figure 9. ^{1}H NMR spectrum of PMMA prepared using MBX

Photopolymerization of St using MBX was found to be significantly different from that of the photopolymerization of MMA. The polymerization mixture became a thick gel on prolonged irradiation especially when higher concentrations of MBX were used as the initiator. Considerable amounts of crosslinked and extremely high molecular weight polymers have been obtained in this case. The amount of soluble polymer obtained was significantly low. This can be explained on the basis of the free radical induced thermal copolymerization behaviour of MBX with styrene (St). As described in Chapter 2 of this thesis, copolymerization of MBX and St leads to the formation of alternate copolymers due to a weak interaction between the electron deficient MBX and electron rich St. Thus, considerable amount of MBX is incorporated into polystyrene backbone when St is photopolymerized using MBX as photoinitiator. The pendant xanthate chromophore thus formed can initiate grafting of St and MBX monomers as shown in Scheme 10. Thus, simultaneous copolymerization and grafting will occur to form highly branched and crosslinked polymers with extremely high molecular weights. Further enhancement in molecular weight may be possible by the photocycloaddition of the end-capped maleimido group to form polymeric bisadducts. Since MBX

has the dual role of a monomer as well as an initiator, increase in its concentration in the polymerization mixture has significant influence on the macromolecular architecture. Therefore, photopolymerization of styrene under high MBX concentration lead to photogelation of the polymerization mixture due to crosslinking reactions. Under high MBX concentration considerable amounts of styrene-MBX alternate copolymers will be formed which can initiate multi-branch grafting and crosslinking leading to complex macromolecular structures.

In order to get a better view of the macromolecular structure and the molecular weights, attempts have been made to restrict the gelation and crosslinking in the case of the photopolymerization of styrene using MBX. This has been achieved by irradiating styrene under extremely low concentrations of MBX and restricting the total monomer conversion to below 10%. In this way, the incorporation of MBX into the polystyrene backbone could be minimized thereby controlling the amount of grafting, branching and crosslinking reactions. The polymers obtained in these cases were soluble in chloroform and THF, which allowed the determination of their molecular weights (Table 7).

Table 7. Results of the photopolymerization of styrene (bulk) using low concentration of MBX*

Run	Time (min)	Conversion (%)	$R_p \times 10^5$ (gs^{-1})	$M_n \times 10^{-6}$	Polydispersity (D) (M_w/M_n)
1	60	2	4.4	1.2	1.1
2	90	3	4.4	1.3	1.1
3	120	4	4.3	1.2	1.1
4	150	5	4.4	1.2	1.1

*[MBX] = 5×10^{-4} M

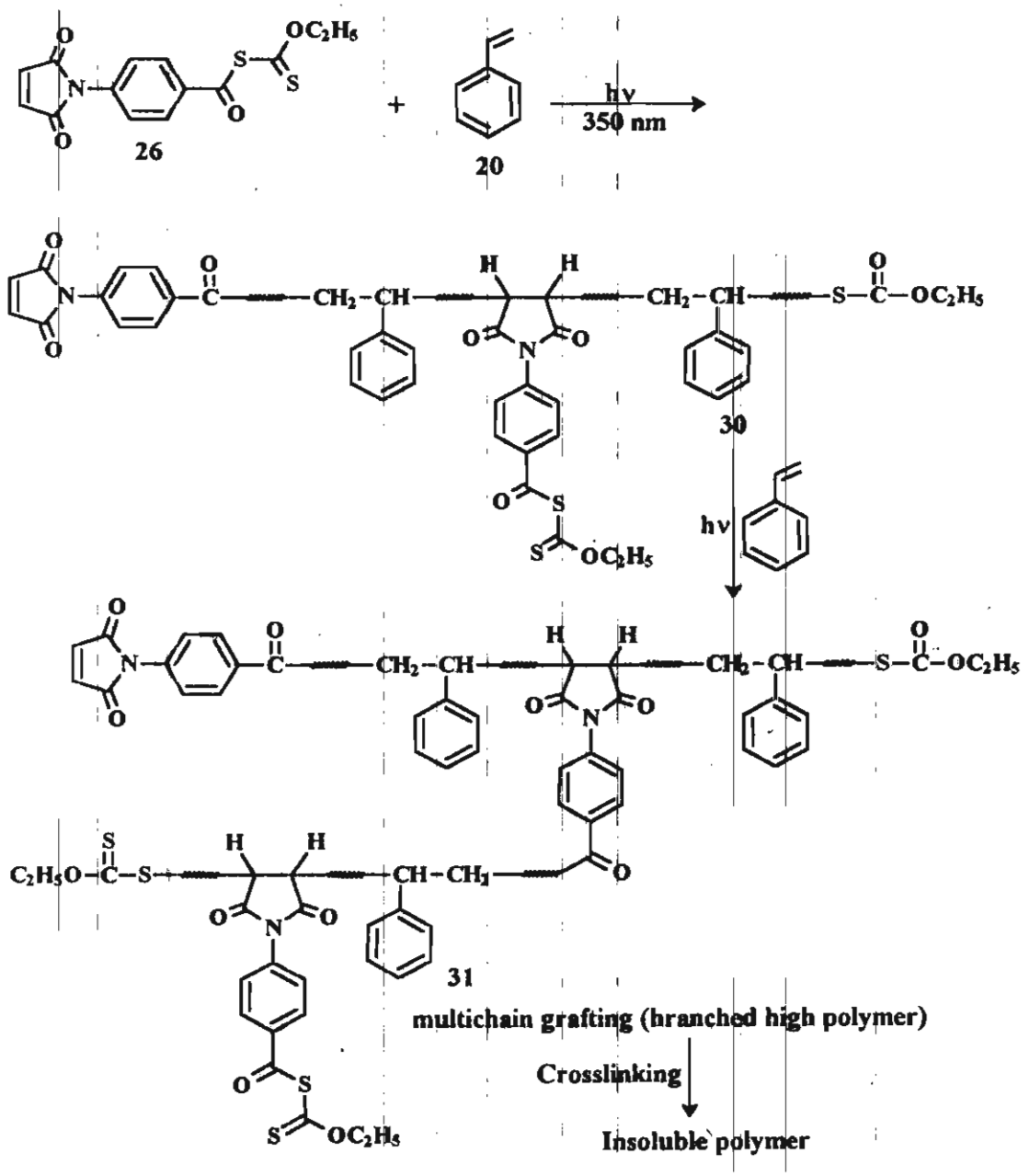
26
20
hν
350 nm
30
hν
31
multichain grafting (branched high polymer)
Crosslinking
Insoluble polymer

Scheme 10

The GPC analysis of soluble polymers showed unusually high molecular weights, which are of the order of 10^6 amu. These extremely high molecular weights could be due to the formation hyper-branched graft copolymers as per the mechanism suggested in Scheme 10. The IR spectra of these copolymers showed weak carbonyl absorption due to the maleimido groups. However, the absorption peak of the thiocarbonylthiyl end functional group was not visible probably due to its extremely low concentration in the high molecular weight hyper-branched polymer.

3.2.3. Photopolymerization of MMA and styrene using VBX

The results of the photopolymerization of MMA using VBX as the photoinitiator are shown in Table 8. As in the case of MAX and MBX a linear increase in percentage yields of the polymer was noticed during the initial periods of irradiation as shown in Figure 10. Interestingly, in contrast to the photopolymerization of MMA using MAX and MBX, a marginal increase in the molecular weight and polydispersity with time of irradiation could be noticed for the photopolymerization of MMA when VBX is used as the photoinitiator. This enhancement in molecular weight has similarity to that in a living free radical polymerization. However, if this is the case the growth in molecular weights should have also occurred with the other two initiators. Since, this is not the case, the living radical mechanism can be ruled out. An alternate possibility for the increase in molecular weights could be due to the incorporation of VBX on to the polymer chain. This dual role of VBX as a photoinitiator as well as a comonomer can be explained on the basis of its high reactivity towards free radical induced polymerization reaction. This will lead to the partial incorporation of VBX on to the PMMA main chain. The pendant xanthate chromophore thus formed will undergo photolysis, which will facilitate the grafting of monomers as shown in Scheme 11.

Table 8. Results of the photopolymerization* of MMA using VBX as photoinitiator

Run	Time (min)	Conversion (%)	$R_p \times 10^4$ (gs^{-1})	$M_n \times 10^{-4}$	Polydispersity (D) (M_w/M_n)
1	10	5	3.8	5.3	1.3
2	20	9	3.8	5.3	1.4
3	30	14	3.8	5.5	1.4
4	40	19	3.8	5.8	1.5
5	50	22	3.7	5.9	1.6

* [MMA] = 5 M, [VBX] = 5×10^{-3} M.

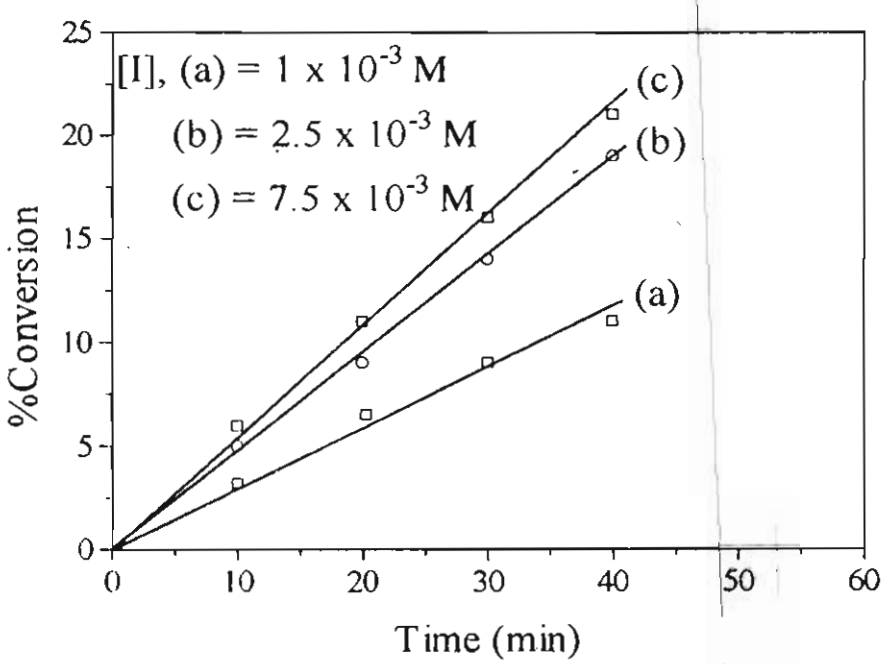

Figure 10. Effect of time on % conversion for the photopolymerization of MMA using VBX as photoinitiator. [MMA] = 5 M

Thus VBX plays a dual role of a photoinitiator as well as a comonomer during photopolymerization of MMA. On the other hand, MAX and MBX show this property only towards styrene. However, the observed decrease in the molecular weights of polymers with increase in VBX concentration is comparable to those of MMA using MAX and MBX (Figure 11).

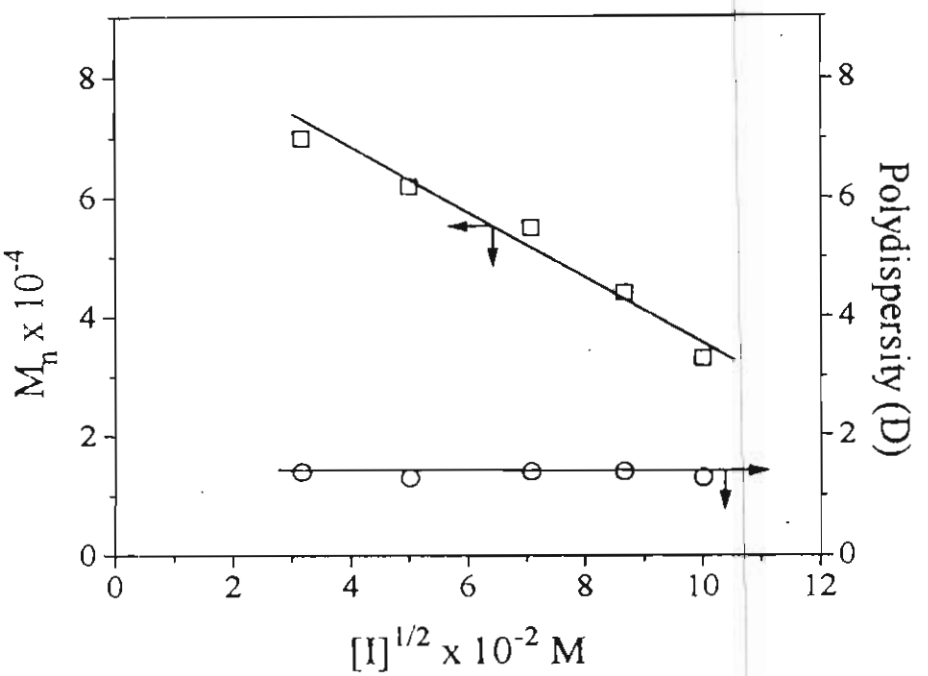

Figure 11. Effect of VBX concentration on M_n and polydispersity for the photopolymerization of MMA

The results of the photopolymerization of styrene using VBX are summarized in Table 9. In contrast to the results obtained for MBX, the photopolymerization of styrene using VBX gave polymers with relatively low molecular weights. As in the case of the polymerization of MMA, marginal increase in molecular weights could be observed for polymerization of styrene. The data obtained for the photopolymerization of styrene using VBX indicates that it does not have any special preference towards styrene during the

photopolymerization reaction. However, the possibility of random incorporation of minor amounts of VBX into PMMA or polystyrene cannot be ruled out which is responsible for the slow increase in molecular weights of polymers formed during photopolymerization.

According to the mechanism suggested in Scheme 11, the polymer formed is expected to contain a vinylic double bond and a thiocarbonylthiyl group at the chain ends. The ^{1}H NMR spectra of the polymer obtained from the photopolymerization of MMA is shown in Figure 12. Weak resonance peaks corresponding to the aromatic and vinylic protons could be observed between δ 4.5-8.0 ppm. In addition, the OCH_2 protons of the thiocarbonylthiyl moiety were visible at δ 4.5 ppm.

Table 9. Results of the photopolymerization of styrene (bulk) using VBX* as photoinitiator

Run	Time (min)	Conversion (%)	$R_p \times 10^5$ (gs^{-1})	$M_n \times 10^{-4}$	Polydispersity (D) (M_w/M_n)
1	30	2	9.4	3.1	1.5
2	50	4	10.7	3.2	1.5
3	70	5	10.5	3.5	1.5
4	100	7	10.4	4.0	1.6
5	150	8	8.1	4.2	1.6
6	240	15	9.5	4.6	1.6

*[VBX] = 7.5×10^{-3} M.

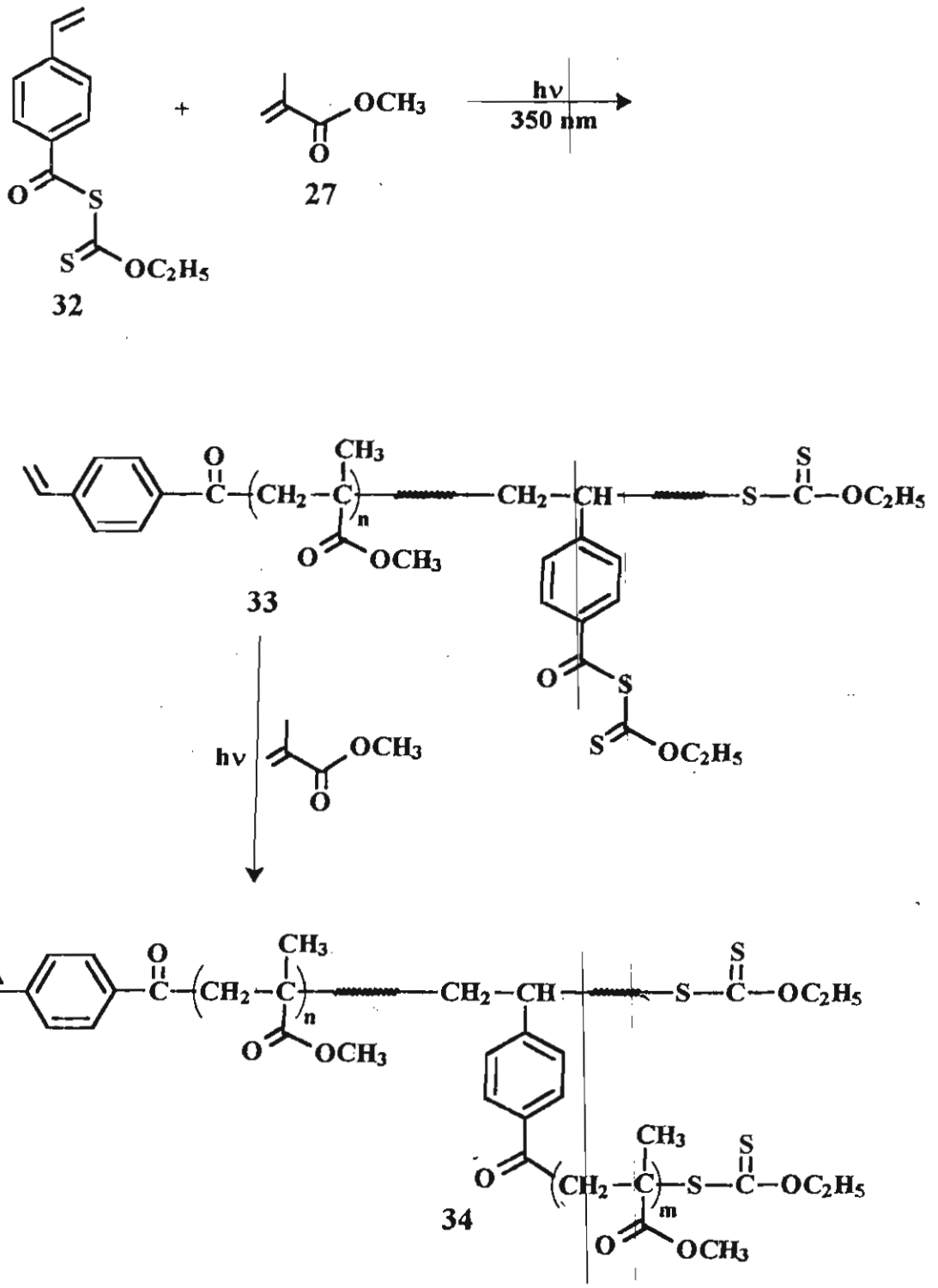

Scheme 11

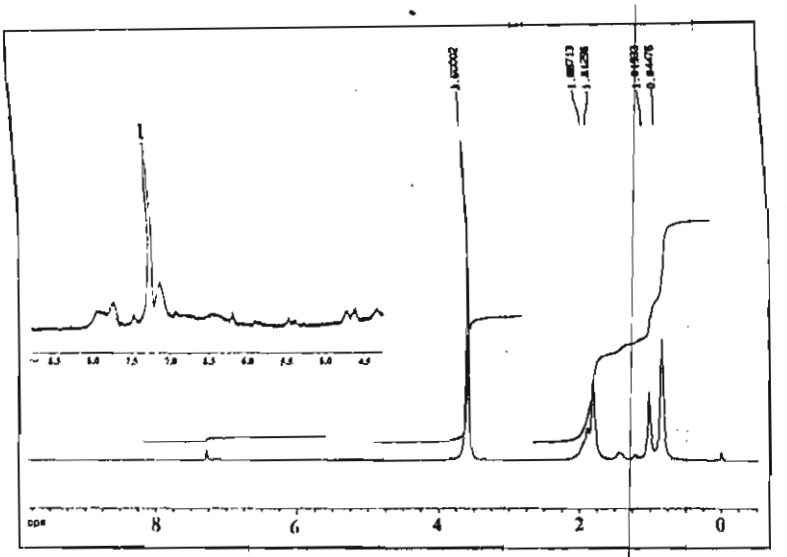

Figure 12. ^{1}H NMR spectrum of PMMA, prepared using VBX

In conclusion, the above results reveal that, even though the photopolymerization of MMA and St using MAX, MBX or VBX has the characteristics of a simple free radical polymerization, their mode of termination is basically different from the conventional free radical polymerization processes. All the three monomeric photoinitiators show distinctly different behaviour towards MMA and St. Novelty of the new photoinitiators for the photopolymerization of MMA is that the molecular weights of polymers can be pre-defined by the initiator concentration. Interestingly, the polydispersity indices of polymers prepared using all the photoinitiators under investigation were lower than 1.5, indicating significant control over the polymerization processes for the photopolymerization of MMA. However, in the case of the photopolymerization of styrene using MAX and MBX, considerable amounts of high molecular weight graft and crosslinked polymers were formed. This has been explained on the basis of a weak interaction between the electron rich St and the electron deficient MAX

and MBX. Interestingly, the photopolymerization of MMA and St using VBX did not show any considerable deference in their polymerization mechanism. The data obtained for the photopolymerization of MMA and styrene using the xanthate derived monomeric photoinitiators such as MAX, MBX and VBX reveal that their thermal free radical copolymerization behaviour with MMA and styrene play a significant role in controlling their polymerization behaviour. The photopolymerization of styrene using MAX and MBX facilitate single step preparation of highly branched graft copolymers. The photopolymerization of styrene with MBX is particularly interesting because of its ability to form extremely high molecular weight graft copolymers. This method would also facilitate the synthesis of macroiniferters with well-defined reactive end functional groups, useful for the designing of block and graft copolymers.

3.3. Experimental Section

Infra-red (IR) spectra were recorded on a Perkin-Elmer model 880 spectrometer. The electronic spectra were recorded on a Shimadzu 2100 A spectrophotometer. ^{1}H nuclear magnetic resonance (NMR) spectra were recorded on a Jeol EX 90 or a Bruker DPX 300 spectrometer using $CDCl_3$ as solvent and tetramethylsilane as internal standard. Gel permeation chromatography (GPC) was carried out on a Shimadzu LC-8A GPC system equipped with a refractive index detector. Calibrations were done with standard polystyrene samples. Tetrahydrofuran (THF) was used as the eluent at a flow rate of 1 mL min^{-1} at 28 °C.

The three photoinitiators S-methacryloyl O-ethyl xanthate (MAX), S-maleimidobenzoyl O-ethyl xanthate (MBX) and S-(*p*-vinyl)benzoyl O-ethyl xanthate (VBX) were prepared according to the procedures discussed in Chapter 2. The monomers MMA and styrene were washed twice with 5% aqueous sodium hydroxide to remove the stabilizer and then several times with distilled water. These were then dried over anhydrous sodium sulphate and

distilled under reduced pressure. All solvents were dried and distilled before use.

3.3.1. Photopolymerization: General procedure

Solutions of known concentrations of the required monomer and the photoinitiator in benzene were taken in pyrex tubes (1.4 cm diameter and 15 cm long) and stoppered with rubber septa. They were purged with argon for 10 min and irradiated in a Rayonet Photochemical Reactor (RPR) containing eight 350 nm fluorescent lamps for known periods of time. After irradiation, the contents were poured in to excess methanol and the precipitated polymers were collected by filtration and washed with methanol. Purification of polymers was achieved by reprecipitation of their chloroform solutions from methanol. The polymers were filtered and dried in a vacuum oven (55°C). In representative cases control experiments were done without the photoinitiator, under identical conditions as employed for the photoinitiator. No polymerization occurred in these cases.

3.3.1.1. Photopolymerization of MMA using MAX as photoinitiator

A stock solution of MMA in dry benzene (5 M) containing MAX (5×10^{-3} M) was prepared and 10 mL each of this solution was transferred into different glass tubes. All the glass tubes were stoppered with rubber septa and purged with dry argon for 10 min. After irradiation for definite intervals, the polymers obtained were collected and purified as described in the general procedure. The yields were calculated after drying the purified polymer in a vacuum oven at 50 °C for 24 h. IR ν_{max} (neat) 1729 (C=O), 1606 (C=C), 1255 and 1043 (C=S) cm^{-1}; ^1H NMR ($CDCl_3$, 300 MHz) δ 6.1 (m, CH_2=C), 4.7 (m, OCH_2), 3.6 (m, CH_3), 1.8-0.8 (m, aliphatic); $M_n = 2.5 \times 10^4$, M_w/M_n (D) = 1.3.

3.3.1.2. Photopolymerization of styrene (bulk) using MAX as photoinitiator

Styrene (9.09 g, 87 mmol) and MAX (190 mg, 1 mmol) were taken in a glass tube and purged with argon for 10 min. The contents were irradiated for 24 h as described above and were poured into excess methanol. After purification, the polymer obtained was dried in a vacuum oven at 50 °C for 24 h. Yield 12 %. IR ν_{max} (neat) 2900 (aromatic), 1729 (C=O), 1606 (C=C), 1255 and 1043 (C=S) cm^{-1}; ^1H NMR ($CDCl_3$, 300 MHz) δ 7.1 (m, aromatic), 4.7 (m, OCH_2), 2.1-1.0 (m, aliphatic); $M_n = 5.6 \times 10^{-3}$, $M_w/M_n = 3.4$.

3.3.1.3. Photopolymerization of styrene (bulk) under higher MAX concentration

MAX (1×10^{-1} M with respect to styrene) was dissolved in styrene (9.09 g, 87 mmol) and this solution was irradiated as described above. After 4 h, the reaction mixture became a thick solid. Chloroform (50 mL) was added to the reaction mixture and the contents were poured into large excess of methanol. The precipitated polymer was collected by filtration, washed with methanol and dried under vacuum. Yield 29%. The molecular weight of the polymer could not be determined since it formed a thick gel in $CHCl_3$, THF and DMF.

3.3.1.4. Photopolymerization of styrene using MAX in benzene

A solution of styrene (4.5 M) and MAX (4.5×10^{-1} M) in dry benzene (10 mL) was taken in a pyrex glass tube and purged with argon for 10 min. The solution was irradiated for 7 h as described earlier. The viscous polymerization mixture was diluted with benzene and poured into methanol. The precipitated polymer was collected, purified as described in the general procedure and dried in a vacuum oven. Yield 29 %. IR ν_{max} (neat) 2900 (aromatic), 1729 (C=O), 1606 (C=C), 1255 and 1043 (C=S) cm^{-1}; ^1H NMR ($CDCl_3$, 300 MHz) δ 7.1 (m, aromatic), 6.1 (m, $CH_2=C(CH_3)$), 4.7 (m, OCH_2), 2.1-1.0 (m, aliphatic); $M_n = 2.5 \times 10^4$, $M_w/M_n = 1.6$.

3.3.1.5. Photopolymerization of MMA using MBX

A stock solution of MMA in dry benzene (5 M) containing MBX (5×10^{-3} M) was prepared and 10 mL each of this solution was transferred into different pyrex glass tubes. All the glass tubes were stoppered with rubber septa and purged with argon for 10 min. Polymerization was performed as described in the general procedure. The yields were calculated after drying the polymer in a vacuum oven at 50 °C for 24 h. IR ν_{max} (neat) 3100 (aromatic), 1729 (C=O), 1606 (C=C), 1255 and 1043 (C=S) cm^{-1}; ^1H NMR ($CDCl_3$, 300 MHz) δ 7.9, 7.4, 6.9 (aromatic), 4.7 (m, OCH_2), 3.6 (s, OCH_3), 1.9-0.8 (m, aliphatic). $M_n = 5.4 \times 10^4$, $M_w/M_n = 1.4$.

3.3.1.6. Photopolymerization of styrene (bulk) using MBX

Styrene (9.09 g, 87 mmol) and MBX (24 mg, 0.07 mmol) were taken in pyrex glass tubes and purged with argon for 10 min. The contents were irradiated as described above. After 20 min, the reaction mixture became a thick solid. Chloroform (50 mL) was added to the reaction mixture and the contents were poured into large excess of methanol. The precipitated polymer was collected by filtration, washed with methanol and dried under vacuum. The molecular weight of the polymer could not be determined since it formed a thick gel in $CHCl_3$, THF and DMF. IR ν_{max} (KBr) 3029 and 2921 (aromatic), 1721 (C=O), 1607 (C=C), 1027 (C=S) cm^{-1}.

3.3.1.7. Photopolymerization of styrene (bulk) under low MBX concentration

MBX (1.6 mg, 5×10^{-3} mmol) was dissolved in styrene (9.09 g, 87 mmol) and this solution was irradiated as described above. After 4 h, the contents were poured into excess methanol. After filtration and washing with methanol, pouring its chloroform solution into methanol further purified the polymer obtained. The precipitated polymer was collected and dried in a vacuum oven. Yield 8 %. IR ν_{max} (neat) 2921 (aromatic),

1702 (C=O), 1219 (C=S) cm^{-1}; ^1H NMR ($CDCl_3$, 300MHz) δ 7.1, 6.5 (aromatic), 1.8-1.4 (aliphatic); $M_n = 1.2 \times 10^6$, $M_w/M_n = 1.1$.

3.3.1.8. Photopolymerization of styrene using MBX in benzene

A solution of styrene (5 M) and MBX (1×10^{-2} M) in dry benzene (10 mL) was taken in a pyrex tube and purged with argon for 10 min. After 6 h of irradiation, the reaction mixture became a thick solid. The contents were diluted with chloroform (20 mL) and poured into excess methanol. The precipitated polymer was collected by filtration, washed with methanol and dried under vacuum. Yield, 30%. The molecular weight of the polymer could not be determined since it formed a thick gel in $CHCl_3$, THF and DMF.

3.3.1.9. Photopolymerization of MMA using VBX

A stock solution of MMA in dry benzene (5 M) containing VBX (5×10^{-3} M) was prepared and 10 mL each of this solution was transferred into different glass tubes. All the glass tubes were stoppered with rubber septa and purged with argon for 10 min. Polymerizations were carried out as per the general procedure. The yields were calculated after drying the polymer in a vacuum oven at 50 °C for 24 h. IR ν_{max} (KBr) 3000 (aromatic), 1731 and 1700 (C=O), 1604 (C=C), 1258 and 1039 (C=S) cm^{-1}; ^1H NMR ($CDCl_3$, 300 MHz) δ 8.1-7.1 (m, aromatic), 6.5-5.5 (m, CH_2=CH), 4.7 (m, OCH_2), 3.6 (s, OCH_3), 1.8-0.8 (aliphatic). $M_n = 5.5 \times 10^4$, $M_w/M_n = 1.4$.

3.3.1.10. Photopolymerization of styrene (bulk) using VBX

Styrene (9.09 g, 87 mmol) and VBX (18.9 mg, 0.075 mmol) were taken in glass tubes and purged with argon for 10 min. The contents were irradiated for 4 h as described above and were poured into excess methanol. The precipitated polystyrene was collected by filtration and washed with methanol. The polymer was redissolved in chloroform and reprecipitated from methanol.

The polymer obtained was dried in a vacuum oven at 50 °C for 24 h. Yield, 15 %. IR ν_{max} (KBr) 3000 (aromatic), 1700 (C=O), 1604 (C=C), 1250 and 1040 (C=S) cm^{-1}. ^1H NMR ($CDCl_3$, 300 MHz) δ 7.1 (m, aromatic), 6.5-5.3(m, CH_2=CH), 4.7 (m, OCH_2), 2.0-1.2 (m, aliphatic). $M_n = 4.6 \times 10^4$, $M_w/M_n = 1.6$.

3.4. References

1. Hirao, A.; Hatttori, I.; Sasagawa, T.; Yamaguchi, K.; Nakahara, S.; Yamazaki, N. *Makromol. Chem., Rapid Commun.* **1982**, *3*, 59.
2. Keszler, B.; Chang, V.S.C.; Kennedy, J. P. *J. Macromol. Sci., Chem.* **1984**, *A21*, 307.
3. Frecht, J.M.J. *Sceince* **1994**, *263*, 1710.
4. Soyali, D. Y.; Hertler, W. R.; Webster, O. W.; Cohen, G. M. *Macromolecules* **1987**, *20*, 1473.
5. Gorman, C. B.; Ginsburg, C. J.; Grubbs, R. H. *J. Am. Chem. Soc.* **1993**, *115*, 1397.
6. Webster, O. *Science* **1991**, *251*, 887.
7. Krstina, J.; Moad, G.; Rizzardo, E.; Winzor, C. L.; Berge, C. T.; Fryd, M. *Macromolecules* **1995**, *28*, 5381.
8. Rizzardo, E. *Chem. Aust.* **1987**, *54*, 32.
9. Solomon, D. H.; Rizzardo, E.; Cacioli, P. *U. S. Patent 4, 581, 429*, March 27, **1985**.
10. Johnson, C. H. L.; Moad, G.; Solomon, D. H.; Spurling, T.; Vearing. D. J. *Aust. J. Chem.* **1990**, *43*, 1215.
11. Georges, M. K.; Veregin, R.P.N.; Kazmaier, P.M.; Hamer, G. K. *Macromolecules* **1993**, *26*, 2987.
12. Geroges, M. K.; Veregin, R. P. N.; Kazmaier, P. M.; Hamer, G. K.; Saban, M. *Macromolecules* **1994**, *27*, 7228.
13. Odell, P.; Veregin, R. P. N.; Michalak, L. M.; Brousmiche, D.; Georges, M. K. *Macromolecules* **1995**, *28*, 8453.
14. Veregin, R. P. N.; Odell, P. G.; Michalak, L. M.; Georges, M. K. *Macromolecules* **1996**, *29*, 3346.
15. Hawker, C. J. *J. Am. Chem. Soc.* **1994**, *116*, 11185.
16. Hawker, C. J. *Angew. Chem. Int. Ed. Engl.* **1995**, *34*, 1456.
17. Hawker, C. J. ; Hedrick, J. L. *Macromolecules* **1995**, *28*, 2993.

18. Hawker, C. J.; Barclay, G. G.; Orellana, A.; Dao, J.; Devonport, W. *Macromolecules* **1996**, *29*, 5245.

19. Wang, J. -S.; Matyjaszewski, K. *J. Am. Chem. Soc.* **1995**, *117*, 5614.

20. Harwood, H. J.; Arvanitopoulos, L. D.; Grenel, M. P. *Polym. Prepr. (Am. Chem. Soc., Div. Polym. Chem.)* **1994**, *35*(2), 549.

21. Wayland, B. B.; Pszmik, G.; Mukerjee, S. L.; Fryd, M. *J. Am. Chem. Soc.* **1994**, *116*, 7943.

22. Minoura, Y.; Utsumi, K.; Lee, M. *J. Chem. Soc., Faraday Trans. 1*, **1979**, *75*, 1821.

23. Gaynor, S.; Mardare, D.; Matyjaszewski, K. *Polym. Propr. (Am. Chem. Soc., Div. Polym. Chem)* **1994**, *36*(1), 700.

24. Mardare, D.; Matyjaszewski, K. *Macromolecules* **1994**, *27*, 645.

25. Kato, M.; Kamigaito, M.; Sawamoto, M.; Higashimura, T. *Macromolecules* **1995**, *28*, 1721,

26. Aiido, T.; Kato, M.; Kamigaito, M.; Sawamoto, M. *Macromolecules* **1996**, *29*, 1070.

27. Kotani, Y.; Kato, M.; Kamigaito, M.; Sawamoto, M. *Macromolecules* **1996**, *27*, 6979.

28. Ando, T.; Kamigaito, M.; Sawamoto, M. *Macromolecules* **1997**, *30*, 4507.

29. Otsu, T.; Yoshida, M. *Makromol. Chem. Rapid Commun.* **1982**, *3*, 127.

30. Otsu, T.; Yoshida, M:; Tazaki, T. *Makromol. Chem., Rapid Commun.* **1982**, *3*, 133.

31. Otsu, T.; Yamashita, K.; Tsuda, K. *Macromolecules* **1986**, *19*, 287.

32. Otsu, T.; Matsunaga, T.; Kuriyama, A,; Yoshioka, M. *Eur. Polym. J.* **1989**, *25*, 643.

33. Turner, R. S.; Blevins, R. W. *Macromolecules* **1990**, *23*, 1856.

34. Weir, D.; Ajayaghosh, A.; Muneer, M.; George, M. V. *J. Photochem. Photobiol. A. Chem.* **1990**, *52*, 425.

35. Muneer, M.; Ajayaghosh, A.; Das, S.; George, M. V. *J. Photochem. Photobiol. A. Chem.* **1995**, *86*, 155.

36. Ajayaghosh, A.; Das, S.; George, M. V. *J. Polym. Sci. Polym. Chem.* **1993**, *31*, 653.

37. Lambrinos, P.; Tardi, M.; Potton, A.; Sig Walt, P. *Eur. Polym. J.* **1990**, *26*, 1125.

38. Kerckhoven, C. V.; den Broeck, H. V.; Smets, G.; Huybrechts, *J. Makromol. Chem.* **1991**, *192*, 101.

39. Nakayama, Y.; Matsuda, T. *Macromolecules* **1996**, *29*, 8622.

40. Delduc, P.; Tailhan, C.; Zard, S. Z. *J. Chem. Soc. Chem. Commun.* **1988**, 308.

41. Crich, D.; Quintero, L. *Chem. Rev.* **1989**, *89*, 1413.

42. Zard, S. Z.; *Angew. Chem. Int. Ed. Engl.* **1997**, *36*, 672.

43. Ajayaghosh, A.; Francis, R. *Macromolecules* **1998**, *31*, 1436.

44. Bryce-Smith, D.; Hems, M. A. *Tet. Lett.* **1966**, 1895.

45. Bradshaw, J. S. *Tet. Lett.* **1966**, 2039.

46. Musa, Y.; Stevens, M. P. *J. Polym. Sci. Part A-1* **1972**, 10, 319.

47. Kardush, N.; Stevens, M. P. *J. Polym. Sci. Part A-1* **1972**, *10*, 1093.

CHAPTER 4

PHOTOINDUCED GRAFT AND BLOCK COPOLYMER SYNTHESIS USING MACROINITIATORS CONTAINING XANTHATE CHROMOPHORES

4.1. Introduction

Synthesis of graft and block copolymers is a novel approach to combine the chemical and physical properties of two or more different monomers to a single polymeric chain.[1-7] This would allow the designing of novel polymeric materials with new and/or improved properties useful for various advanced technological applications. Block copolymers are synthesized by the incorporation of a required monomer to a polymer containing reactive end functional groups. On the other hand, graft copolymers are prepared by incorporating an appropriate monomer through pendant (side chain) reactive functional groups. Free radical induced polymerization is the easiest and widely accepted procedure for graft and block copolymer synthesis. However, a major drawback of the free radical polymerization approach is the unwanted homopolymerization, which generally proceeds in parallel with the block and graft copolymerizations. In addition, there is no control over molecular weight and polydispersity of the block and graft polymers obtained by free radical induced polymerization.

Graft and block copolymer synthesis by anionic or cationic mechanisms has the advantages of minimized homopolymer formation.[8,9] Apart from that, significant control over molecular weight and polydispersity can be achieved by ionic mechanisms.[10-13] On the other hand, from the practical point of view, cationic or anionic techniques severely limit their use in polymerization processes due to the stringent requirements on reaction conditions and monomer purity.[14-17]

These problems have led to considerable interest in free radical induced controlled synthesis of block and graft copolymers. Recently, the concept of "living" free-radical polymerization has attracted considerable interest in block and graft copolymer synthesis due to the accurate control of molecular weight, polydispersity, chain ends and macromolecular structural characteristics.[18-21] Several macromonomers and mocroinitiators have been used for block and graft copolymer synthesis, even though, many of these methods lack the ability to control polydispersity and purity of products.[22, 23]

When compared to other modes of free radical initiated graft and block copolymer synthesis, light-induced initiation has the advantage of being applicable at low temperatures, especially at room temperature. Moreover, because of the selective absorption of certain chromophores, it is possible to produce free radical initiation sites at definite positions in the macromolecules. In such cases, the polymerization processes can also be controlled by varying the intensity and wavelength of the light used. Several reports pertaining to the light-induced block and graft copolymer synthesis are available in recent literature.[24-27] Almost all photoinitiators which are known in the literature have been exploited for the photochemical synthesis of block and graft copolymers. However, the major problems involved are the formation of considerable amount of homopolymers and lack of control on molecular weights and polydispersity of the block and graft copolymers.

Several methods have been proposed for the control of homopolymer formation during photoinduced block and graft copolymer synthesis. One of the efficient methods involves the use of polymers containing halogen atom in the presence of compounds of certain transition metals such as manganese and rhenium carbonyls as photoinitiators.[28-32] The mechanism involves photoinduced electron transfer from the transition metal to the polymer halide to form a macroradical and a metal halide. Homopolymerization in this case is prevented

because no free radicals are generated in the reaction mixture other than the macroradical.

It has been reported earlier that sulfur containing compounds such as tetraethylthiuram disulfide (1) and bis(isopropylxanthogen) disulfide (2) can be used for the photoinduced block copolymer synthesis.[33,34] Otsu et al., during early 1980 s, have found that a new class of sulfur-containing photoinitiators namely dithiocarbamates can be used for the efficient block and graft copolymer synthesis thereby minimizing the homopolymer formation.[35-39] These photoinitiators are referred to as photoiniferters which means that they function as initiator, transfer agent and terminator during photopolymerization. A pseudo living free radical mechanism has been suggested for polymerization using photoiniferters which involves the stepwise incorporation of monomers leading to growth of the molecular weight with increase in monomer conversion. Several people have used the dithiocarbamate photochemistry for the block and graft copolymer synthesis.[40-43] The major drawback of the dithiocarbamate based photoiniferter method is the formation of block and graft copolymers with high polydispersity. This observation reveals that the original mechanism proposed for the block and graft copolymerization using dithiocarbamates is complicated by some secondary reactions.[41,42] Since dithiocarbamates absorb light in the short wavelength region, the photoinitiation has to be performed around 280-290 nm region. Under such conditions, the monomer may also absorb light thereby facilitating the self-initiation of the monomer leading to the formation of considerable amounts of homopolymers. Therefore, design of better methods for photoinduced synthesis of block and graft copolymers of high purity has great significance.

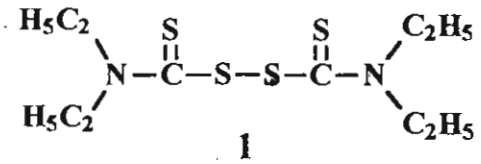

1

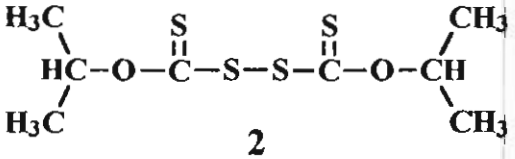

2

In the present Chapter, the use of copolymers containing pendant xanthate groups as macroinitiators for the photoinduced synthesis of extremely pure graft copolymers are described. In addition, polymers containing thiocarbonylthiyl end functional groups have been used for the photoinduced block copolymer synthesis.

4.2. Results and Discussion

4.2.1. Photoinitiated grafting of MMA and styrene using macroinitiators containing pendant xanthate chromophores

Macroinitiators used for the present studies have been prepared by the thermal copolymerization of S-methacryloyl O-ethyl xanthate (MAX) with MMA and styrene (St) as described in Chapter 2 of the present thesis. MAX-co-MMA and MAX-co-St having various copolymer compositions and molecular weights were employed for the grafting studies. Photografting of MMA and St on MAX-co-St and MAX-co-MMA respectively were performed either using bulk monomer or in benzene solution under 350 nm irradiation. The data obtained for the photografting of St on to MAX-co-MMA are shown in Table 1. The initial grafting reactions were performed using 50 mg of MAX-co-MMA having 16 mole percentage of the MAX photoinitiator group. The molecular weight of

MAX-co-MMA before the grafting of MMA was 2700 amu. The yield and molecular weights of the graft copolymers are found to increase gradually with the time of irradiation, as shown in Table 1. It is also observed that the polydispersity of the graft copolymers increases with the time of irradiation. Upon prolonged irradiation, considerable amounts of crosslinked polymers are also formed.

Table 1. Photografting[a)] of styrene (bulk) onto MAX-co-MMA[b)] copolymer at various time intervals

Run	Time of irradiation (min)	Graft yield (%)	Crosslink yield (%)	Mol. wt. of the graft copolymer (M_n)	M_w/M_n
1	45	4	0	14000	1.3
2	90	9	0	17000	1.3
3	140	15	2	20000	1.4
4	240	32	6	28000	1.9

[a)] λ_{irr} = 350 nm; [b)] MAX-co-MMA = 0.017 g/mL (M_n = 2700, MAX mol % = 16)

Results obtained for the photografting of St on to MAX-co-MMA having different copolymer compositions and molecular weights are summarized in Table 2. These data reveal that the graft yields and the molecular weights of the graft copolymers decrease with decrease in the mole percentage of the MAX groups in the initial copolymers irrespective of their initial molecular weights. On the other hand, the polydispersity of the graft copolymers did not vary much with the copolymer composition or molecular weights of the initial copolymer. A plot of the molecular weights of graft copolymers obtained against the mole percentage of MAX in the MAX-co-MMA is shown in Figure 1. A linear increase in molecular weights of the graft copolymers could be noticed with increase in mole percentage

of MAX in the copolymer. In all these cases the homopolymer formation could be suppressed to a considerable extent.

Table 2. Photografting[a)] of styrene (bulk) onto MAX-co-MMA[b)] having different copolymer compositions and molecular weights

Run	Mol % of MAX in the copolymer	Initial copolymer mol. wt. (M_n)	Graft yield (%)	Crosslink yield (%)	Mol. wt. of the graft copolymer (M_n)	M_w/M_n
1	21	2200	15	5	23000	1.4
2	16	2700	13	0	19000	1.4
3	14	2500	12	0	18000	1.4
4	12	1500	11	0	14000	1.4

[a)] λ_{irr} = 350 nm, Time of irradiation = 140 min; [b)] MAX-co-MMA = 0.017 g/mL

The Results of the photografting of MMA using MAX-co-St as the macroinitiator as a function of irradiation time is shown in Table 3. MAX-co-St of molecular weight 3400 amu, containing 20 mole percentage of pendant MAX moieties has been used for the grafting. The percentage yields of the graft polymers are found to increase with irradiation time. Considerable amounts of crosslinked polymers are also formed with increase in graft yield. The increased formation of crosslinked polymer with increasing yield of graft copolymer can be explained on the basis of the decrease in monomer concentration in the polymerization mixture. In addition, under higher graft yield the reaction mixture becomes highly viscous thereby limiting the mobility of macroradicals, which facilitate macroradical recombination leading to their crosslinking.

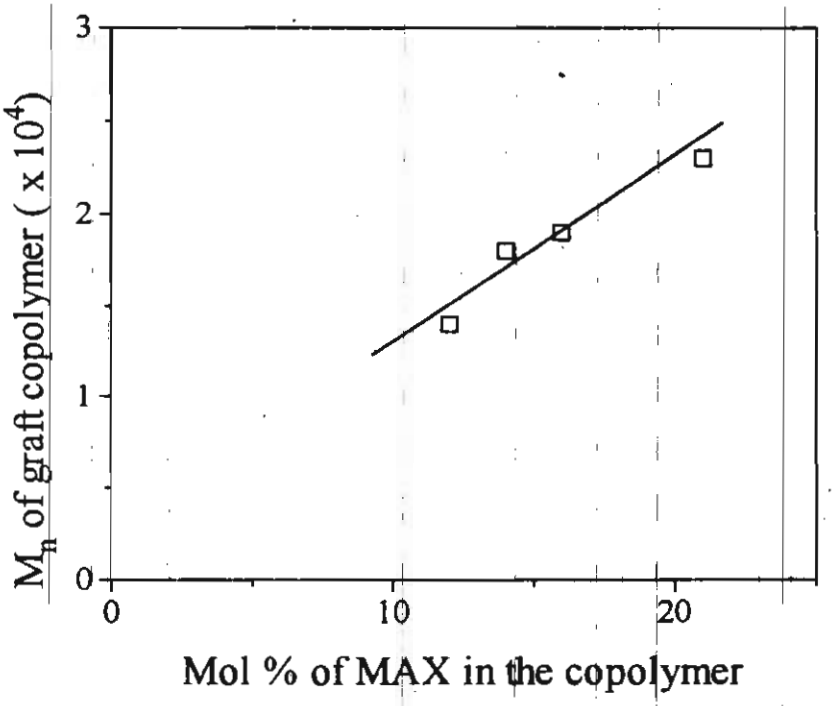

Figure 1. Effect of mol % of MAX in MAX-co-MMA on the molecular weight of MAX-co-MMA-g-St.

Table 3. Photografting[a)] of MMA[b)] onto MAX-co-St[c)] copolymer at various time intervals

Run	Time of irradiation (min)	Graft yield (%)	Crosslink yield (%)	Total conversion (%)	Mol. wt. of the graft copolymer (M_n)	M_w/M_n
1	10	8	0	8	13000	1.3
2	30	22	0	22	16000	1.3
3	60	41	4	45	20000	1.4
4	90	50	10	60	28000	1.3

[a)] λ_{irr} = 350 nm; [b)] MMA = 5 M in benzene; [c)] MAX-co-St = 0.017 g/mL (M_n = 3400, MAX mole % = 20)

A plot of the molecular weights of the MAX-co-St-g-MMA copolymers against the time of irradiation is shown in Figure 2. A linear increase in molecular weight is noticed which is analogous to that observed for a living radical polymerization. However our earlier studies have revealed that photopolymerization of MMA using low molecular weight xanthate-derived photoinitiators does not show any characteristic property of a living radical polymerization. Therefore, the increase in molecular weights of the graft copolymers is unique in the case of macroinitiators. In the case of photografting using macroinitiators, new radical centers will be generated within the macroinitiator with the time of irradiation, which in turn will initiate the formation of new graft polymer chains. The growth in the molecular weights of graft copolymers can be understood by comparing Scheme 2 with the normal photopolymerization using a low molecular weight photoinitiator as shown in Scheme 1. In the case of the low molecular weight photoinitiators each initiating radical will lead to the formation of individual polymer chains with time of irradiation whereas photografting using macroinitiators leads to a collective addition of polymer chains onto the macroradicals.

The effect of the copolymer compositions of MAX-co-St used for the photografting of MMA has been summarized in Table 4. A plot of the molecular weight of the graft copolymer against mole percentage of the MAX in the parent copolymer showed a linear increase as shown in Figure 3. However, the polydispersity indices of the graft copolymers did not show any considerable change. It has been found that the yields of the grafted and crosslinked polymers increased with increase in the mole percentage of MAX in the MAX-co-St copolymer. When MAX-co-St having higher mole percentage of MAX was used for the grafting of MMA, considerable amount of crosslinked polymer was also formed along with the graft copolymer. The reason for this could be the formation of large number of immobilized radical centres within the macroinitiator. High

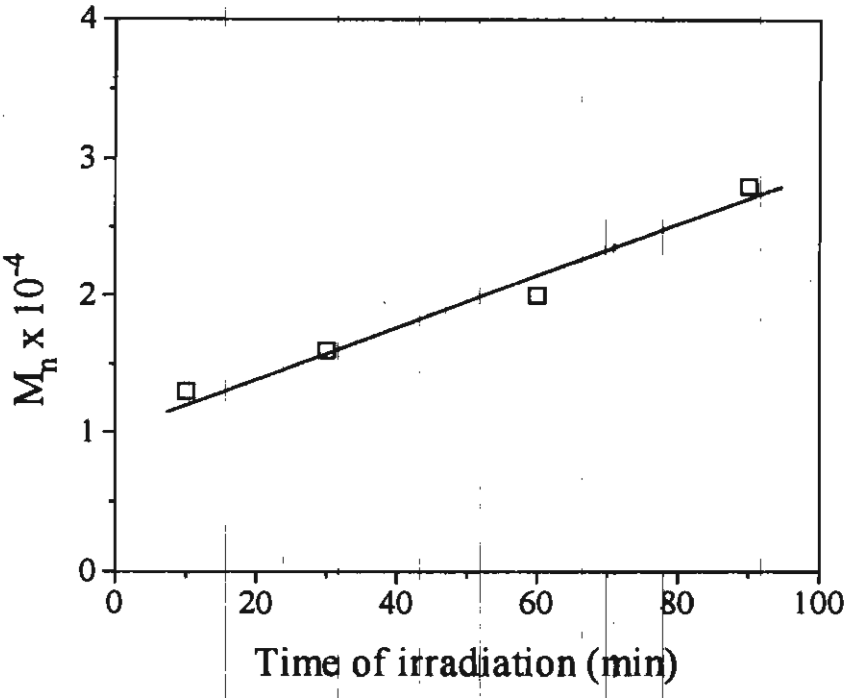

Figure 2. Effect of time of irradiation on molecular weight of MAX-co-St- g-MMA.

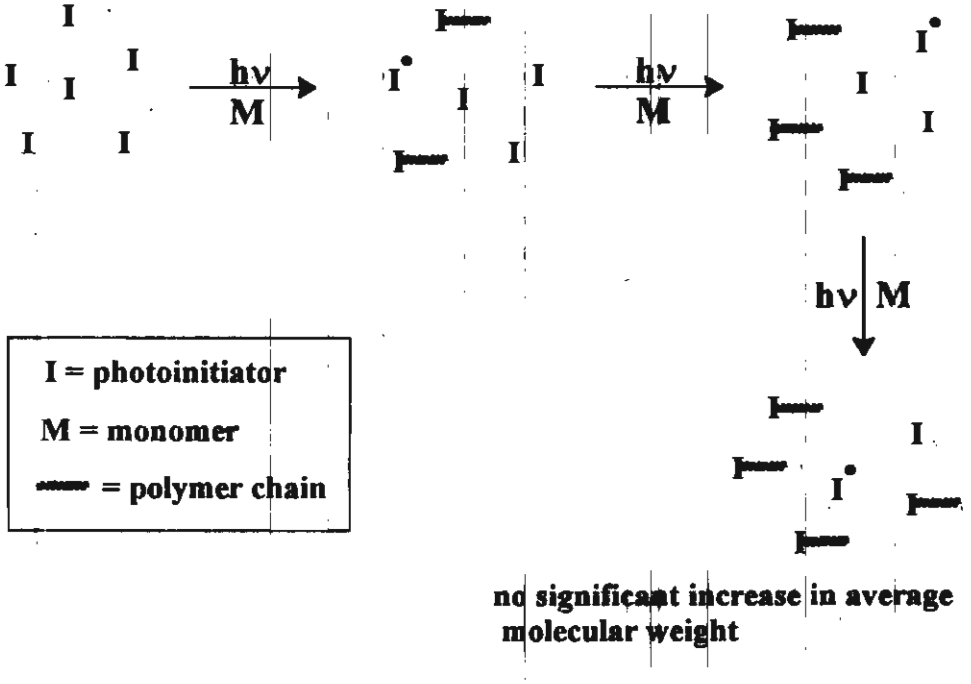

Scheme 1

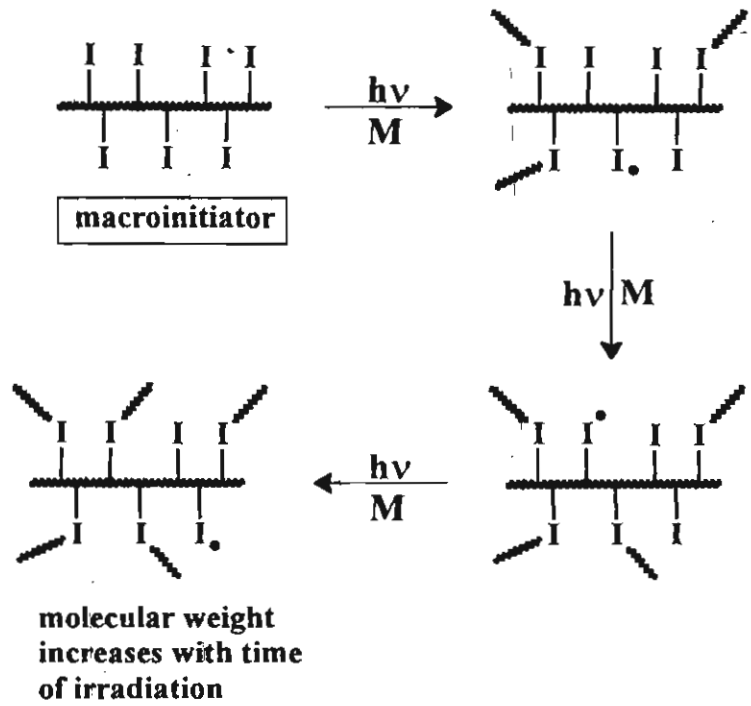

Scheme 2

Table 4. Photografting[a)] of MMA[b)] on MAX-co-St[c)] of various compositions and molecular weights

Run	Mol % of MAX in MAX-co-St	Initial copolymer mol. wt.	Graft yield (%)	Crosslink yield (%)	Total conversion (%)	Graft copolymer mol. wt. (M_n)	M_w/M_n
1	20	3400	43	5	48	32000	1.5
2	15	2800	42	1	43	26000	1.4
3	11	3300	39	1	40	24000	1.3
4	9	2900	38	0	38	20000	1.4

[a)] λ_{irr} = 350 nm, Time = 70 min [b)] MMA = 5M in benzene; [c)] MAX-co-St = 0.017 g/mL.

local concentration of radical centres on the macroinitiator compete for photografting as well as the intramolecular radical-radical recombination resulting in the formation of the crosslinked copolymer of the structure **3** as shown in Chart 1. Nevertheless, the intermolecular crosslinking between the graft chain radicals cannot be completely ruled out.

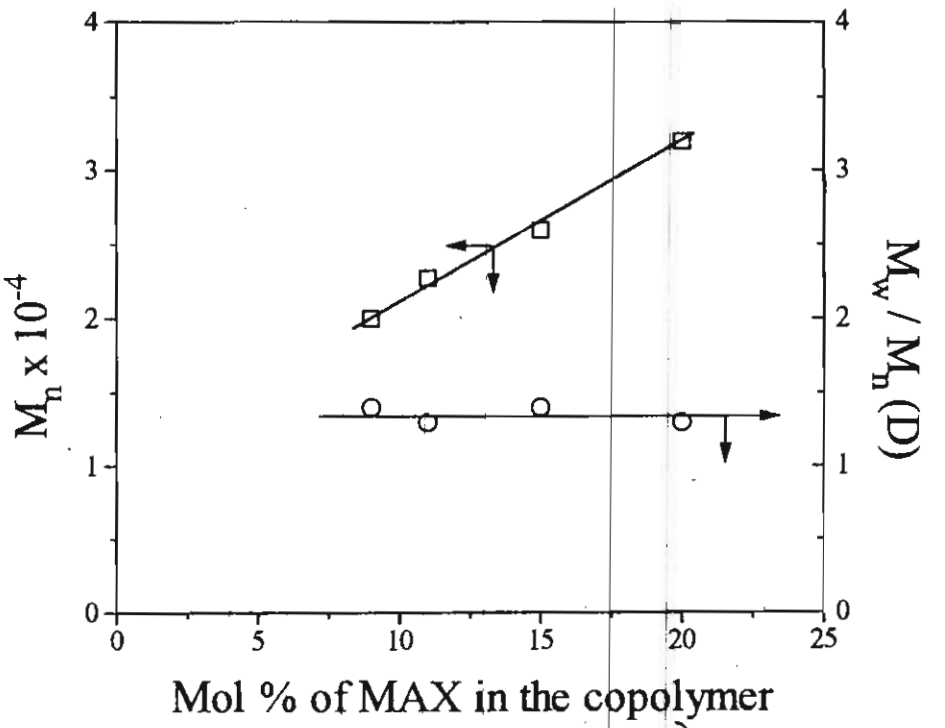

Figure 3. Effect of MAX mol % in MAX-co-St on the molecular weight and poydispersity of MAX-co-St-g-MMA.

The effect of the macroinitiator concentrations on the photografting of MMA using MAX-co-St is shown in Table 5. The total conversion of the monomer is found to increase with the increase in the concentration of MAX-co-St while the yields and the molecular weights of the graft copolymers decreased. The

decrease in the yields of the graft copolymers with increase in concentration of MAX-co-St is due to the increased formation of crosslinked polymers. The effect of the concentration of MAX-co-St on the crosslinked and grafted polymer yields is shown in Figure 4. Under high concentration of MAX-co-St, the possibility for interpolymer crosslinking will be higher thereby facilitating the formation of the crosslinked polymers and the consequent decrease in isolable graft copolymer yields.

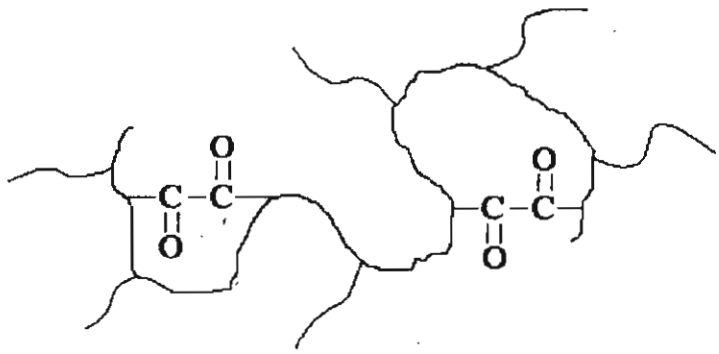

3

Chart 1

Table 5. Effect of macroinitiator concentration for the photografting[a)] of MMA[b)] onto MAX-co-St[c)]

Run	MAX-co-St (mg/L)	Total conversion (%)	Graft yield (%)	Crosslink yield (%)	Graft copolymer mol. wt. (M_n)	M_w/M_n
1	10	43	40	3	24000	1.3
2	50	46	34	12	14000	1.4
3	80	59	29	30	12000	1.4
4	100	68	20	48	12000	1.3

[a)] λ_{irr} = 350 nm; [b)] MMA = 5 M in benzene; [c)] M_n = 3500 (MAX mole % = 18)

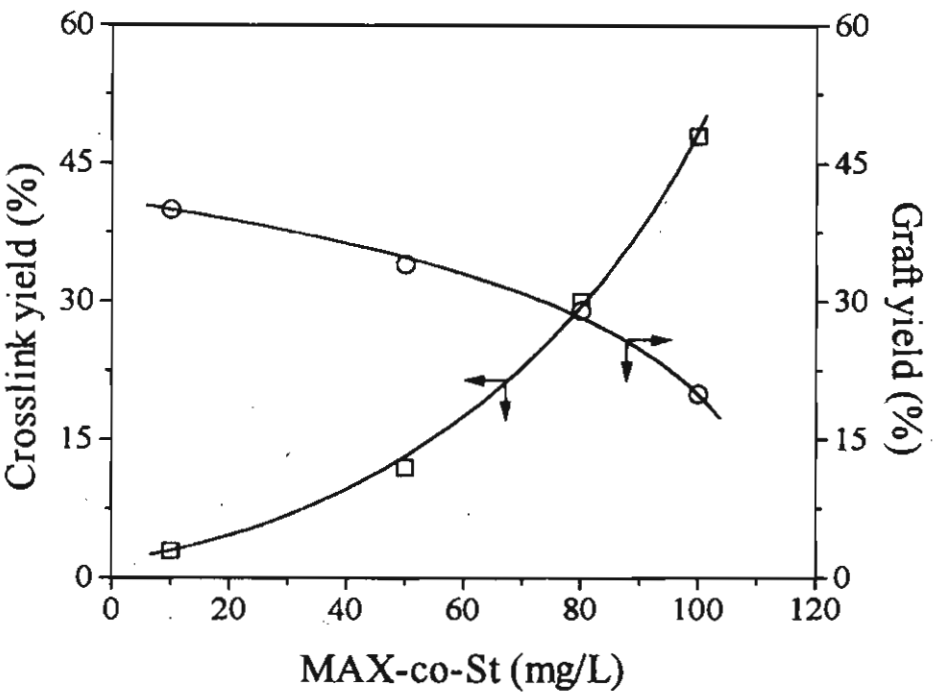

Figure 4. Effect of the weight of MAX-co-St on crosslink and graft yields of MAX-co-St-g-MMA

Evidence for the photoinduced grafting of St and MMA on to MAX-co-MMA and MAX-co-St, respectively can be obtained from their spectral analysis. The UV spectra of MAX-co-MMA and MAX-co-St are compared with their respective graft copolymers in Figures 5 and 6, respectively. Before initiating the graft copolymerization, both MAX-co-MMA and MAX-co-St showed broad absorptions around 395 nm, which is due to the pendant xanthate chromophore. After graft copolymerization, the absorption at 395 nm disappeared indicating the cleavage of the (C=O)-S bond of the parent polymers.

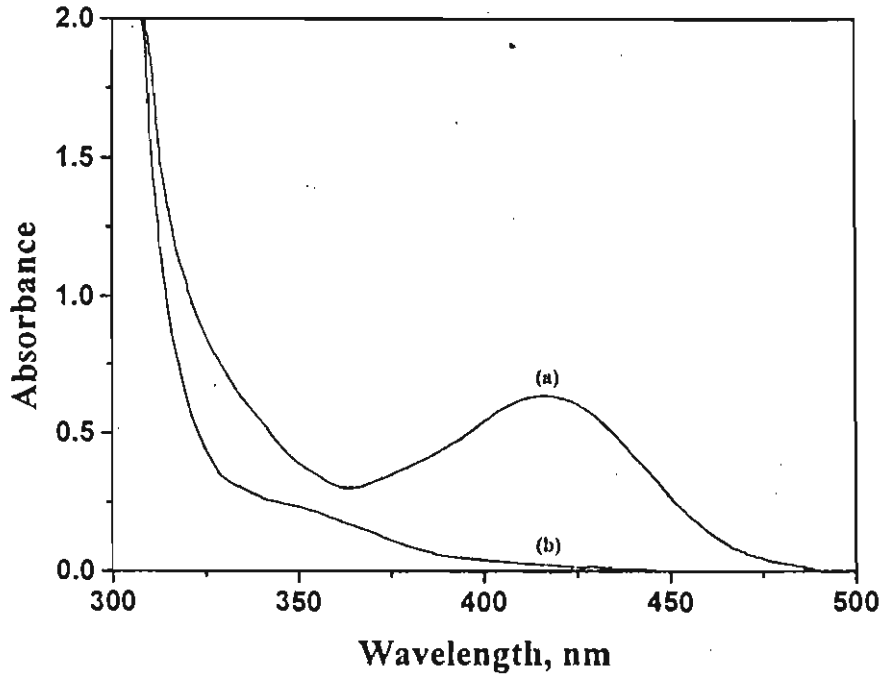

Figure 5. UV spectrum of (a) MAX-co-MMA and (b) MAX-co-MMA-g-St

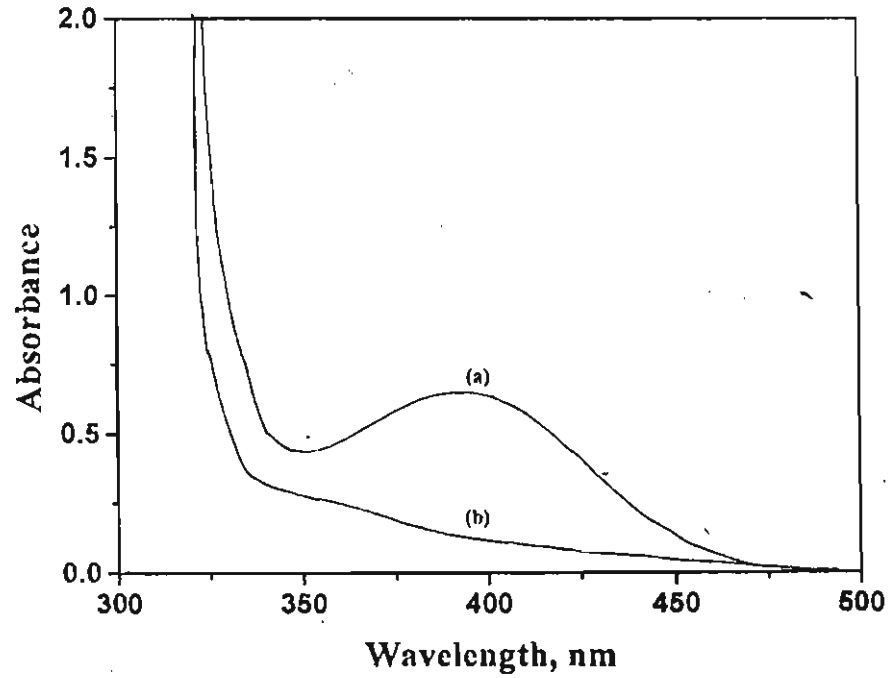

Figure 6. UV spectrum of (a) MAX-co-St and (b) MAX-co-St-g-MMA

The IR spectra of MAX-co-MMA and MAX-co-MMA-g-St are shown in Figure 7, whereas the IR spectra of MAX-co-St and MAX-co-St-g-MMA are shown in Figure 8. The IR spectrum of MAX-co-MMA (Figure 7(a)) shows absorption peaks at 1739 cm^{-1} due to carbonyl groups and 1251 and 1046 cm^{-1} due to the thiocarbonylthiyl groups. In the IR spectrum of the graft copolymer MAX-co-MMA-g-St (Figure 7(b)), the intensities of absorption of the carbonyl group at 1739 cm^{-1} and the thiocarbonylthiyl group at 1251 and 1046 cm^{-1} have been considerably reduced and new absorption peaks at 1605, 756 and 696 cm^{-1} characteristic of the aromatic ring of polystyrene have appeared. The IR spectrum of MAX-co-St (Figure 8(a)) shows considerable decrease in the intensity of absorption at 1252 and 1041 cm^{-1} due to the thiocarbonylthiyl groups after grafting of MMA (Figure 8(b)).

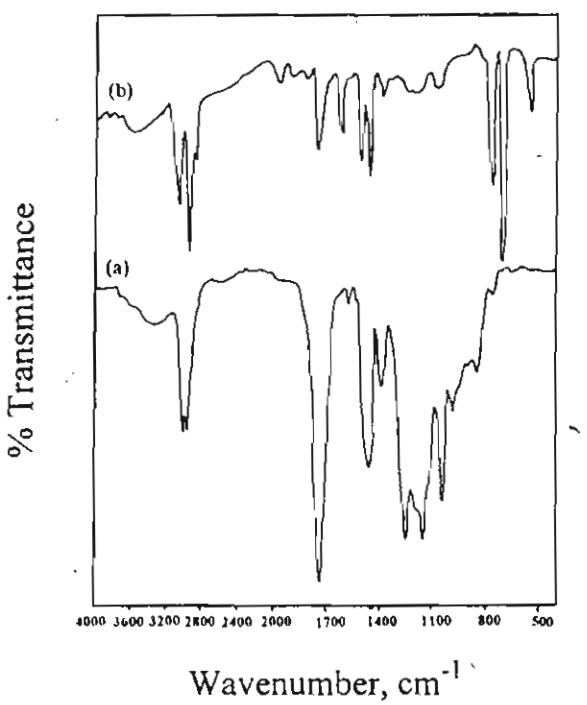

Figure 7. IR spectrum of (a) MAX-co-MMA and (b) MAX-co-MMA-g-St

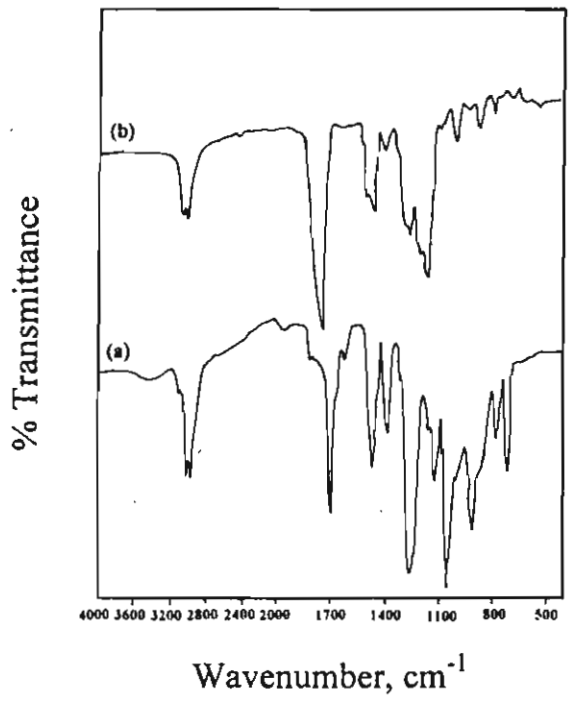

Figure 8. IR spectrum of (a) MAX-co-St and (b) MAX-co-St-g-MMA

Comparison of the ^{1}H NMR spectra of MAX-co-MMA before (Figure 9) and after grafting of styrene (Figure 10) indicates considerable reduction in the intensity of the OCH_3 protons of the PMMA in the latter spectrum at δ 3.6 ppm. At the same time, two new peaks between δ 6-7.5 ppm due to the aromatic protons appeared after grafting (Figure 10), indicating the presence of grafted polystyrene chains. The results of the thermogravimertic analysis of MAX-co-MMA and MAX-co-St and their respective graft copolymers are shown in Figures 11 and 12, respectively. The weight loss at 170 °C in the thermal degradation patterns of MAX-co-MMA and MAX-co-St are associated with the pendant xanthate chromophores. After grafting of MMA and styrene, no weight loss could be seen at 170 °C and the thermal stability of the grafted copolymers increased considerably.

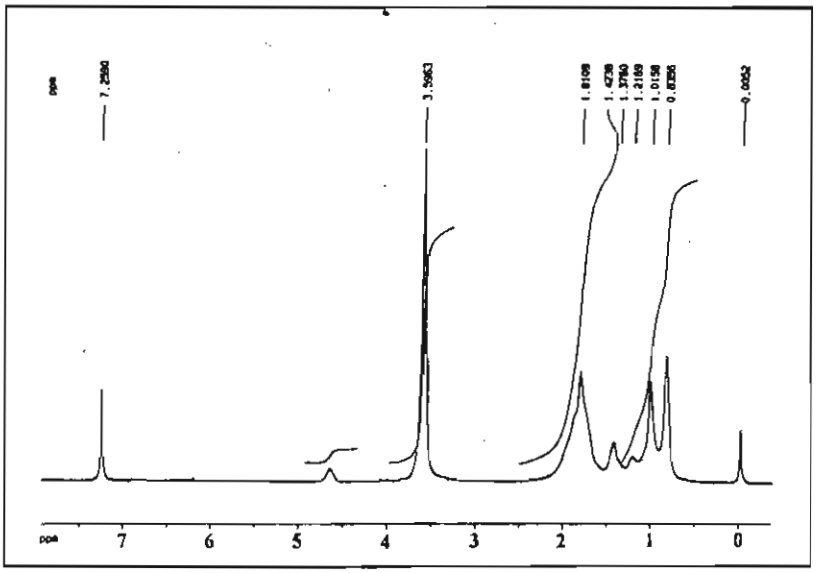

Figure 9. ^{1}H NMR spectrum of MAX-co-MMA

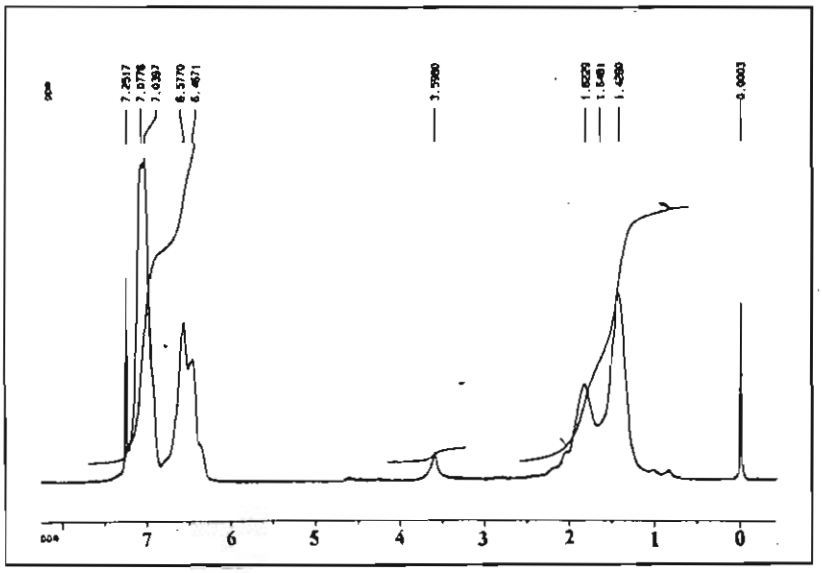

Figure 10. ^{1}H NMR spectrum of MAX-co-MMA-g-St

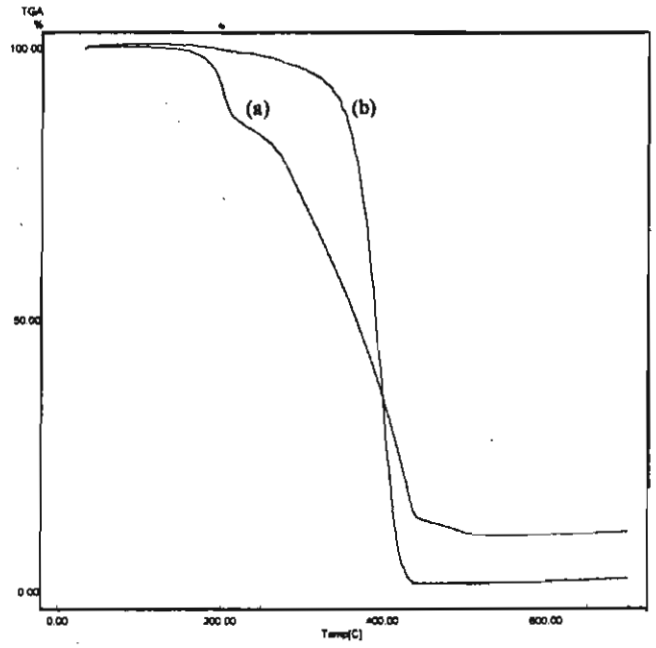

Figure 11. Thermal analysis data of (a) MAX-co-MMA and (b) MAX-co-MMA-g-St

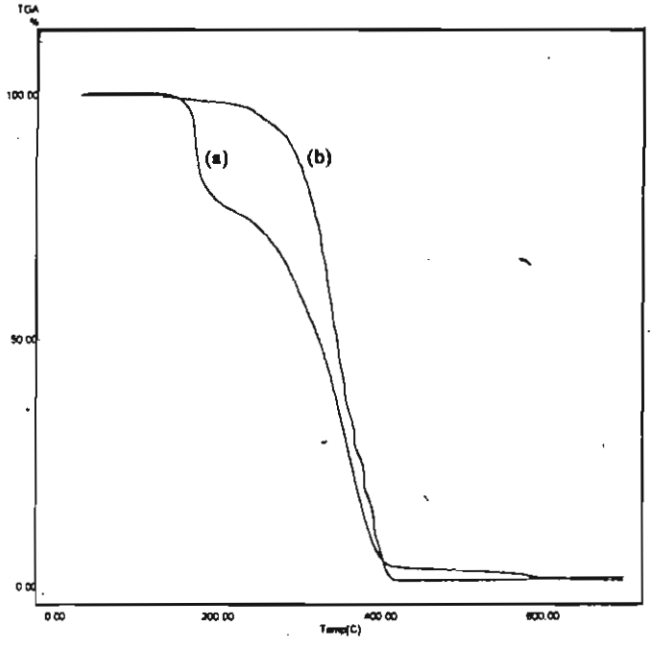

Figure 12. Thermal analysis data of (a) MAX-co-St and (b) MAX-co-St-g-MMA

The photografting of St and MMA using MAX-co-MMA and MAX-co-St are shown in Schemes 3 and 4, respectively. Analogous to our earlier observations, both MAX-co-MMA and MAX-co-St on photolysis undergo homolytic bond cleavage at the C(=O)-S bond position of the pendant MAX chromophore.[44, 45] As a result, macroradicals and thiocarbonylthiyl radicals will be generated. The macroradicals thus formed initiate the graft copolymerization of

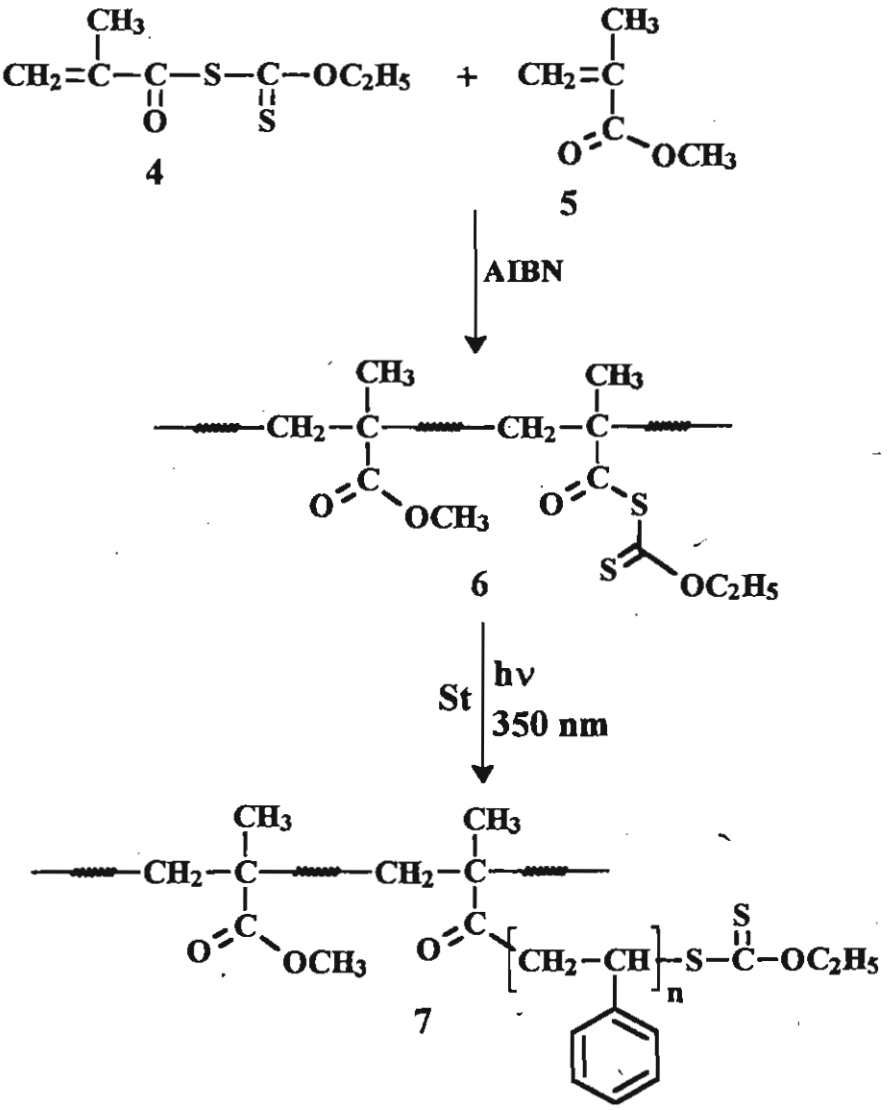

Scheme 3

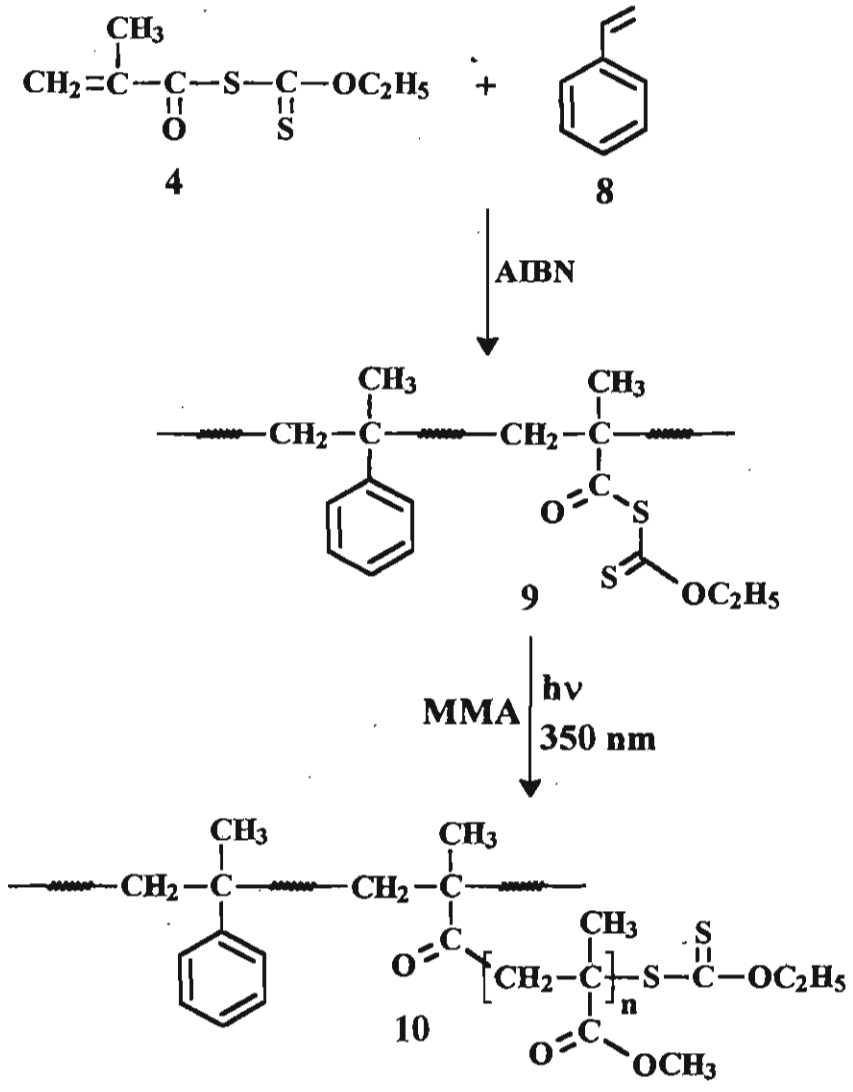

Scheme 4

the surrounding monomers whereas the thiocarbonylthiyl radicals mainly act as the terminator. This property of the thiocarbonylthiyl radicals plays a significant role in controlling the formation of crosslinked polymers as well as homopolymers during photografting of various monomers. The suppressed homopolymer formation during the photografting of monomers to MAX-co-MMA and MAX-co-St clearly indicates the strong primary radical termination efficiency of the thiocarbonylthiyl radicals and their inefficiency to initiate homopolymerization process.

4.2.2. Photografting of MMA using a heterogeneous photoinitiator containing xanthate chromophore.

The termination efficiency of the thiocarbonylthiyl radicals and the suppressed homopolymer formation during photografting of monomers on to macroinitiators containing xanthate chromophores can be proved by a reverse photografting experiment. This is possible by doing surface photografting of MMA on to a crosslinked heterogeneous polymer containing xanthate groups, which on photolysis generate a thiocarbonylthiyl radical on the heterogeneous polymer and a ketyl radical in the solution. If the macroradical acts exclusively as the terminator, the ketyl radical initiated growing polymer chains will eventually get attached to the macroradical leading to the formation of graft polymers with high graft efficiency. The use of a crosslinked polymer for this purpose has the advantage that the graft polymer will be in the heterogeneous form whereas any homopolymer, if formed, will be in solution. Therefore, it is easy to isolate the homopolymer in this case.

The photografting of MMA was carried out using the polymer-bound S-benzoyl O-ethyl xanthate which has been prepared according to Scheme 5.[46] Poly(2-hydroxyethyl methacrylate) (PHEMA) which is crosslinked with 5 % ethyleneglycol dimethacrylate (100-200 mesh) was prepared as per a known procedure.[47] This was subsequently treated with NaOH and CS_2 to form the corresponding polymer-bound sodium xanthate **12**. Reaction of the polymer **12** with benzoyl chloride afforded the macrophotoinitiator **13**. The IR spectrum of the polymer-bound photoinitiator **13** showed the characteristic absorption peaks at 1700 and 1055 cm^{-1} corresponding to the C=O and C=S groups of the xanthate moiety, respectively. The amount of the initiator moieties of the polymer **13** was determined by elemental sulfur analysis which gave 1.78 mmol of xanthate groups/g of the polymer.

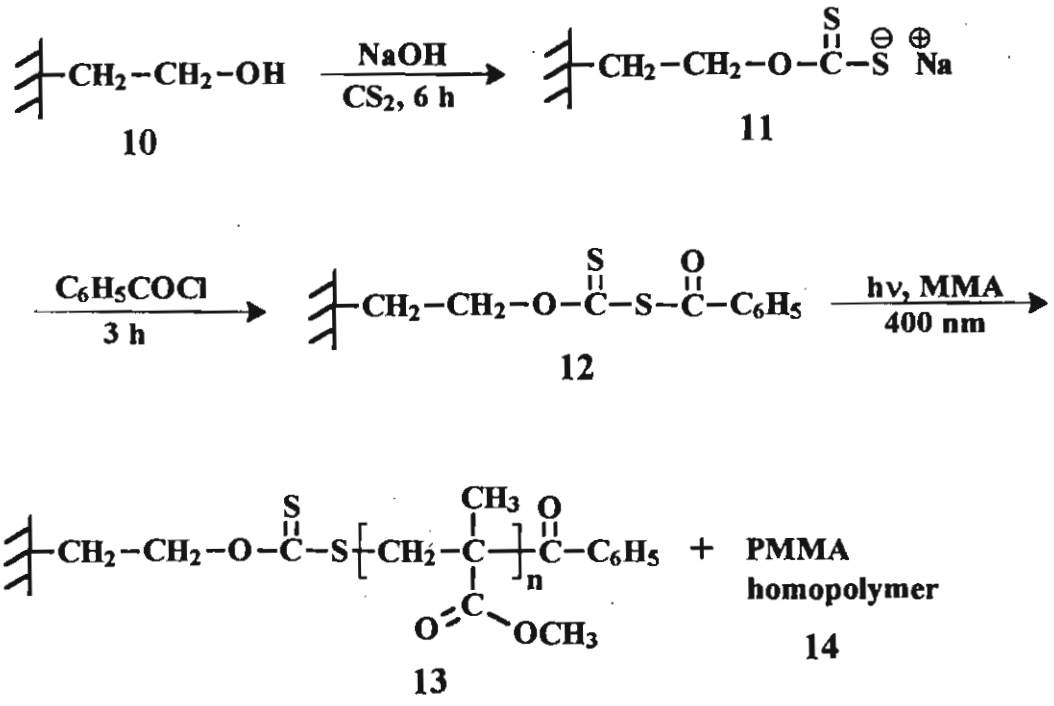

Scheme 5

The results of the photografting of MMA using the polymeric photoinitiator **13** are shown in Table 6. It is found that as in the case of the soluble macroinitiators, MAX-co-MMA and MAX-co-St, the total conversion increases with time of irradiation. A plot of the monomer conversion against the irradiation time indicates that after 20 min of irradiation there is a sudden increase in the total conversion of the monomer (Figure 13). Correspondingly, the yields of the graft polymers were also showed rapid increase with the time of irradiation (Figure 14). On the other hand, the yields of the homopolymers were relatively lower which showed a linear increase with time of irradiation as shown in Figure 14. The yield of the graft polymer after 40 min of irradiation is found to be around 41 %, whereas the corresponding yield of the homopolymer was only 5 %. These results reveal that, in the case of the polymer-bound initiator **13**, even though the initiation and growth of polymer chain occur in homogeneous solution, majority of

Table 6. Photografting[a] of MMA[b] using polymer-bound photoinitiator[c] **13**

Run	Time of irradiation (min)	Total conversion (%)	Yield of graft polymer (%)	Yield of homopolymer (%)
1	20	2.4	2	0.4
2	24	6.8	5	0.8
3	28	15.6	13	2.6
4	35	36.3	32	4.3
5	40	46.1	41	5.1

[a]λ_{irr} = 400 nm; [b]MMA = 8 mL; [c]Photoinitiator = 100 mg

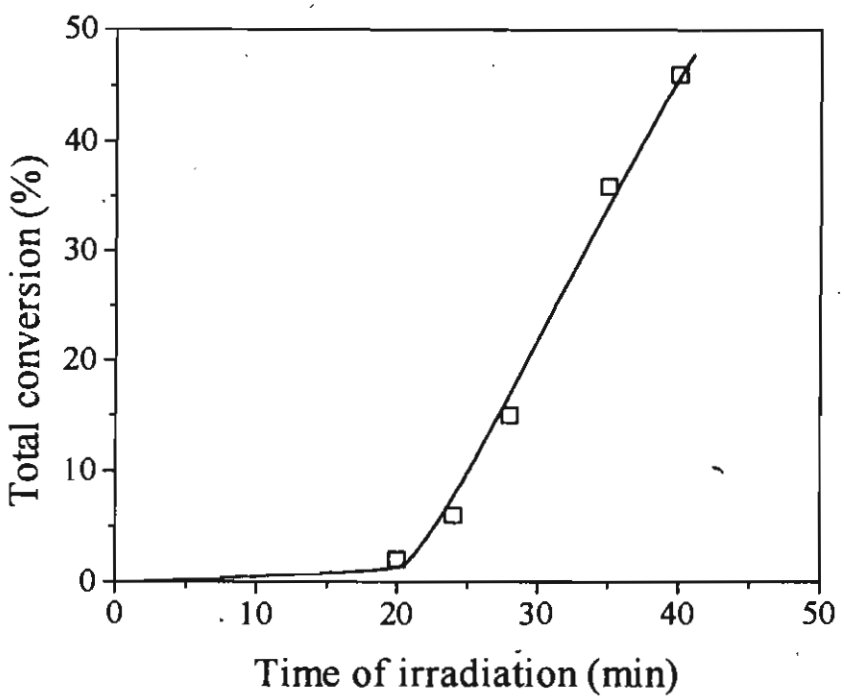

Figure 13. Effect of time of irradiation on total conversion for the photopolymerization of MMA using polymer-bound initiator **13**

the growing polymer radicals eventually get trapped by the heterogeneous polymer-bound thiocarbonylthiyl radicals. This observation clearly proves the efficiency of the thiocarbonylthiyl radicals in the termination of polymerization reaction.

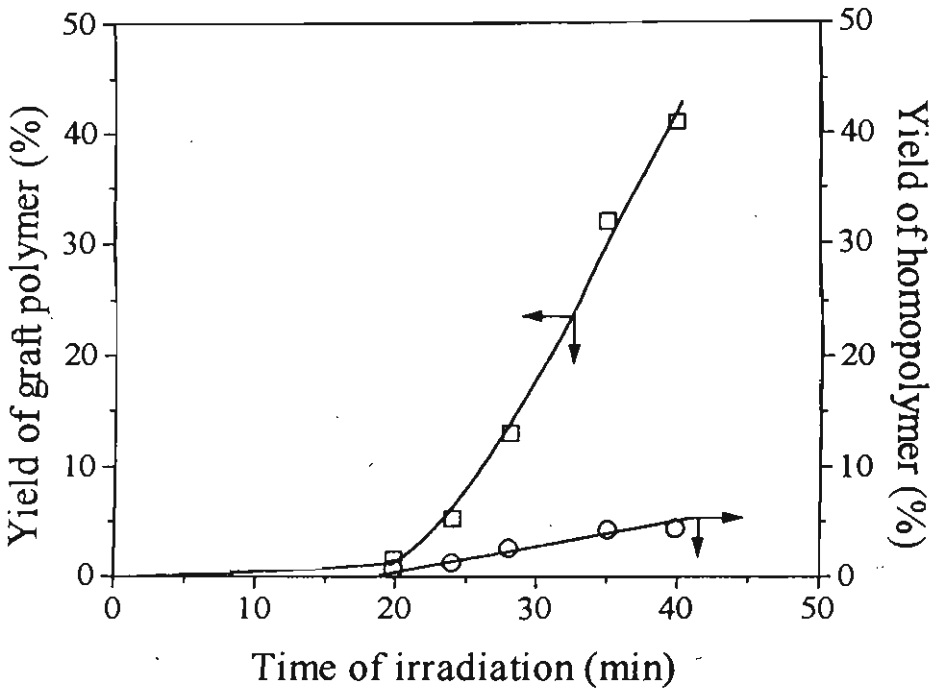

Figure 14. Effect of time of irradiation on graft and homopolymer yields for the photopolymerization of MMA using polymer-bound initiator **13**

4.2.3. Photoinduced block copolymerization using macrophotoinitiators end-capped with xanthate moieties

The xanthate end-capped macroinitiator **16** employed for the block copolymerization was prepared by the photopolymerization of MMA using S-methacryloyl O-ethyl xanthate (MAX) as described in Chapter 3 of the present thesis. The IR, UV and NMR analysis have been used to confirm the structure of the macroinitiator **16**. The initial molecular weight of **16** used for the block

copolymerization was 16000 amu having a polydispersity index of 1.7. Block copolymerizations were carried out using methyl acrylate (MA) as the monomer under 300 nm irradiation. MA was chosen as the monomer because it does not have much absorption at 300 nm.

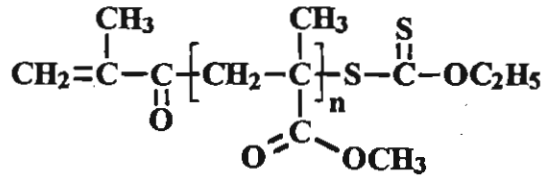

16

The results of the block copolymerization of MMA on to the macroinitiator 16 at various intervals of time are shown in Table 7. Considerable increase in molecular weights could be noticed with the time of irradiation (Figure 15). For example, after 30 min of irradiation the molecular weight of the block copolymer prepared from the macroinitiator **16** (M_n = 16000 amu) was around 39000 amu. After 90 min of irradiation the molecular weight of the block copolymer was further enhanced to 210000 amu. The GPC elution patterns of the block copolymers obtained under different irradiation times are shown in Figure 16, which are compared with the molecular weight of the starting polymer.

Table 7. Block copolymerization[a)] of MA[b)] onto the macroinitiator **16**[c)]

Run	Time (min)	Block copolymer yield (%)	Mol. wt. of the block copolymer (M_n)	M_w/M_n
1	30	5	39000	2.1
2	60	12	88000	1.9
3	90	25	210000	1.2

[a)] λ_{irr} = 300 nm; [b)] MA = 4 M; [c)] **16** = 5 mg/mL (M_n = 16000)

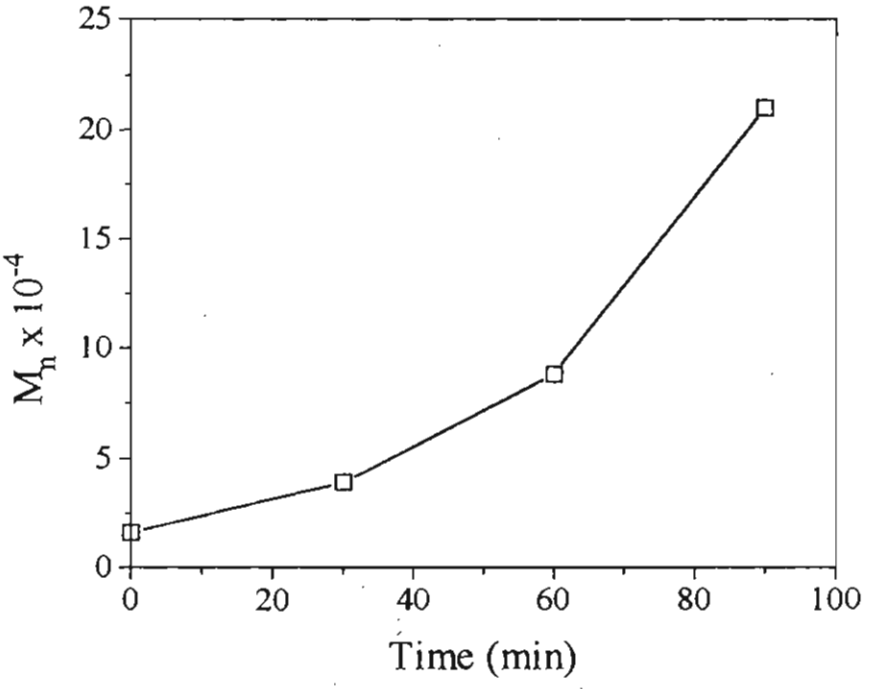

Figure 15. Plot of the molecular weight of the block copolymers of MMA prepared using the macroinitiator **16** at 300 nm

The observed increase in molecular weights of the block copolymers as a function of the irradiation time is analogous to that observed in the cases of block copolymerization using photoiniferters such as dithiocarbamates.[35-39] Therefore the mechanism of block copolymerization using the macroinitiator **16** may involve the cleavage of the end thiocarbonylthiyl group at 300 nm irradiation and the subsequent reversible monomer addition and termination processes (Scheme 6). Thus the whole polymerization can be considered as a photoiniferter mediated pseudo living radical process.

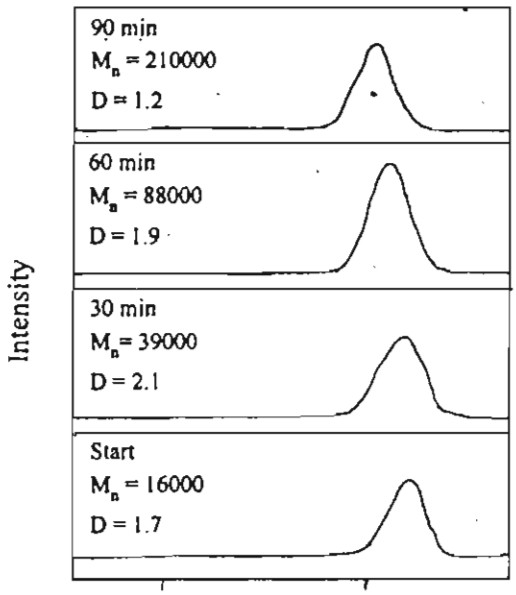

Figure 16. GPC elution patterns of block copolymers prepared under different irradiation times

4.2.4. Conclusions

In the present study soluble and crosslinked macroinitiators containing xanthate chromophores have been used for the photoinduced graft and block copolymer synthesis. Efficient grafting of monomers with suppressed homopolymer formation could be achieved by using copolymers of S-methacryloyl O-ethyl xanthate (MAX) with MMA and St. The homopolymer formation could be efficiently suppressed due to the inability of the resonance stabilized thiocarbonylthiyl radical to initiate polymerization. Photografting of MMA using a crosslinked polymer-bound xanthate photoinitiator unraveled the suppressed homopolymer formation in this reaction which is due to the ability of the heterogeneous polymer-bound thiocarbonylthiyl radicals to trap the growing polymer radicals which are present in the homogeneous solution. Macroinitiators end-capped with thiocarbonylthiyl radicals have been shown to undergo efficient

block copolymerization by a pseudo living radical mechanism as in the case of the iniferter polymerization reported by Otsu and coworkers.

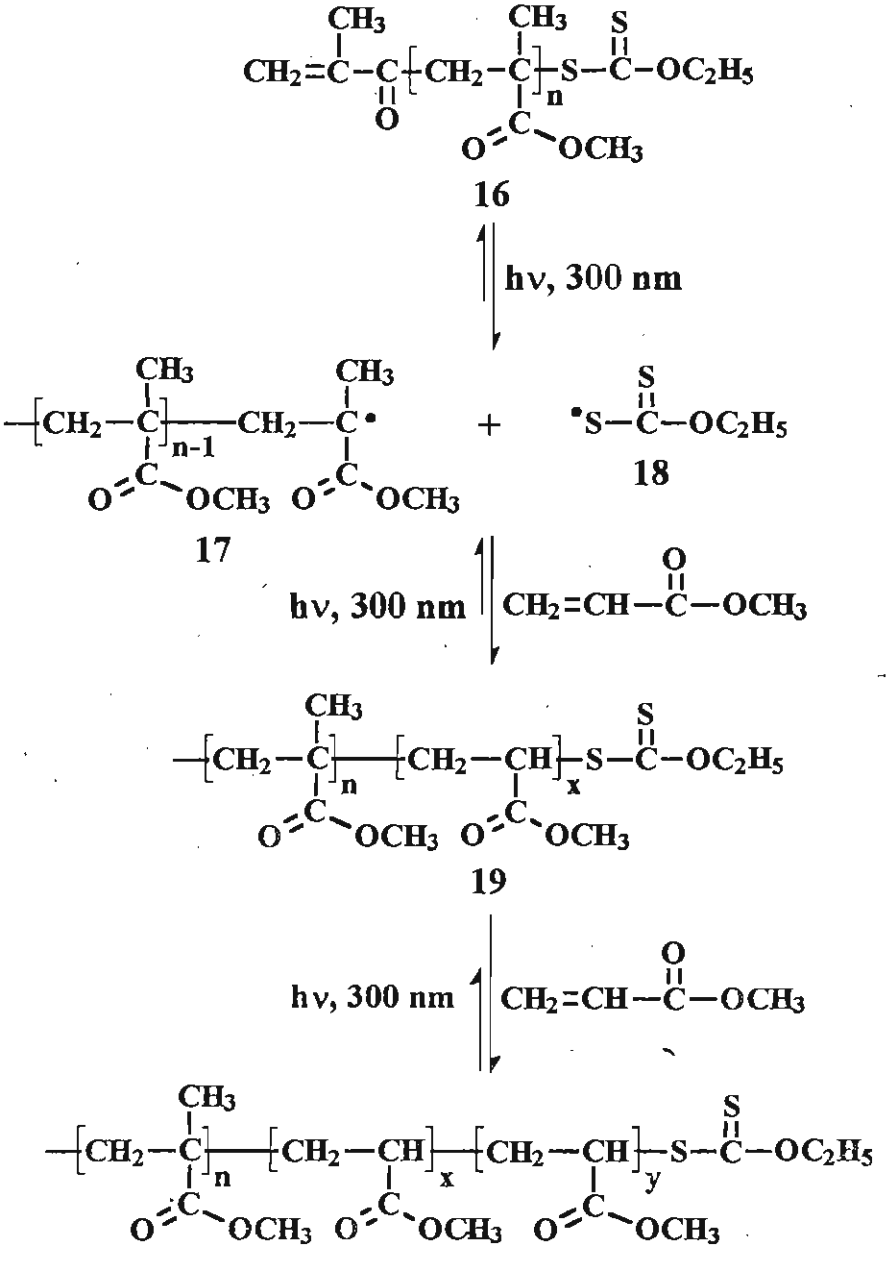

Scheme 6

4.3. Experimental

Infra-red (IR) spectra were recorded on a Perkin-Elmer model 880 spectrometer. The electronic spectra were recorded on a Shimadzu 2100 A spectrophotometer. ^{1}H nuclear magnetic resonance (NMR) spectra were recorded on a Jeol EX 90 or a Bruker DPX 300 spectrometer using $CDCl_3$ as solvent and tetramethylsilane as internal standard. Gel permeation chromatography (GPC) was carried out on a Shimadzu LC-8A GPC system equipped with a refractive index detector. Calibrations were done with standard polystyrene samples. Tetrahydrofuran (THF) was used as the eluent at a flow rate of 1 mL min^{-1} at 28 ^{o}C. Thermal analysis data (TGA) were recorded on a Shimadzu TGA-50H thermal analyser.

The monomers MMA, MA and styrene were purified by washing twice with 5 % aqueous NaOH and then several times with distilled water. These were then dried over anhydrous sodium sulphate and distilled under reduced pressure. 2-Hydroxyethyl methacrylate (HEMA) and ethyleneglycol dimethacrylate (EGDM) were distilled under reduced pressure and stored in a refrigerator. AIBN was recrystallized twice from methanol. All solvents used were dried and distilled before use.

S-Methacryloyl O-ethyl xanthate (MAX), MAX-co-MMA and MAX-co-St were prepared as described in Chapter 2 of the present thesis. Thiocarbonylthiyl group end-capped macroinitiator **16** was prepared by the photopolymerization of MMA using MAX as the photoinitiator as described in Chapter 3 of the present thesis. Crosslinked poly(2-hydroxyethyl methacrylate) beads (PHEMA) were prepared as per a reported procedure.[47]

4.3.1. Preparation of S-benzoyl O-PHEMA xanthate resin 13

PHEMA (4 g) was suspended in NaOH solution (3 N, 50 mL) and stirred for 1 h. To this suspension, CS_2 (18 mL, 0.15 mol) was added and the stirring was continued for an additional 5 h. The reaction mixture was decanted and the

polymer beads were washed thoroughly with water, methanol and chloroform. The sodium O-PHEMA xanthate resin **12** thus obtained was suspended in a mixture of chloroform and acetone (1:1, 20 mL), followed by the addition of benzoyl chloride (5 mL). The reaction mixture was stirred in the dark for 4 h. The resulting yellow resin was collected by filtration, washed several times with chloroform, acetone, water and methanol. The S-benzoyl O-PHEMA xanthate resin **13** thus obtained was dried in vacuum to give 6.2 g. IR ν_{max} (KBr) 1700 (C_6H_5C=O), 1055 (C=S) cm^{-1}. Anal S, 6.7 % (2.09 mmol S/g).

4.3.2. Photografting of MMA using MAX-co-St

MAX-co-St (170 mg, 20 mole % of MAX) and MMA (10 mL, 5M in benzene) was taken in a pyrex glass vial and stoppered with a rubber septum. The solution was purged with dry argon for 10 min and irradiated for 70 min using a Rayonet Photo Reactor (RPR) equipped with eight 350 nm fluorescent lamps. The viscous polymerization mixture obtained was diluted with chloroform (50 mL) and poured into excess methanol. The precipitate obtained was Soxhlet extracted with THF. The extract was concentrated under reduced pressure and poured into methanol. The polymer obtained was collected and dried in a vacuum oven for 24 h. Yield of the graft copolymer was 43 %. IR ν_{max} (KBr) 1738 (C=O), 1252 and 1041 (C=S) cm^{-1}; ^{1}H NMR (300 MHz, $CDCl_3$) δ 7.1 (aromatic), 4.6 (OCH_2), 3.6 (OCH_3); M_n = 32000, M_w/M_n = 1.5.

4.3.3. Photografting of St using MAX-co-MMA

MAX-co-MMA (170 mg, 21 mole % of MAX) and styrene (10 mL) was irradiated for 140 min and the graft copolymer was isolated as described in Section **4.3.2**. Yield 15 %. IR ν_{max} (KBr) 1739 (C=O), 1605 (aromatic), 1251 and 1046 (C=S), 756 and 696 (aromatic); ^{1}H NMR (300 MHz, $CDCl_3$) δ 7.5–6 (aromatic), 3.6 (OCH_3); M_n = 23000, M_w/M_n = 1.4.

4.3.4. Photografting of MMA using S-benzoyl O-PHEMA xanthate resin 13

All photografting experiments using the macroinitiator **13** were carried out in cylindrical reaction vessels of pyrex glass (2.5 cm x 2 cm). Suspensions of known amounts of the polymeric photoinitiator **13** and MMA were purged with dry argon for 10 min. The suspensions were then irradiated at 400 nm, selected from a 500 W high pressure Hg lamp housed on an Oriel Optical Rail, using 340 nm long pass and 400 nm band pass filters. After irradiation for known periods at 30 ± 1 °C, the contents of the tubes were filtered, washed several times with benzene, dried under vacuum and weighed. The filtrate was concentrated and poured into excess methanol. The polymer formed was collected, washed with methanol, dried and weighed. The conversion was calculated from the total weight of the homopolymer and the polymer grafted onto the polymer-bound photoinitiator.

4.3.5. Block copolymerization of MA using the macroinitiator 16

The macroinitiator **16** (50 mg) having a molecular weight of 1.6 x 10^4 amu which was dissolved in MA (4 M, 10 mL) was taken in a quartz reaction vial and closed with a rubber septum. The polymerization mixture was purged with dry argon for 10 min and irradiated in a Rayonet Photochemical Reactor (RPR) using eight 300 nm fluorescent lamps. After 90 min, the polymerization mixture was diluted with chloroform and precipitated from methanol. The polymer obtained was purified again by redissolving in THF and reprecipitating from hexane. Yield, 25 %. M_n = 2.1 x 10^5, M_w/M_n = 1.2.

4.4. References

1. Ceresa, R. J. (Ed.), *Block and Graft Copolymers*, Wiley, New York, Vol. 1, **1973** and Vol. 2, **1976**.
2. Stannett, V.; Memetea, T. *J. Polym. Sci.Polym. Symp. Ed.* **1978**, *64*, 57.
3. Riess, C.; Hurtrez, G.; Bahadur, P. *Block Copolymers, Encyclopedia of Polymer Science and Engineering*, Mark, H. (Ed.), Wiley, New York, Vol. 2, p. 324, **1985**.
4. Jerome, R.; Tayt, R.; Quhadi, T. *Prog. Polym. Sci.* **1984**, *10*, 87.
5. Simionescu, C. I.; Comanita, E.; Pastravanu, M.; Dumitriu, S. *Prog. Polym. Sci.* **1986**, *12*, 1.
6. Nuyken, O.; Weidner, R. *Adv. Polym. Sci.* **1986**, *73-74*, 145.
7. Samal, R. K.; Sahoa, P. K.; Samantary, H. S. *J. Macromol. Sci., Rev. Chem. Phy.* **1986**, *26*, 81.
8. Mishra, M. K., Ed. *Macromolecular Design: Concept and Practice*; Polymer Frontiers International, Inc. New York, **1994**.
9. Mishra, M. K. *Macromolecular Engineering: Recent Advances*; Mishra, M. K. ; Nuyken, O.; Kobayashi, S.; Yagci, Y.; Sar, B., Eds.; Plenum: New York, **1995**
10. Van Beylen, M.; Scwarz, M.; *Ionic Polymerization and Living Systems*; Chapman and Hall: New York, **1993**.
11. Kennedy, J. P.; Ivan, B. *Designed Polymers by Carbocationic Macromolecular Engineering*; Hanser: Munich, **1991**.
12. Quirk, R. P.; Lynch, T. *Macromolecules* **1993**, *26*, 1206.
13. Frechet, J. M. J. *Science* **1994**, *263*, 1710.
14. Webster, O. *Science*, **1991**, *251*, 887.
15. Quirk, R. P.; Ren, J.; Bidinger, G. *Macromol. Chem. Macromol. Symp.* **1993**, *67*, 351.
16. Jenkins, A. D. *Eur. Polym. J.* **1993**, *29*, 449.

17. Fayt, R.; Forte, R.; Jacobs, C.; Jerome, R.; Ouhadi, T.; Teyssie, P. H.; Varshney, S. K. *Macromolecules* **1987**, *20*, 1442.

18. Hawker, C. J. *Angew. Chem. Int. Ed. Engl.* **1995**, *34*, 1456.

19. Listigovers, N. A.; Georges, M. K.; Odell, P. G.; Keoshkerian, B. *Macromolecules* **1996**, *29*, 8992.

20. Hawker, C. J.; Elee, E.; Dao, J.; Volksen, W.; Russell, T.; Barelay, G. G. *Macromolecules* **1996**, *29*, 2686.

21. Fukuda, T.; Teranchi, T.; Goto, A.; Tsujii, Y.; Miyamoto, T. *Macromolecules* **1996**, *29*, 3050.

22. Krstina, J.; Moad, G.; Rizzardo, E.; Winzor, C. L.; Berge, C. T.; Fryd, M. *Macromolecules* **1995**, *28*, 5381.

23. Mishra, M. K. *Macromolecules* **1996**, *29*, 5228.

24. Smets, G.; Dor, T. *New Trends in Photochemistry of Polymers*, Allen. N. S.; Rabek, J. F. Eds.; Elsevier Applied Science Publishers, London, pp 113-128, **1985**.

25. Arthur, J. C. Jr. *Developments in Polymer Photochemistry 2*. Allen, N. S. Ed. Applied Science Publishers, London, pp 39-53, **1981**.

26. Fouassier, J. P. *Graft Copolymerization of Lignocellulosic Fibers*. David, N.; Hohn, S. Eds.; ACS Symp. Ser. 187, American Chemical Society, New York, pp 83-141, **1982**.

27. Yagchi, Y.; Schnabel, W. *Prog. Polym. Sci.* **1990**, *15*, 551.

28. Bamford, C. H. *Reactivity, Mechanism and Structure in Polymer Chemistry*, Jenkins, A. D.; Ledwith, A. Eds. John Wiley, New York, p. 52, **1974**.

29. Bamford, C. H. *New Trends in the Photochemistry of Polymers*, Allen, N. S.; Rabek, J. F.; Elsevier Applied Science Publishers, London, p. 129, **1985**.

30. Bamford, C. H.; Crowe, P. A.; Wayne, R. P. *Proc. R. Soc. A*. **1965**, *284*, 455.

31. Bamford, C. H.; Crowe, P. A.; Hobbs, J.; Wayne, R. P. *Proc. R. Soc. A*, **1965**, *292*, 153.

32. Bamford, C. H.; Han, X. Z. *Polymer* **1981**, *22*, 1299.

33. Otsu, T.; Yoshida, M. *Makromol. Chem., Rapid Commun.* **1982**, *3*, 127.

34. Niwa, M.; Matsumoto, T.; Izumi, H. *J. Macromol. Sci. Chem.* **1987**, A *24*, 567.

35. Otsu, T.; Yoshida, M.; Tazaki, T. *Makromol. Chem., Rapid Commun.* **1982**, *3*, 133.

36. Otsu, T.; Yamashita, K.; Tsuda, K. *Macromolecules* **1986**, *19*, 287.

37. Otsu, T.; Ogawa, T.; Yamamoto, T. *Macromolecules* **1986**, *19*, 2089.

38. Otsu, T.; Matsunaga, T.; Kuriyama, A.; Yoshioka, M. *Eur. Polym. J.* **1989**, *25*, 643.

39. Otsu, T.; Matsunaga, T.; Doi, T.; Matsumoto, A. *Eur. Polym. J.* **1995**, *31*, 67.

40. Kerckhoven, C. V.; den Broeck, H. V.; Smets, G.; Huybrechts, J. *Makromol. Chem.* **1991**, *192*, 101.

41. Turner, S. R.; Blevins, R. W. *Macromolecules* **1990**, *23*, 1856.

42. Lambrinos, P.; Tardi, M.; Potton, A.; Sigwatt, P. *Eur. Polym. J.* **1990**, *26*, 1125.

43. Nakayama, Y.; Matsuda, T. *Macromolecules* **1996**, *29*, 8622.

44. Ajayaghosh, A.; Das, S.; Kamat, P. V.; Das, P. K.; George, M. V. *Polymer* **1993**, *34*, 3605.

45. Ajayaghosh, A. *Polymer* **1995**, *36*, 2049.

46. Ajayaghosh, A.; Francis, R.; Das, S. *Eur. Polym. J.* **1993**, *29* (1), 63.

47. Jayakrishnan, A.; Sunny, M. C.; Chithambara Thanoo, B. *Polymer* **1990**, *31*, 1339.

VITAE

Born on May 15, 1969, in Kottayam, Kerala, India, Raju Francis has completed his early school education from the Mar Thoma Seminary High School, Kottayam in 1984. He obtained the degree of Bachelor of Science from C. M. S. College, Kottayam, under Mahatma Gandhi University in 1989 and Master of Science from the School of Chemical Sciences, Mahatma Gandhi University, Kottayam in 1991.

He joined the Photochemistry Research Unit of RRL, Trivandrum as a Junior Research Fellow (CSIR) in July 1992. Presently he is a Lecturer in the Department of Chemistry of St.Joseph's College, Calicut, Kerala.